VATNAJÖKULL:
Mass balance, meltwater drainage and surface velocity of the glacial year 2010_11

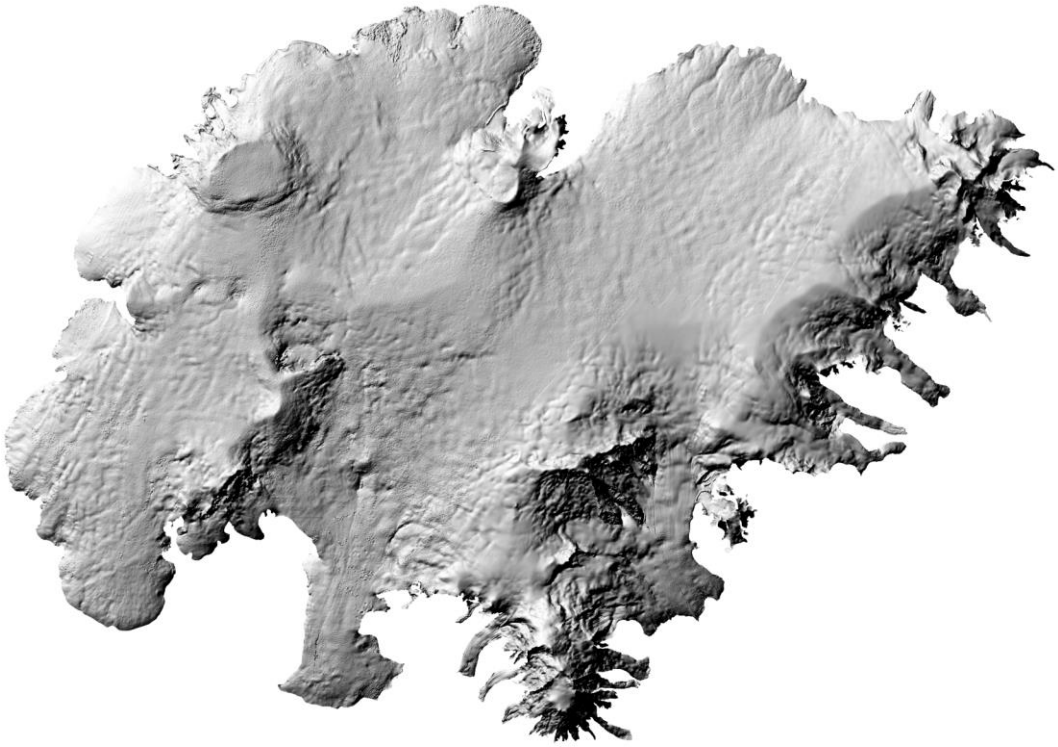

Institute of Earth Sciences
University of Iceland
and
National Power Company

Finnur Pálsson
Helgi Björnsson
Sverrir Guðmundsson
Hannes H. Haraldsson

RH-24-2013

Contents:

Figures:

Tables:

Appendixes:

1. INTRODUCTION

In 1992 (glacial year 1991_1992) a program of mass balance measurements was started for Vatnajökull by the Science Institute University of Iceland (now Institute of Earth Sciences, IES) in collaboration with the National Power Company (NPC). For the first year the program was limited to the western part of the glacier, but then expanded to include the northern outlets as well. In 1996 this study was further expanded to include southern outlets, with support from The European Union (Framework IV - Environment and Climate, TEMBA project 1996-1997). This program was extended 1998–2000 with further support from EU (Framework IV - Environment and Climate, ICEMASS project, 1998-2000). In 2000-2002 NPC and IES continued the program. In 2003-2005 IES participated in a multinational research project, which was financially supported by The European Union (EVK2-CT-2002-00152 SPICE). IES was responsible for obtaining data sets for calibration of models of the mass balance and dynamics of Vatnajökull. This work was also supported by The National Power Company of Iceland and The National Road Authority, and is a continuation of the TEMBA-project of 1996-97 and ICEMASS project 1998-2001.
In 2010-11 IES and NPC continued a similar program. Mass balance measurements on the southeast outlets Breiðamerkurjökull and Hoffellsjökull is financially supported by the National Road Authority.
The aim of the collaborative work of NPC and IES is to improve our understanding of the mass balance and melt water runoff from glaciers. This work in combination with energy balance measurements by NPC and IES on Vatnajökull will be used for calibration of models of the energy and mass balance of Vatnajökull.

This report describes the field measurements and the initial results, the mass balance and melt water runoff for the glacial year 2010_11.

2. DIARY

January 11: "Autumn" survey at the lowest mass balance sites on Tungnaárjökull and Síðujökull (impassable in autumn 2010).
March 25-26: GPS survey of sites on Tungnaárjökull.
April 4-6: winter mass balance measurements, maintenance of AWS on Breiðamerkurjökull and Hoffellsjökull.
May 4 - 11: measurements of the winter balance.
May 30 - June 3: measurements of the winter balance.
June 30 – July 1: mass balance wires and lower AWS on Tungnaárjökull visited.
July 25 and 30: AWS at site B16 serviced.
June 16, July 10 and September 3: maintenance of AWS and mass balance site on Breiðamerkurjökull.
October 19 - 24: summer balance measurements.

In all expeditions and short visits to the glacier the locations of mass balance stakes were measured with Kinematic GPS (or fast static GPS and a few with DGPS) for surface velocity calculation.

The following members of staff of the Institute of Earth Sciences, University of Iceland, carried out the fieldwork on Vatnajökull: Finnur Pálsson, Þorsteinn Jónsson, Sveinbjörn Steinþórsson and Snævarr Guðmundsson. Also Hannes H. Haraldsson and Andri Gunnarsson (National Power Company), Hlynur Skagfjörð Pálsson (Reykjavík Rescue Team). Members of the Iceland Glaciological Society assisted in the June fieldwork.

3. MASS BALANCE MEASUREMENTS

The purpose of the mass balance measurements is to describe the temporal and spatial distribution of the components of the mass balance. The mean annual values of the components and their variation from year to year are analyzed and related to meteoro-logical conditions and climatic variability. The results will be used in studies of changes in the glacier volume, estimates of meltwater contribution to glacial rivers, mass balance modeling, evaluation of altitudinal and regional variations of mass balance in response to climatic variations, and to assess the hydrometeorological and dynamic response of the ice cap to climate change.

The mass balance was determined by a stratigraphic method, measuring changes in thickness and density relative to the summer surface. The winter balance was estimated by drilling ice cores through the winter layer in the spring. Ablation was monitored from markers; snow stakes were put up on the glacier and wires were drilled down in the ablation area. The summer balance was measured in the autumn.

3.1 Methods

Measurements of the surface mass balance on a large ice cap like Vatnajökull are impractical in terms of cost with conventional techniques and sampling density that are typically used on small glaciers. The spatial variability of the mass balance may, however, be predictable on the flat large outlets of such an ice cap given data on several profiles extending over the elevation range of the glacier. The precipitation generally increases with elevation and decreases with the distance from the coast, but both the distribution of snowfall and redistribution of snow by drift depend on the prevailing wind direction during the winter. The summer melting depends mainly on the altitude and the albedo of the glacier surface. Therefore, we have used observations along a limited number of flowlines, which span the elevation range of the outlets to assess aerial estimates of surface mass balance. Each profile describes the variation with elevation, but together they also describe the lateral variation of the mass balance. Recently, modern over-snow vehicles and helicopters have allowed fast traverses to ensure successful fieldwork in spite of frequently poor weather conditions. The error for individual point measurement is estimate ~30 cm_{we} for both summer and winter balance. The error for the area integral of mass balance is however considered smaller, since the error for individual survey sites is independent.

The winter mass balance (b_w) is defined as the mass of snow accumulated during the winter months, the summer balance (b_s) is the mass balance during the summer, and the net balance (b_n) is defined as their sum. The specific mass balance is expressed in terms of the equivalent thickness of water. All mass balance components apply to a time interval between given measurement dates, which are not fixed from one year to another. The dates in the autumn are separated by approximately one calendar year, which roughly coincides with the glaciological year defined as October 1st to September 30th. Snow cores are drilled in April-May through the winter layer and profiles of the density are measured. The summer balance is derived in the autumn from measurements of the changes in the snow core density during the summer in the accumulation area and from readings at stakes and wires drilled into the ice in the ablation areas.

Digital maps are created for winter, summer and net balance for the whole ice cap based on site measurements. The mass balance is calculated over both the ice and water drainage basins. The summer balance over the water basin is an estimate of meltwater contribution to rivers and groundwater storage. This estimate, however, does not include precipitation that falls as rain on the glacier or snow, which falls and melts during the summer. The meltwater contribution is compared with river runoff at stream flow gauges closest to the glacier. For this comparison, we define the glaciological year from the start of October to the end of September and the period draining meltwater from the glacier during the summer from June through September. It would be misleading to include May in the summer period because runoff from the glacier melt in May is delayed due to refreezing during elimination of the cold wave.

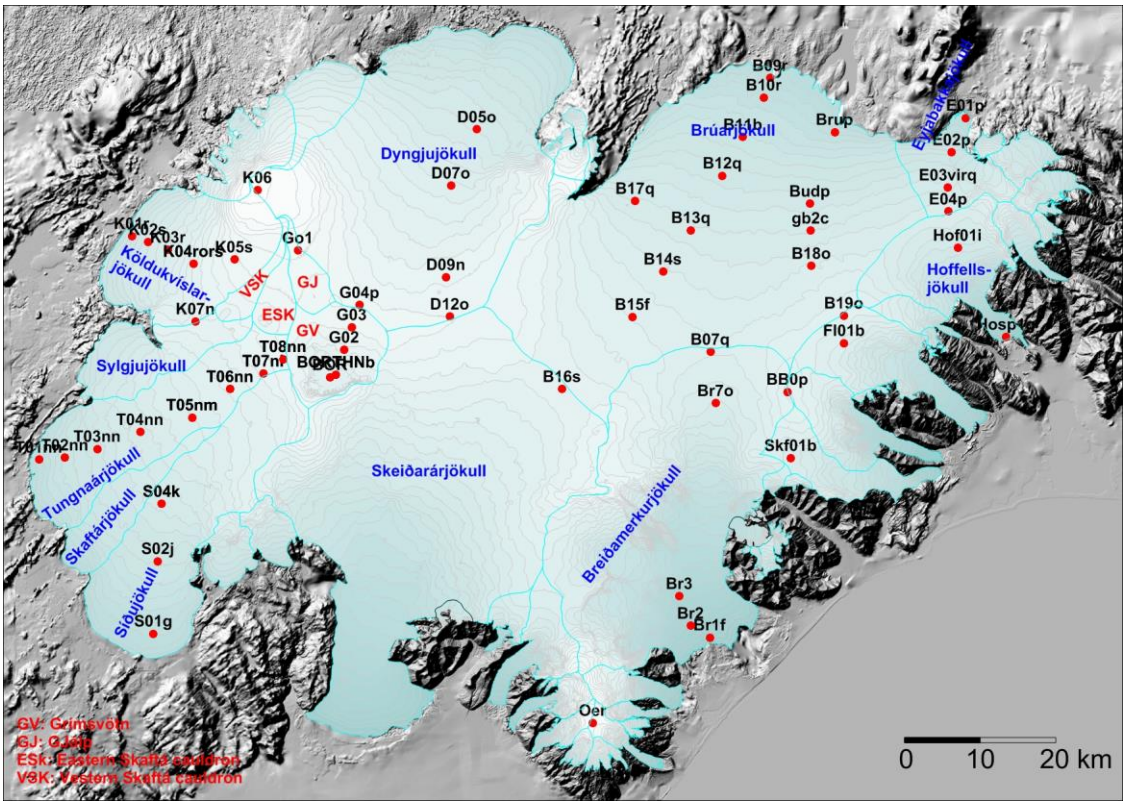

Figure 1. Outlets of Vatnajökull and location of mass balance measurement sites 2010_11.

3. 2 Results of mass balance measurements.

Mass balance measurements were done at 57 sites in spring 2011 (Fig. 1). The specific mass balance at individual sites is shown in Fig. 2. Most sites are on central flow lines at individual outlets. The specific mass balance along flow lines is given in Fig. 3 as a function of elevation for each glacier outlet: Síðujökull, Tungnaárjökull, Dyngju-jökull, Köldukvíslarjökull, Brúarjökull (west and east), Eyja-bakkajökull, Hoffellsjökull and Breiðamerkurjökull.

Digital maps for winter, summer and net balance are shown in Figure 4. Although no balance measurements are available for Skeiðarárjökull, the balance has been estimated by interpolating the balance values from the neighboring outlets, based on our experience from previous years. The mass balance of individual large outlets is discussed in the following

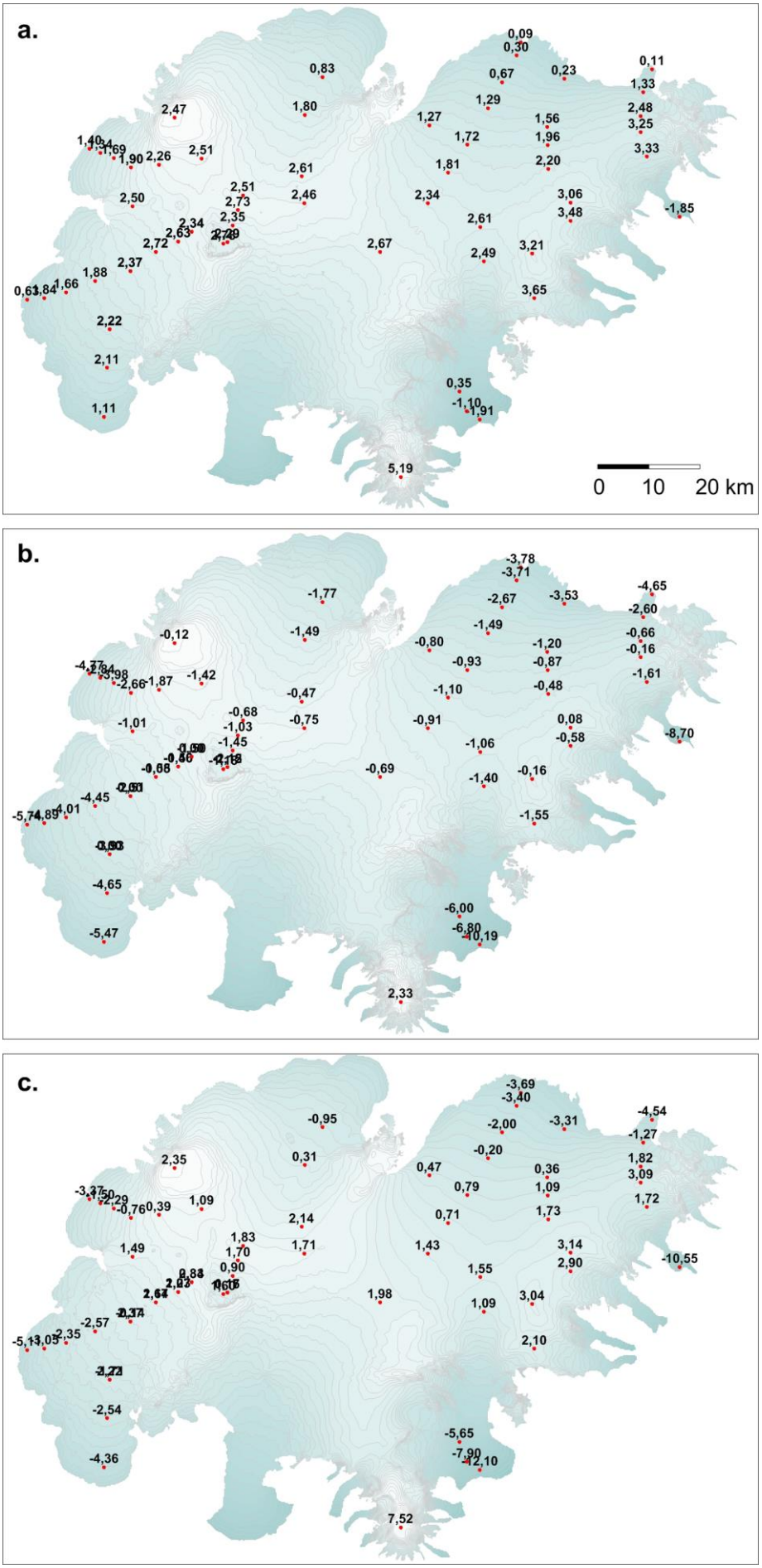

Figure 2. Maps showing point values of specific mass balance in m water equivalent (m_{we}), 2010_11. a. winter, b. summer, c. net balance.

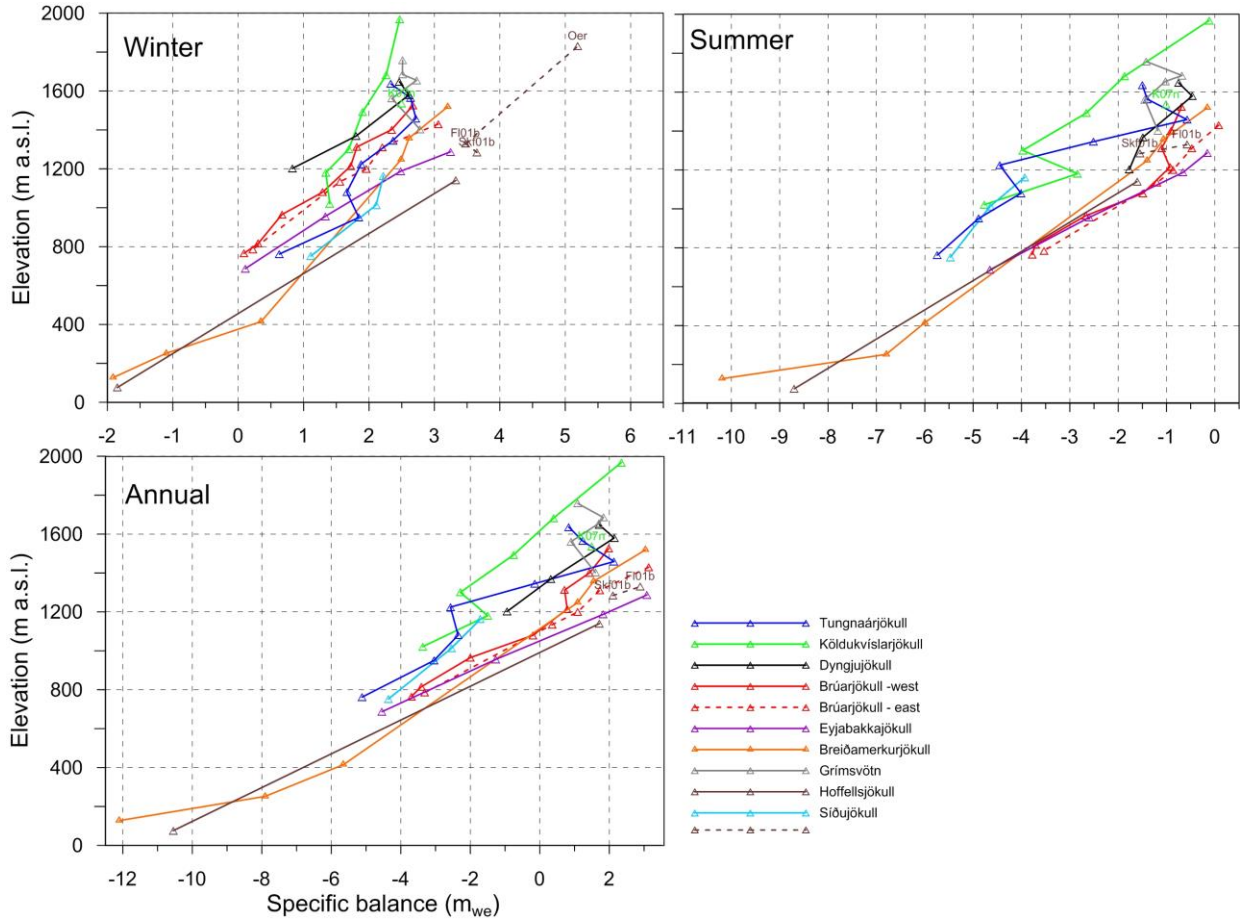

Figure 3a. Specific mass balance (m_{we}), along all mass balance profiles 2010_11.

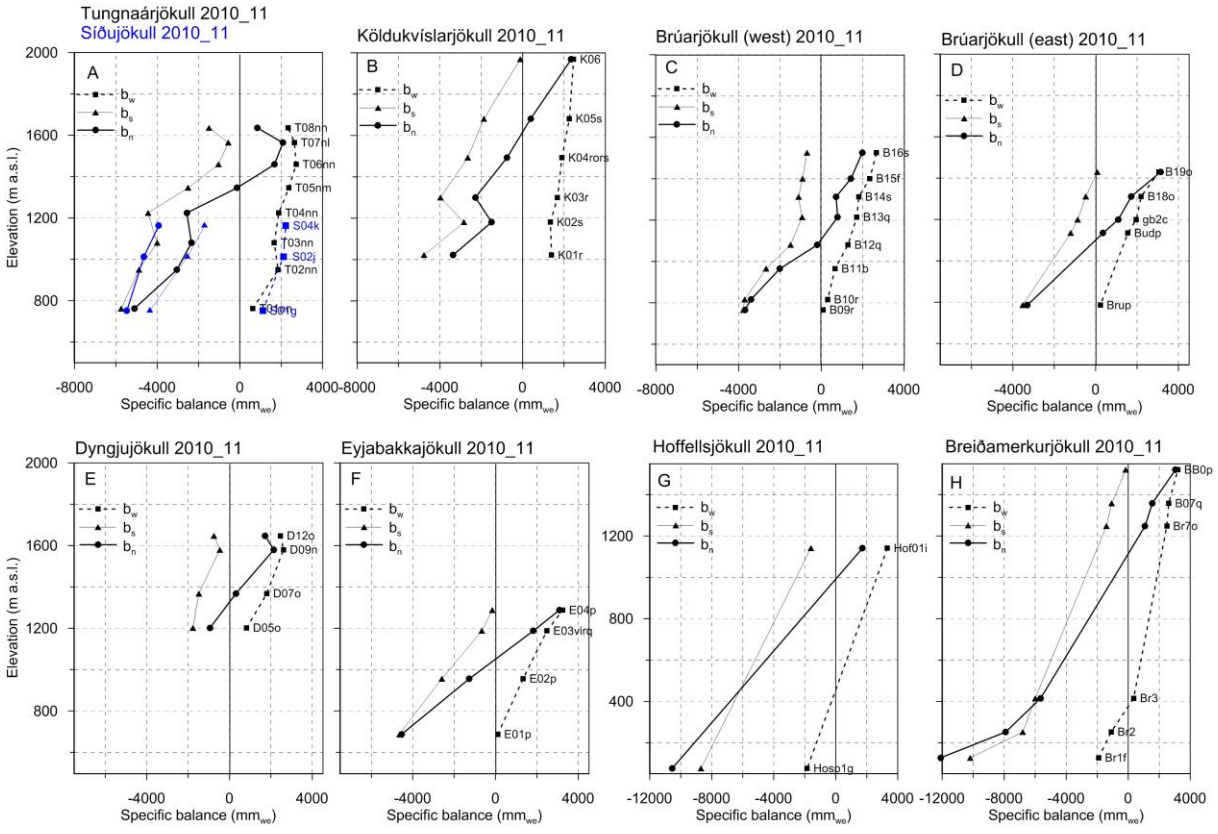

Figure 3b. Specific mass balance (mm_{we}) 2010_11 as a function of elevation on central flow lines on Vatnajökull outlets.

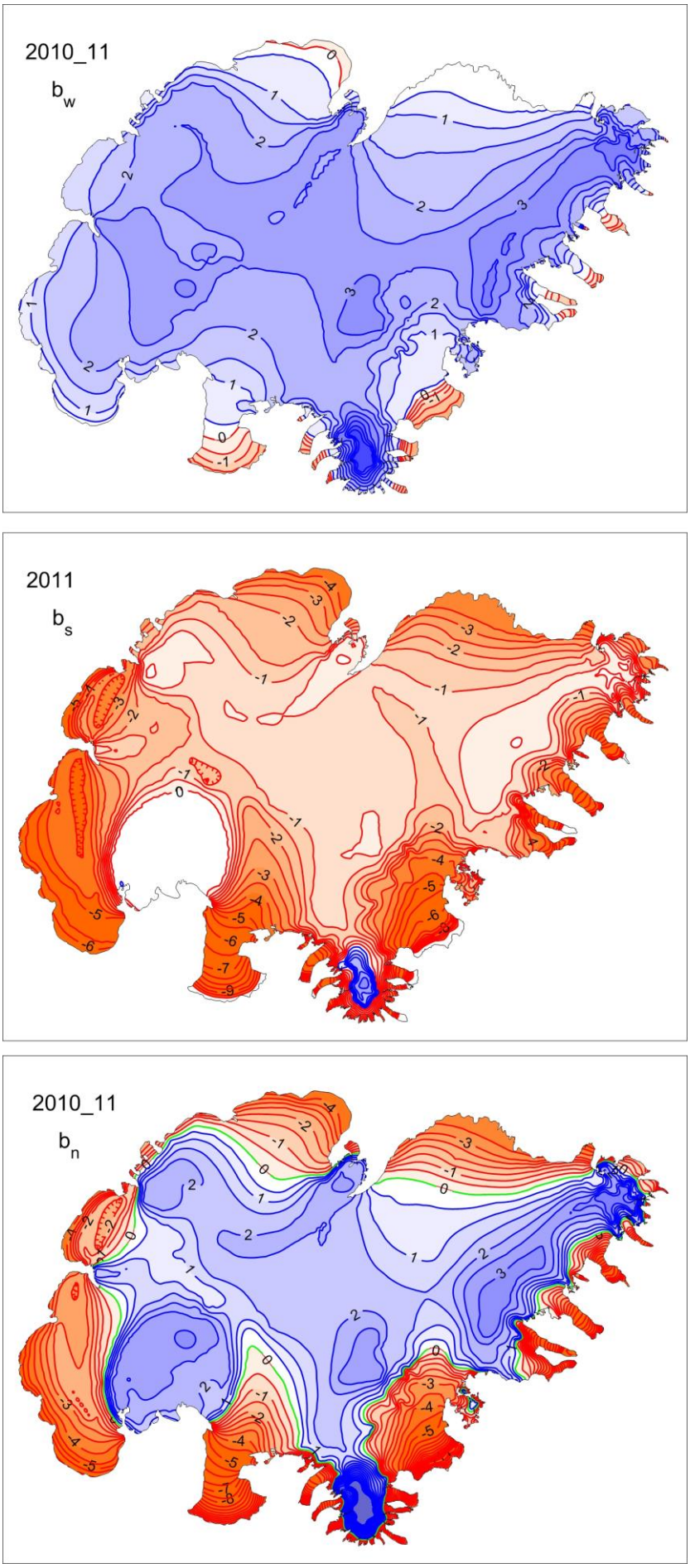

Figure 4. Specific mass balance (m_{we}) maps of Vatnajökull 2010_11. Top: winter, Centre: summer, Bottom: net balance.

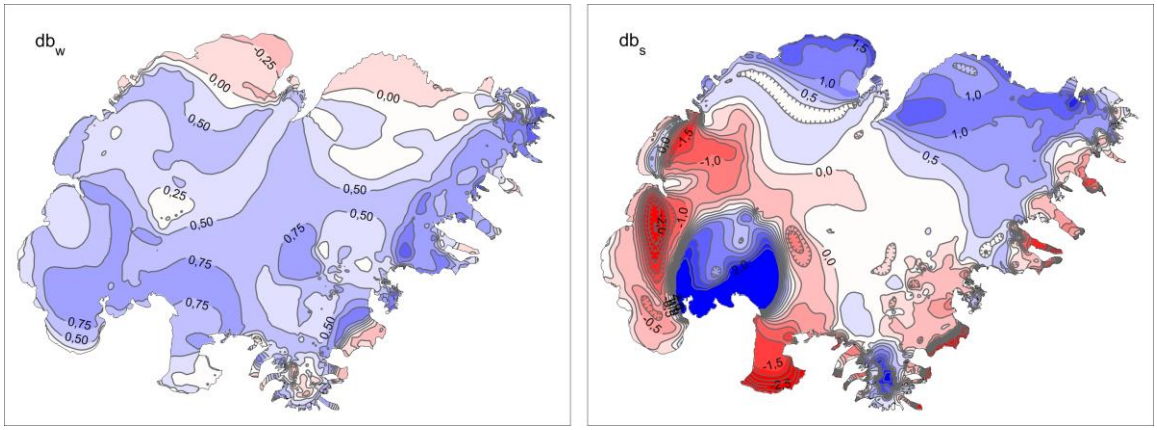

Figure 5. The left frame shows the difference between winter balance in 2010_11 and the average winter balance 1995_96 to 2009_10. *(Positive (blue) is higher than average).* *The left frame shows the difference between summer balance in 2011 and the average summer balance 1996 to 2010; the dark blue area south of Grímsvötn is where the tephra cover from the eruption prohibited ablation.* *(Negative (red) is higher than average ablation).*

subsections. A DEM of Vatnajökull mostly based on SPOT5 HRS images (stereo images from the SPOT5 satellite) in 2010, and partly from LiDAR survey 2010, is used for surface area distribution and delineation of ice divides for individual outlets and catchments.

The autumn and winter were unusually warm, precipitation close to average in the SW but slightly higher than average in the north and east. In section of the chosen Modis images (appendix F) show that in late November almost no snow had accumulated in the highland west and NW of Vatnajökull and the south lowland was snow-free the whole winter. The snow accumulation was ~0.5 m over average on Vatnajökull except on the north outlets where accumulation was close to average. The summer was warm and sunny in the SW (~1 °C above average, and sunny hours ~35% more than average). However the June was cold in the east and north, on Vatnajökull; summer came late; there were frequent snowfall events on the northern and higher outlets. July was warm and dry on SW Vatnajökull but colder in the north and east, and wet cloudy in the SE. The temperature and precipitation in August was close to average, but September was stormy and wet, winter turned in early. (Information about weather is from the web site of the Iceland met office written by Trausti Jónsson).

Inspection of the MODIS monthly overview of the summer months in Appendix F show that days with clear skies over Vatnajökull were ~7 in June, ~5 in July, ~7 in August. September was stormy with occasional snowfall in cold northern winds. In all the summer 2011 was short on Vatnajökull; it started late (after mid-June) and ended abruptly in late August.

On the MODIS images for May 22nd the Grímsvötn eruption plume over Vatnajökull can be seen. The eruption started on the 21st and terminated on May 30th. Most of the tephra fell out south of Grímsvötn in strong northern winds, some in a NNW section over Köldukvíslarjökull. However some tephra fell out all over Vatnajökull, and greatly enhanced melting in the short summer period, especially NW of Grímsvötn. In a large area south of Grímsvötn the tephra insulated the snow surface and there was no ablation.

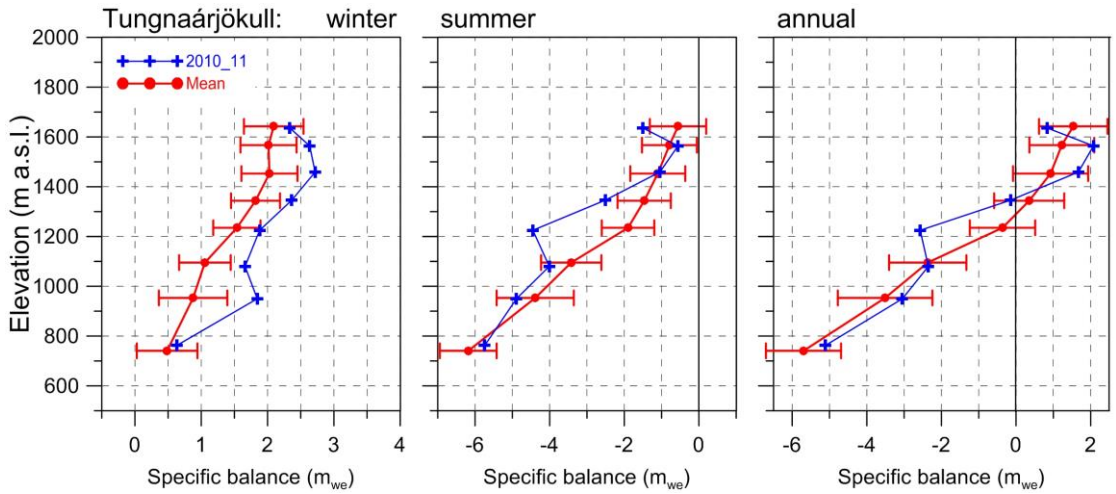

Figure 6. Mass balance at a central flow line of Tungnaárjökull 2010_11, and average mass balance 1991_92 to 2009_10.

3.2.1 Tungnaárjökull.

Area = 345 km^2
B_w= 0.66 km^3 ; b_w = 1.92 m
B_s = -1.19 km^3 ; b_s = -3.47 m
B_n = -0.53 km^3 ; b_n = -1.55 m
ELA = 1345 m (at profile)
AAR = 29 %

(The terms are defined at the foot of this page)

Variation of mass balance along a central flow line on Tungnaárjökull is shown in Fig. 6. The winter balance was higher more than 1 std. higher than average at most sites of the survey sites, except the lowest. The low value at the lowest site may be explained by warm winter. The total winter balance was 30% higher than average. The summer ablation was greatly affected by tephra from the Grímsvötn eruption in May. In the lower areas the tephra washed off as the snow cover melted away. Above average ELA the tephra stayed in the surface and enhanced melting throughout summer, resulting in 2fold the average melt at elevations between 1200 and 1400 m. Above ~1400 m the tephra was thick enough to insulate the winter snow resulting in very little melt. The tephra thickness varied in few m wide bands (with S-N direction), with excessive melt in the bands with thin cover (this was the case at the top site). The net balance was negative the 18th year in a row; the net loss was ~0.4 m_{we} less than average during the survey period (30% more than average).

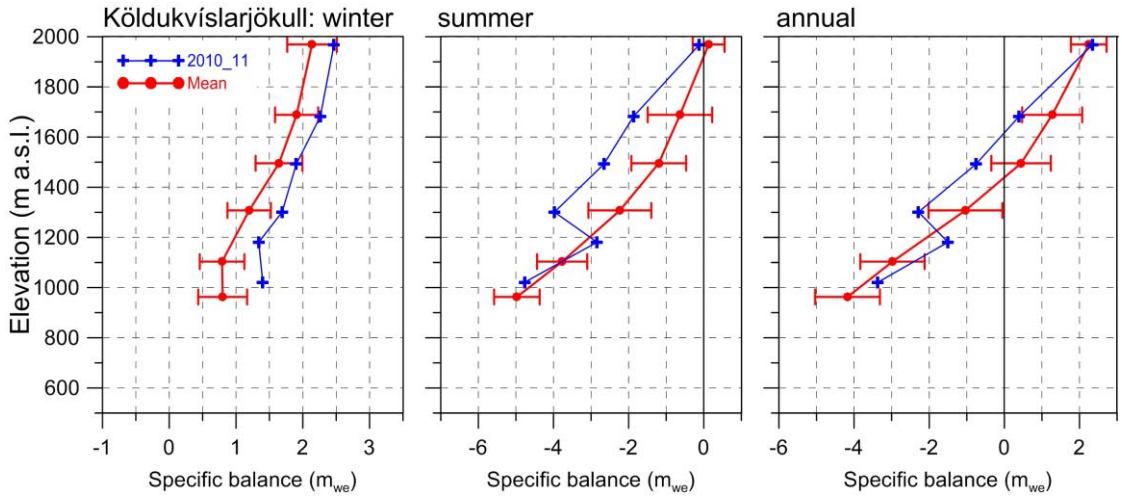

Figure 7. Mass balance at a central flow line of Köldukvíslarjökull 2010_11, and average mass balance 1991_92 to 2009_10.

B_w,B_s and B_n are water equivalent volumes of winter, summer and net balance, ELA the equilibrium line altitude, and AAR is the accumulation area ratio.

3.2.2 Köldukvíslarjökull

Area = 301 km^2
B_w = 0.56 km^3 ; b_w = 1.86 m
B_s = -0.79 km^3 ; b_s = -2.64 m
B_n = -0.23 km^3 ; b_n = -0.78 m
ELA = 1615 m (at profile)
AAR = 39 %

Variation of mass balance along a central flow line on Köldukvíslarjökull is shown in Fig. 7. Accumulation was about one st.var. over the average at all survey sites. The winter balance was about 28% higher than average since 1991_92. The summer ablation was greatly affected by tephra from the Grímsvötn eruption in May. In the lower areas the tephra washed off as the snow cover melted away. Above average ELA the tephra stayed in the surface and enhanced melting throughout summer, resulting in 2fold the average melt at elevations between 1200 and 1600 m. At the top site on Bárðarbunga the tephra was very thin and much of the summer it was covered with fresh snowfall. The summer balance was 32% lower than average. The net balance was negative the 18th year in a row, 54% (0.24 m_{we}) more mass was lost than the average during the survey period.

3.2.3 Dyngjujökull

Area = 1064 km^2
B_w= 1.89 km^3 ; b_w= 1.78 m
B_s = -1.47 km^3 ; b_s = -1.39 m
B_n = 0.42 km^3 ; b_n = 0.39 m
ELA = 1325 m (at profile)
AAR = 65 %

Variation of mass balance along a flow line on Dyngjujökull is shown on Fig. 8. The winter balance in 2010_11 was more than std.var. above average in the uppermost survey sites, but more than std. var. less at 1200 m, and almost nothing was accumulated in the ablation zone (no sites but this is obvious from the MODIS images in appendix F.) In total the winter balance was 22% higher than average.
The summer ablation was close to average at all sites. Although some tephra from the Grímsvötn eruption was deposited all over Dyngjujökull, large areas were covered by fresh snow much of summer; this resulted in summer balance very close to average above average ELA, less than average at the lowest site. The resulting summer balance was 85% of the average over the survey period. The net balance was positive due to the high winter balance.

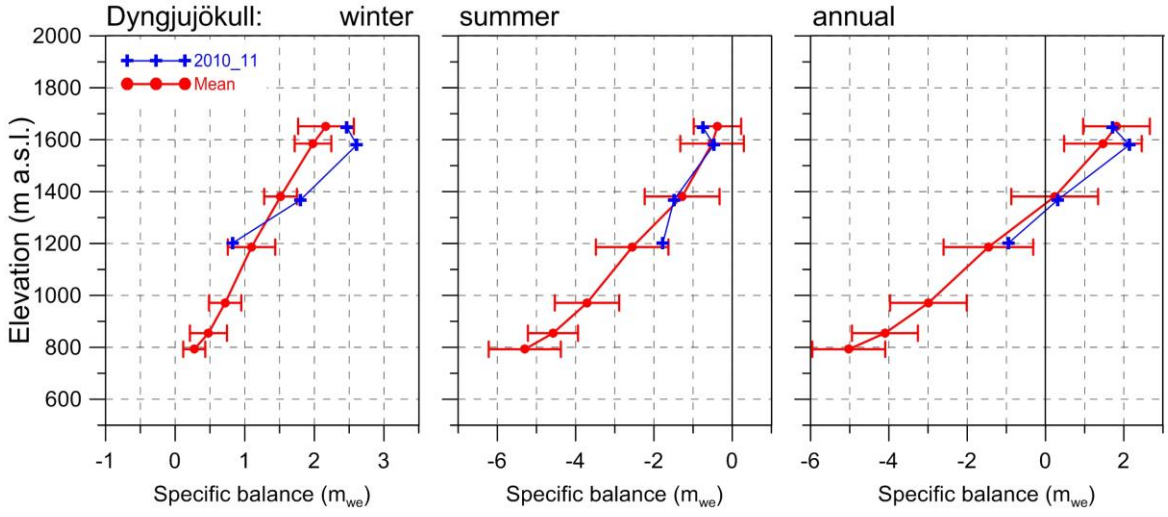

Figure 8. Mass balance at a central flow line on Dyngjujökull 2010_11, and average mass balance 1991 92 to 2009 10 (except 1998 99 – 2003 04 at all but the top elevation).

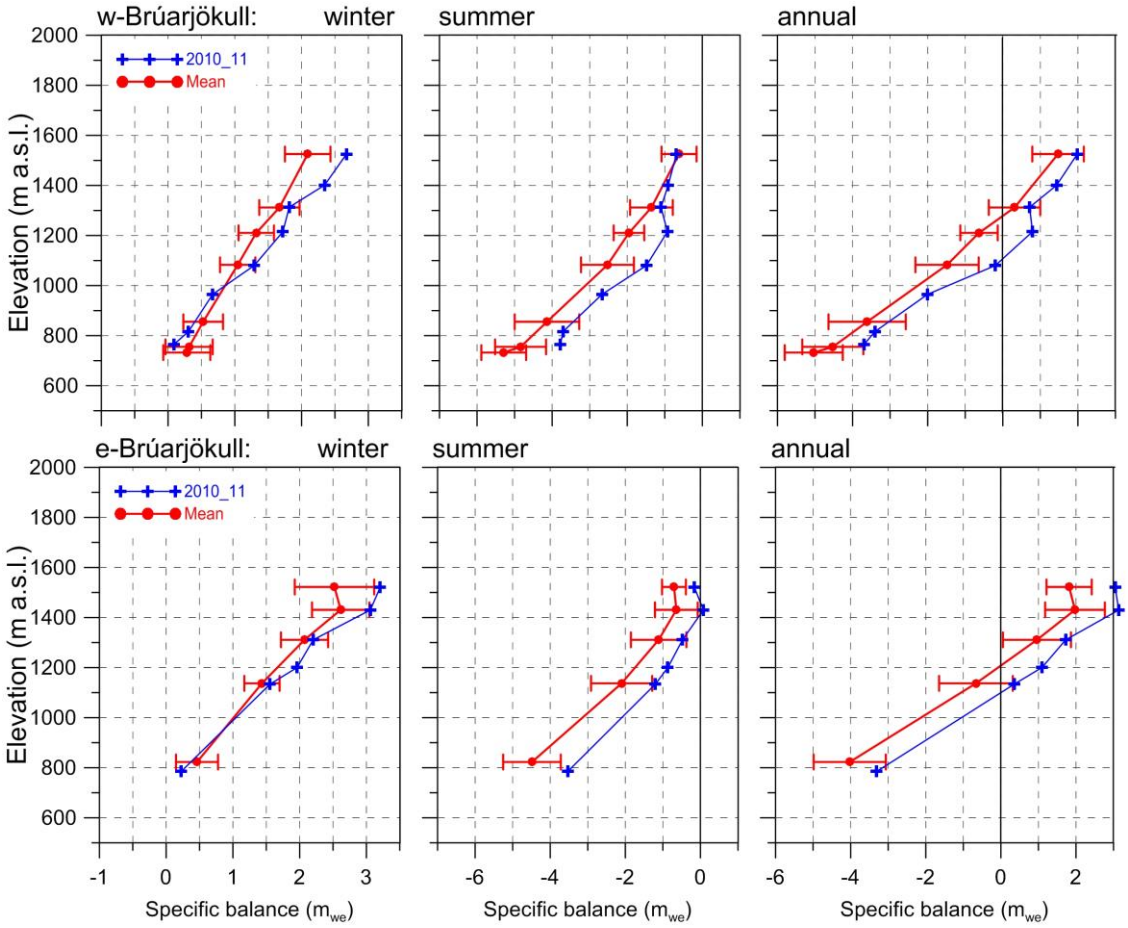

Figure 9. Mass balance at two flow lines on Brúarjökull 2010_11, and average mass balance 1992_93 to 2009_10.

3.2.4 Brúarjökull

Area = 1526 km^2
B_w= 2.72 km^3 ; b_w = 1.78 m
B_s = -1.96 km^3 ; b_s = -1.28 m
B_n = 0.76 km^3 ; b_n = 0.50 m
ELA = 1105 m (western flow line)
ELA = 1100 m (eastern flow line)
AAR = 73 %

Variation of mass balance along two flow lines on Brúarjökull is shown on Fig. 9. At all the lower survey sites accumulation was less than average, but at sites above 1000 m the winter snow accumulation was well above average, more than one std. dev. at sites above 1400 m. The total winter balance is 17% higher than average. The summer ablation was much less than average on all sites except the highest on the western profile. Although some tephra from the Grímsvötn eruption was deposited all over Brúarjökull, large areas were covered by fresh snow much of summer; and in the E and NE the summer was not only short, but also wet and colder than average. The resulting summer balance was 87% of the average over the survey period. The net result of the higher than average winter balance and less than average summer melt was positive net balance; +0.5 m_{we} in contrast to the average loss of -0.4 m_{we} of the survey period.

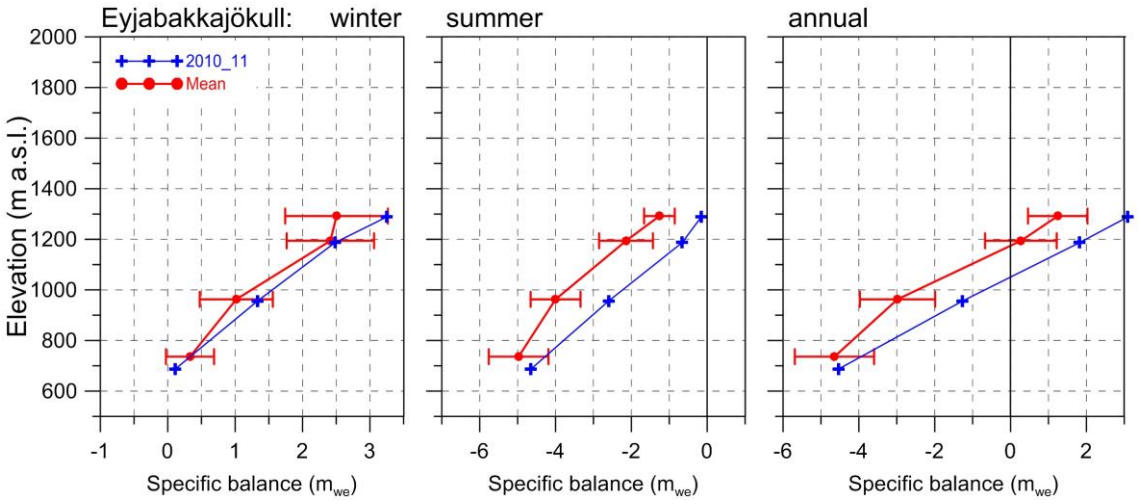

Figure 10. Mass balance at a central flow line of Eyjabakkajökull 2010_11 and average mass balance 1995_96 to 2009_10.

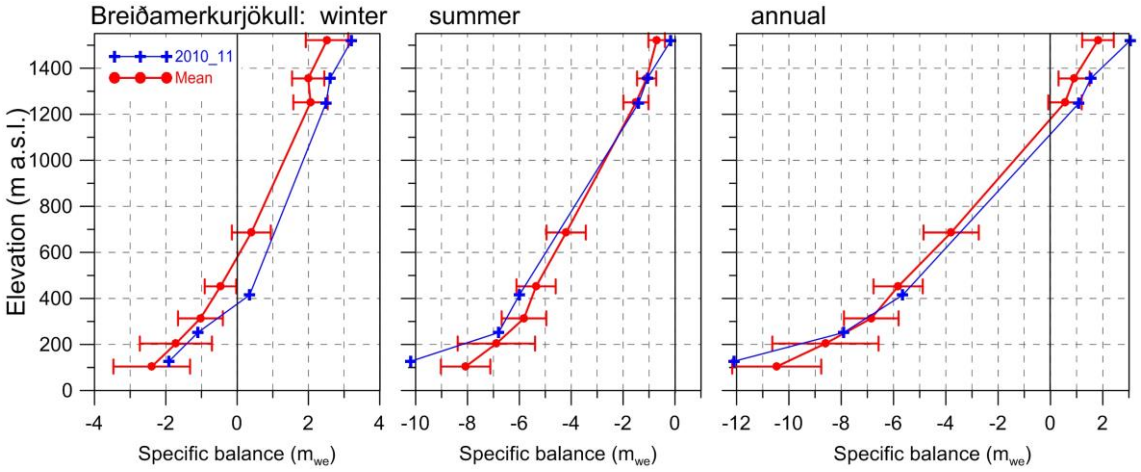

Figure 11. Mass balance at a central flow line of Breiðamerkurjökull 2010_11, and average mass balance 1995_96 to 2009_10.

3.2.5 Eyjabakkajökull

Area = 112 km^2
B_w= 0.22 km^3 ; b_w = 1.99 m
B_s = -0.16 km^3 ; b_s = -1.47 m
B_n = 0.06 km^3 ; b_n = 0.51 m
ELA = 1150 m (at profile)
AAR = 63 %

Variation of mass balance along a central flow line on Eyjabakkajökull is shown on Fig. 10. Winter balance was close to average at all sites except he highest, where it was more than one std. var. higher. In total the winter balance was 16% higher than average. The short, cold and wet summer resulted in exceptionally little ablation, at all survey sites. The total summer balance was only 55% of the average. The net result of the higher than average winter balance and much less than average summer melt, was positive net balance; +0.5 m_{we} in contrast to the average loss of -1.0 m_{we} of the survey period (since 1995_96).

3.2.6 Breiðamerkurjökull

Area = 938 km^2
B_w= 1.73 km^3 ; b_w = 1.85 m
B_s = -2.40 km^3 ; b_s = -2.56 m
B_n = -0.67 km^3 ; b_n= -0.71 m
ELA = 1110 m (at profile)
AAR = 57 %

Variation of mass balance along a central flow line on Breiðamerkurjökull is shown on Fig. 11. Snow accumulation was more than one std. dev. more than average above 400 m, but the winter ablation at the lowest survey sites was close to average. Here the Grímsvötn tephra significantly enhanced summer ablation at the lower sites. The winter balance was 39% above average, and summer balance 98% of the average (since 1995_96). The net balance was negative but only 56% of the average.

3.3 The mass balance record for Vatnajökull.

From the digital maps the total volumes of winter, summer and net balance have been calculated by integration (appendix D, gives balance values as a function of elevation) and are as follows (in water equivalent):

B_w= 15.66 km^3 ; b_w = 1.97 m
B_s = -15.83 km^3 ; b_s = -1.99 m
B_n = -0.17 km^3 ; b_n = -0.02 m
AAR = 63%

Most of the latter half of winter was wet, with prevailing southerly winds. This lead to higher than average winter balance by 29% (over the observation period 1991_92-2009_10, Fig. 12 and 13). The zero mass balance turnover for Vatnajökull (current topography) is close to 13.4 km^3 (1.64 m_{we}) and the winter balance 2010_11 is about 20% higher. The summer was short, June was cold and winter turned on early just after mid-August. However the Grímsvötn eruption in late May deposited tephra all over the glacier, extremely thick south of Grímsvötn (up to a few m), a substantial amount in a section NNW (~ mm - cm) of Grímsvötn but a thin layer elsewhere. East of Grímsvötn the tephra was covered with fresh snow most of May and June and ablation rates were very low. On western Vatnajökull the tephra cover greatly enhanced melting in May and June, especially in the accumulation zone of Tungnaárjökull, Sylgjujökull and Köldukvíslarjökull. However in a ~420 km^2 area south of Grímsvötn nothing melted due to the thick tephra cover (thicker than a few cm). In July the tephra became visible all over Vatnajökull, enhancing melt rates everywhere. The high melt rates in the west compensated for the low melt rates elsewhere, the total summer ablation was only ~2% less than average over the survey period, ~20% higher than for zero balance turnover.
The net balance was only slightly negative; the mass loss is the smallest

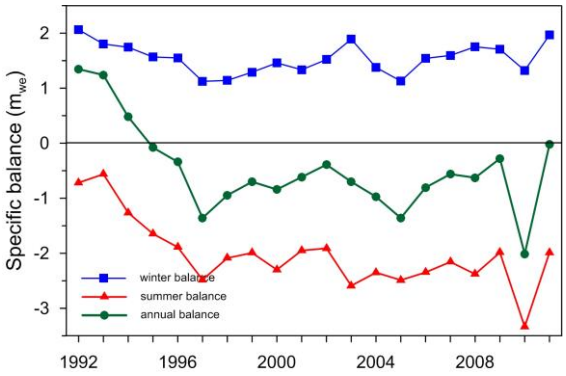

Figure 12. Specific mass balance record for Vatnajökull 1991_92 – 2010_11.

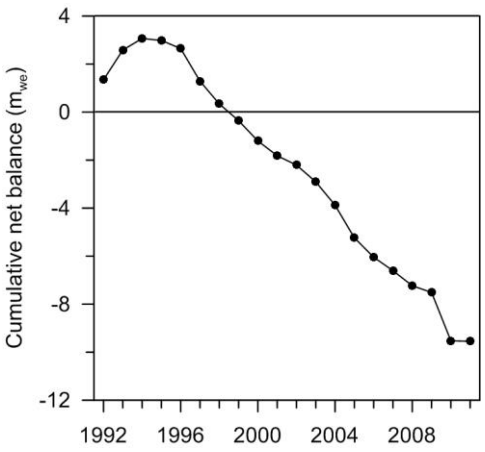

Figure 13. Cumulative specific mass balance record for Vatnajökull 1991_92 – 2010 11.

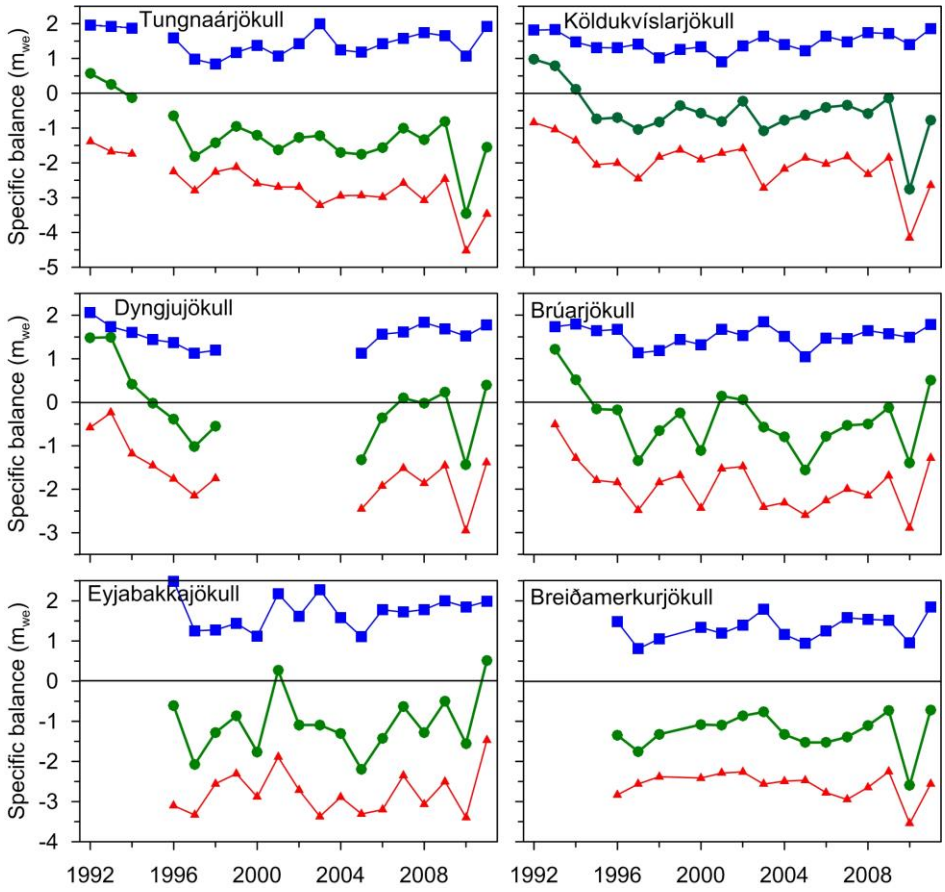

Figure 14. Specific mass balance record for Vatnajökull outlets 1991_92-2010_11.

during the survey period, only 3% of the average loss (-0.74 m) of the past 16 consecutive years of negative balance.

The glacial year of 2010_11, although with only slight mass loss, was the 18th in a row with negative mass balance for Vatnajökull (Fig. 12, Fig. 13), contributing to a total loss of 12.5 m_{we} (ice volume of ~112 km^3) since 1994_95.

The temporal variability of mass balance for different outlets is shown in Fig. 14. In 2010_11 on all the northern outlets net mass balance was positive, the winter snow layer was thicker than average and the summer was short. The net balance of the western outlets was highly negative due to hectic ablation in the accumulation areas, caused tephra on the surface deposited in the Grímsvötn eruption in May, and relatively dry and cloud free period in May and June. The tephra fallout increased total ablation on all of Vatnajökull outlets; without the tephra net balance would have been positive to a degree not seen since the early 1990's.

The greatest variability of the winter balance is for Eyjabakkajökull, the eastern most of studied outlets. This part of the glacier receives precipitation from all south- and east- and north-easterly wind directions, and thus has high snow accumulation in winters when the paths of the North Atlantic lows is just east of Iceland. This is also the case for the eastern part of Brúarjökull.

Breiðamerkurjökull shows lowest variability. It is a maritime glacier with climate controlled by the stable sea temperature and humid air mass. The longest winter balance records seem to reveal periodic behaviour,

with peaks in ~1991_92 and 2002_03 and a low in ~1998. During the period of net mass loss since 1994_95, the northern outlets have had several years of close to zero and positive mass balance. The cumulative net balance curves for the outlets of Vatnajökull in Fig. 15 show that all outlets have been losing mass since 1994_95. The slope for mass loss is about 0.7 ma^{-1} for the northern outlets, but 1.5 ma^{-1} for the south and western outlets.

In Fig. 16 the relation of the annual net balance to the accumulation area ratio (AAR) and equilibrium line altitude (ELA) is shown for different outlets over the survey period. The b_n-AAR gradient is similar for all outlets, about 0.5 m_{we} for 10% change in AAR. The zero-balance AAR varies for different outlets from about 60-65%, similar for all outlets except for the southern outlet Breiðamerkurjökull.

Breiðamerkurjökull is not in dynamic or mass balance equilibrium, the ablation area is too large. A large part of the glacier has carved 200-300 m through the former sediment bed, and the surface elevation has lowered accordingly. Breiðamerkurjökull is now retreating at a high rate.

Similarly the zero-balance ELA varies from about 1000-1100 m for the southern outlets to 1400 m for the NW outlets. The b_n-ELA slope is similar for all outlets -0.7 m_{we} per 100 m.

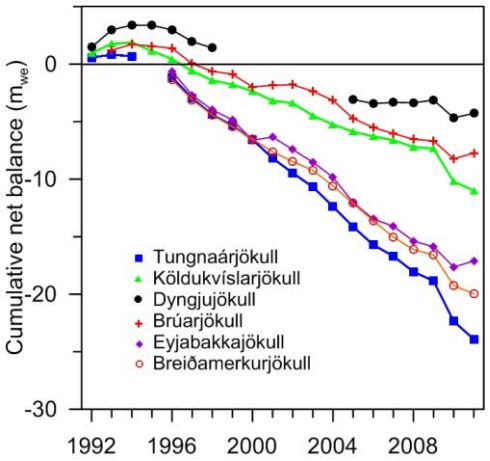

Figure 15. Cumulative specific mass balance for several of Vatnajökull outlets 1991_92 – 2010_11.

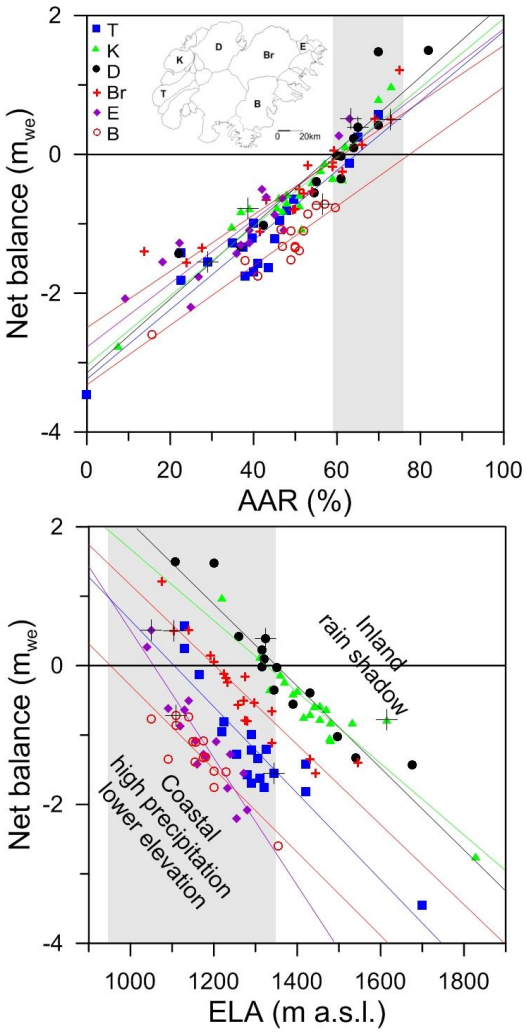

Figure 16. The relation between net annual balance (b_n) and accumulation area ratio (AAR)(upper) and b_n and equilibrium line altitude (ELA), for Vatnajökull outlets during the survey period. (This year's points are marked with a black +).

4. SURFACE VELOCITY MEASUREMENTS

The surface velocity of the glacier was calculated from DGPS (accuracy within 1 m), fast static (accuracy about 1 cm) and kinematic GPS (accuracy about 3 cm) positioning of the ablation stakes. All sites were surveyed in spring and autumn (most kinematic, some DGPS), and many also in June (kinematic), August (fast static) and October (kinematic). At a few sites stakes from previous years were found and resurveyed, making it possible to calculate surface velocity over a year or longer time span. The average summer surface velocity is shown on Figure 17.

The use of more accurate instruments and setup, allows estimation of vertical as well as horizontal velocities. Two 6 metre long 4 inch metal poles where set up in the accumulation zone of the western outlet Tungnaárjökull and one on east Brúarjökull to directly measure the vertical displacement. Small GPS units are also attached to the poles and run continuously. At sites close to the glacier edge very small horizontal movement is measured. This indicates that the glacier snouts are almost stagnant. In the centre areas of some of the outlets especially close to the equilibrium line, there is an increase in velocity during summer compared to winter. The summer velocity is of the order of two-fold the winter velocity. This suggests that basal sliding is increased in the melting season, and is of the same magnitude as the deformation velocity.

From previous velocity measurements, surging of outlets has been predicted. No signs of a starting surge are seen from this year's survey.

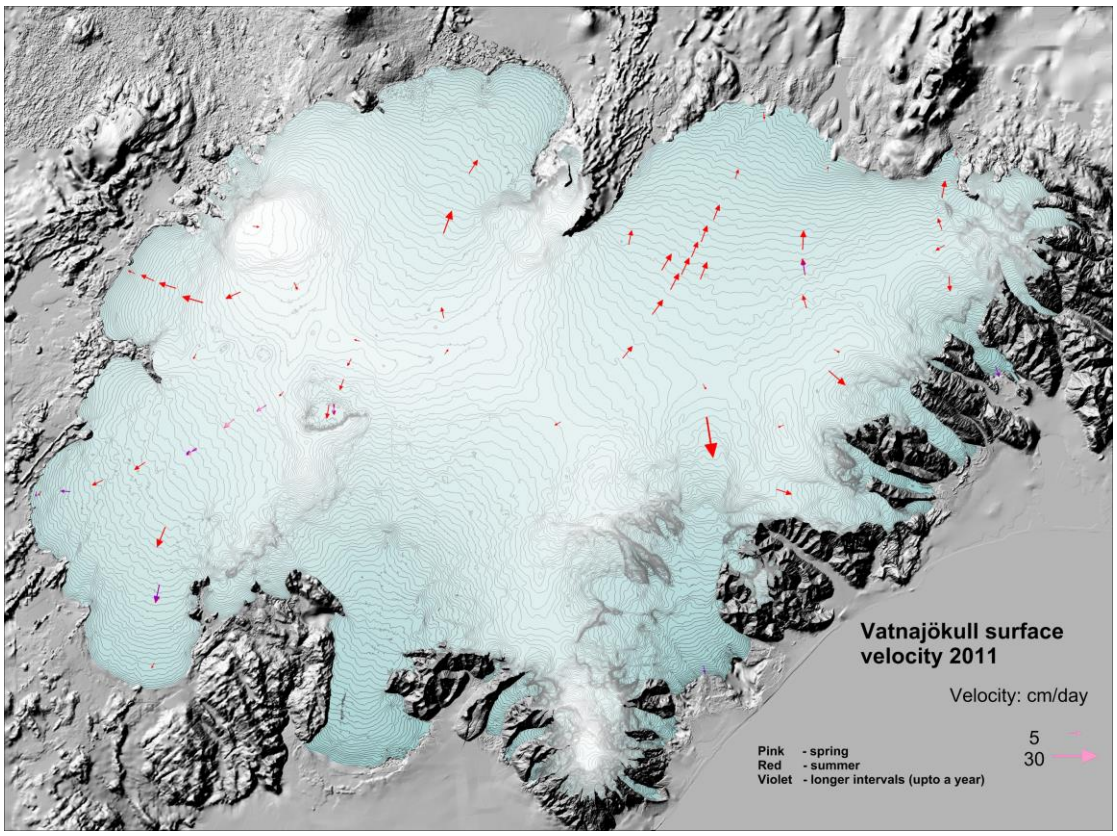

Figure 17. Average surface velocity at survey sites in 2010_11.

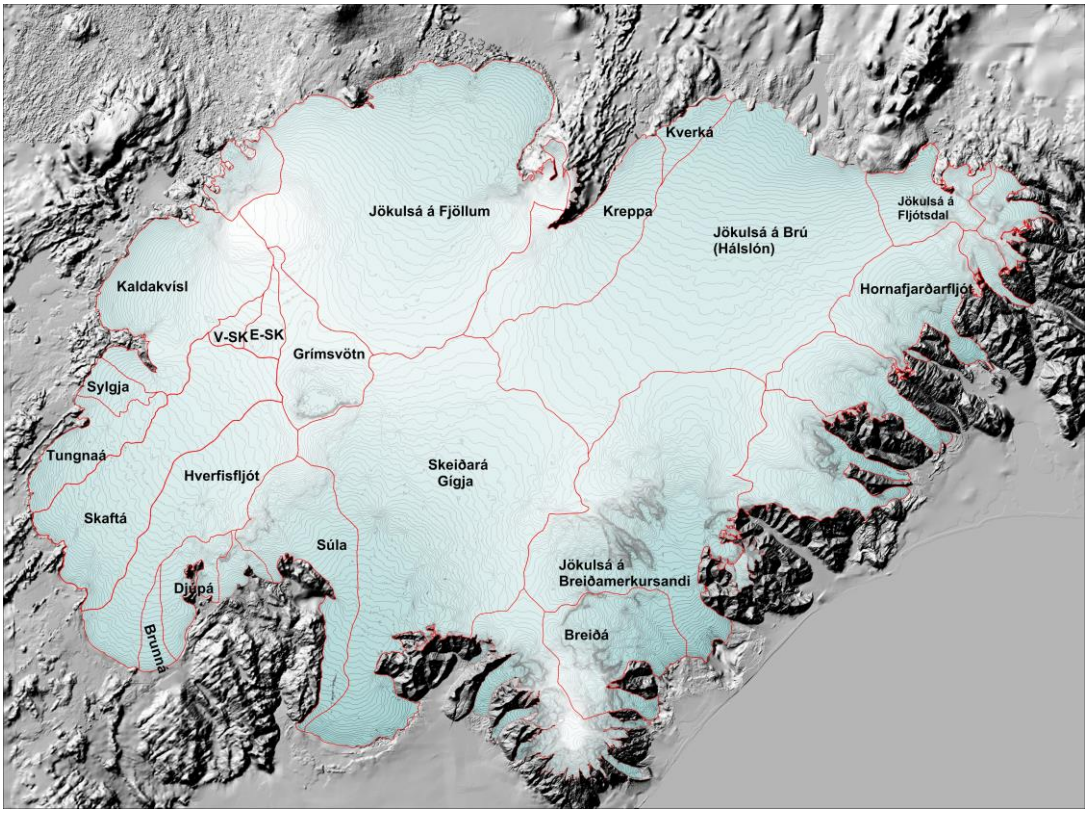

Figure 18. Water divides and drainage basins of selected rivers draining water from Vatnajökull.

5. Melt water runoff.

Water divides and drainage basins for rivers draining water from Vatnajökull have been defined from water pressure potential maps. The potential maps were produced from existing surface (year 2010) and bedrock digital elevation models.

Figure 18 shows the water divides and drainage areas for selected rivers draining melt water from Vatnajökull. The summer balance over the water basin is an estimate of meltwater contribution to rivers and groundwater storage. This estimate, however, does not include precipitation that falls as rain on the glacier, nor snow which falls and melts during the summer. The meltwater contribution can be compared with river runoff at stream flow gauges closest to the glacier. For this comparison, we define the glaciological year from the start of October to the end of September and the period draining meltwater from the glacier during the summer from June through September. It would be misleading to include May in the summer period because runoff from

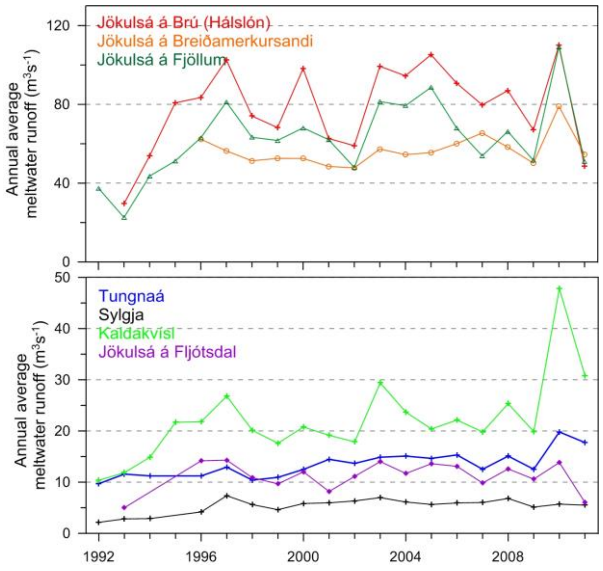

Figure 19. The temporal variation of average annual meltwater runoff to selected river catchments.

the glacier melt in May is delayed due to refreezing during elimination of the cold wave and because of the contribution of the spring melt from the highlands to the runoff. Some melting also occurs during winter, especially in the low snouts of the southern outlets.

Average melt water runoff to different rivers is given in Table I, and temporal variation of the average meltwater runoff in Fig. 29. The average specific runoff (q_s) differs from basin to basin from 32 to 169 $ls^{-1}km^{-2}$. This is mainly due to different elevation distributions, for example, the water drainage basins for Tungnaá and Kverká are within the ablation area, while that of Grímsvötn and Skaftárkatlar are high in the accumulation zone.

Table I. Melt water drainage to selected rivers in 2010_11.

Water Catchment:	**Area (km^2)**	**ΣQ_s ($10^6 m^3$)**	**Q_s ($m^3 s^{-1}$)**	**Q_a ($m^3 s^{-1}$)**	**q_s ($ls^{-1}km^{-2}$)**
Vatnajökull	7968,0	15980,5	1516,06	506,74	63,60
Tungnaá	121,8	559,4	53,07	17,74	145,64
Sylgja	39,7	174	16,51	5,52	138,98
Kaldakvísl	367,9	972,4	92,25	30,83	83,81
Jökulsá á Fjöllum	1188,3	1609,9	152,73	51,05	42,96
Kreppa	291,2	295,1	28,00	9,36	32,13
Kverká	47,0	148,8	14,12	4,72	100,39
Jökulsa a Brú	1214,8	1530,8	145,23	48,54	39,96
Jökulsá á Fljótsdal	130,6	190,8	18,10	6,05	46,33
Jökulsá í Lóni	101,3	202,5	19,21	6,42	63,39
Hornafjarðarfljót	239,1	491,3	46,61	15,58	65,16
Jökulsá á Breiðamerkursandi	739,5	1721	163,27	54,57	73,80
Breiðá-Fjallsá	234,6	869,1	82,45	27,56	117,47
Skeiðará-Gígja	1165,2	2572,6	244,06	81,58	70,01
Súla	255,8	411,8	39,07	13,06	51,05
Brunná	35,8	190,8	18,10	6,05	169,00
Djúpá	83,7	186,3	17,67	5,91	70,58
Hverfisfljót	317,7	561,2	53,24	17,80	56,01
Skaftá	394,9	1335,1	126,66	42,34	107,21
Grímsvötn	173,3	202,3	19,19	6,41	37,02
Eystri Skaftárketill	39,4	59,9	5,68	1,90	48,21
Vestari Skaftárketill	25,1	37,5	3,56	1,19	47,38
Hólmsá	164,9	371,8	35,27	11,79	71,50
Heinabergsvötn	229,6	586,6	55,65	18,60	81,01
Skjálfandafljót	71,9	75,9	7,20	2,41	33,47

ΣQ_s: total summer melt water; Q_s : average runoff (averaged over summer, 4 months, June – September)
Q_a : average runoff (averaged over a whole year); q_s : average runoff per km^2 (averaged over a whole year)

6. Conclusions

The winter snow accumulation 2010_11 was 29% over the average during the survey period.
On Vatnajökull the summer 2011 was short, June was cold and winter turned on early just after mid-August. However the Grímsvötn eruption in late May deposited tephra all over the glacier, extremely thick south of Grímsvötn (up to a few m), a substantial amount in a section NNW (~ mm - cm) of Grímsvötn but a thin layer elsewhere. East of Grímsvötn the tephra was covered with fresh snow most of May and June and ablation rates were very low. On western Vatnajökull the tephra cover greatly enhanced melting in May and June, especially in the accumulation zone of Tungnaárjökull, Sylgjujökull and Köldukvíslarjökull. However in a ~420 km^2 area south of Grímsvötn nothing melted due to the thick tephra cover (thicker than a few cm). In July the tephra became visible all over Vatnajökull, enhancing melt rates everywhere. The high melt rates in the west compensated for the low melt rates elsewhere.

The winter balance (15.56 km^3) was higher than average by 29% (over the observation period 1991_92-2009_10). The summer ablation (-15.83 km^3) was ~2% less than average over the survey period. The net balance was almost zero, negative by only -0.17 km^3 (-0.02m_{we}).
The accumulation area ratio was 63% for the total glacier (close to the text book values for zero balance).
Although the glacial year of 2010_11 was the 17th in a row with negative mass balance for Vatnajökull (since 1994_95) the measured mass loss this year is less than the estimated survey error limits (~0.3 m_{we}).
The close to zero net balance is explained by excessive winter balance and short summer; however without the Grímsvötn tephra net balance would have been positive to a degree not seen since the early 1990's.

Summary:

B_w of 15.66 km^3, B_s : -15.83 km^3 and B_n : -0.17 km^3 , AAR = 63%
Specific values:
b_w= 1.97 m, b_s= -1.99, b_n= -0.02 m

Appendix A: Mass balance at measurement sites 2010_11.

b_w: specific winter balance, **b_s**: specific summer balance, **b_n**: specific net balance, **l_a**: new snow in autumn (all in water equivalent).

Site	Position				Elevation	Date	Date	b_w	b_s	b_n	la
	Latitude		Longitude		(m a.s.l.)	in spring	in autumn	(mm)	(mm)	(mm)	(mm)
B09r	64	45,045	16	5,474	765,4	110505	111021	88	-3780	-3692	18
B10r	64	43,685	16	6,701	815,9	110505	111021	305	-3710	-3405	35
B11b	64	40,940	16	10,492	964,9	110505	111021	668	-2670	-2002	35
B12q	64	38,271	16	14,177	1079,8	110505	111021	1290	-1490	-200	77
B13q	64	34,498	16	19,771	1214,6	110506	111020	1720	-930	790	210
B14s	64	31,644	16	24,692	1312,6	110506	111020	1815	-1100	715	224
B15f	64	28,501	16	29,993	1400,9	110506	111020	2344	-910	1434	364
B16s	64	23,570	16	42,054	1525,4	110506	111021	2672	-690	1982	385
B17q	64	36,731	16	28,802	1210,7	110506	111020	1270	-800	470	105
Br1f	64	5,522	16	19,484	127,3	110501	111001	-1910	-10190	-12100	0
Br2	64	6,418	16	22,551	252,1	110501	111001	-1100	-6800	-7900	0
Br3	64	8,549	16	24,166	415,0	110501	111001	350	-6000	-5650	0
Br7o	64	22,143	16	16,917	1247,6	110511	111020	2490	-1404	1086	193
B07q	64	25,796	16	17,434	1357,4	110511	111020	2610	-1060	1550	340
BB0p	64	22,720	16	5,056	1519,7	110503	111019	3205	-160	3045	595
B19o	64	27,931	15	55,169	1430,2	110504	111019	3058	80	3138	602
B18o	64	31,571	16	0,134	1311,4	110505	111020	2203	-477	1726	378
gb2c	64	34,079	16	0,017	1199,7	110505	111020	1960	-868	1092	172
Budp	64	35,994	15	59,909	1134,1	110505	111020	1556	-1200	356	133
Brup	64	40,99	15	55,22	785,2	110505	111020	225	-3533	-3308	35
D05o	64	42,223	16	54,631	1201,8	110507	111021	827	-1772	-945	53
D07o	64	38,294	16	59,257	1368,1	110507	111021	1800	-1488	312	168
D09n	64	31,803	17	0,568	1579,7	110507	111021	2610	-470	2140	382
D12o	64	28,989	17	0,138	1647,6	110507	111021	2465	-750	1715	546
E01p	64	41,515	15	33,408	687,2	110504	111020	110	-4650	-4540	35
E02p	64	39,134	15	35,981	955,8	110504	111020	1331	-2600	-1269	158
E03virq	64	36,647	15	36,909	1187,1	110504	111020	2481	-660	1821	175
E04p	64	34,943	15	37,076	1287,6	110504	111020	3246	-160	3086	105
Hof01i	64	32,332	15	35,850	1140,5	110504	111019	3328	-1610	1718	147
Hosp1g	64	25,834	15	28,680	75,6	110501	111001	-1850	-8700	-10550	0
K01r	64	35,266	17	52,350	1021,4	110510	111024	1400	-4770	-3370	18
K02s	64	34,828	17	49,700	1180,7	110510	111024	1340	-2840	-1500	88
K03r	64	34,248	17	46,386	1300,7	110510	111024	1690	-3976	-2286	70
K04rors	64	33,210	17	42,239	1492,4	110510	111024	1902	-2660	-758	
K05s	64	33,4631	17	35,475	1681,6	110510	111024	2262	-1870	392	350
K06	64	38,3517	17	31,368	1968,0	110531	111024	2467	-120	2347	581
K07n	64	29,1228	17	42,084	1535,7	110510	111024	2501	-1010	1491	
S01g	64	7,00113	17	49,997	751,3	110509	111023	1110	-5470	-4360	53
S02j	64	12,143	17	49,038	1012,7	110509	111023	2107	-4648	-2541	161
S04k	64	16,2048	17	48,244	1162,8	110509	111023	2220	-3930	-1710	

T01nn	64	19,485	18	8,228	762,0	110509	111023	629	-5742	-5113	0
T02nn	64	19,612	18	3,955	950,1	110509	111023	1844	-4891	-3047	35
T03nn	64	20,193	17	58,631	1080,3	110508	111023	1660	-4010	-2350	140
T04nn	64	21,343	17	51,562	1224,7	110508	111023	1880	-4450	-2570	
T05nm	64	22,302	17	42,962	1345,5	110508	111023	2365	-2510	-145	70
T06nn	64	24,27	17	36,63	1459,0	110508	111024	2717	-1046	1671	630
T07nl	64	25,316	17	31,114	1564,2	110508	111024	2635	-560	2075	368
T08nn	64	26,303	17	27,799	1636,4	110508	111023	2335	-1500	835	175
BORTHNb	64	25,111	17	19,148	1399,0	110508	111023	2295	-2150	145	350
BOR	64	24,937	17	20,156	1402,3	110531	111023	2781	-1180	1601	312
G02	64	26,859	17	17,716	1561,2	110531	111023	2350	-1450	900	210
G03	64	28,4459	17	16,3507	1655,2	110531	111023	2727	-1026	1701	438
G04p	64	29,9979	17	14,9831	1685,4	110507	111023	2510	-680	1830	424
Go1	64	34,0047	17	24,9437	1757,6	110531	111024	2513	-1420	1093	266
Skf01b	64	18,0080	16	5,0160	1284,1	110503	111019	3650	-1550	2100	350
Fl01b	64	25,9889	15	55,3522	1330,0	110504	111019	3475	-580	2895	413
Oer	63	59,7900	16	39,0400	1830,0	110430		5192	2329	7521	

Appendix B: Balance distribution by elevation in 2010_11.

ΔS : area in elevation range, $\sum\Delta S$: cumulative area above given elevation, b_w: specific winter balance, b_s: specific summer balance. b_n: specific winter balance, ΔB_w : winter balance at a given elevation range, $\sum\Delta B_w$: cumulative winter balance above given elevation, ΔB_s summer balance at a given elevation range, $\sum\Delta B_s$: cumulative summer balance above given elevation, ΔB_n: net annual balance in a given elevation range, $\sum B_n$: cumulative net annual balance above given elevation.

Vatnajökull

Elevation (m a.s.l.)			ΔS (km^2)	$\sum\Delta S$ (km^2)	b_w (mm)	b_s (mm)	b_n (mm)	ΔB_w ($10^6 m^3$)	$\sum\Delta B_w$ ($10^6 m^3$)	ΔB_s ($10^6 m^3$)	$\sum\Delta B_s$ ($10^6 m^3$)	ΔB_n ($10^6 m^3$)	$\sum B_n$ ($10^6 m^3$)
2000	2050	2025	0,5	0,5	4678	2273	6952	2,2	2	1,1	1	3,3	3
1950	2000	1975	16,3	16,8	2705	258	2963	44,1	46	4,2	5	48,4	52
1900	1950	1925	44,6	61,4	2604	-70	2533	116,2	163	-3,1	2	113,1	165
1850	1900	1875	35,8	97,2	2910	51	2962	104,5	267	1,8	4	106,3	271
1800	1850	1825	40,4	137,6	3210	321	3531	129,8	397	13,0	17	142,9	414
1750	1800	1775	55,5	193,1	2867	-367	2500	159,8	557	-20,5	-4	139,3	553
1700	1750	1725	102,5	295,6	2666	-870	1796	274,0	831	-89,4	-93	184,6	738
1650	1700	1675	223,9	519,5	2612	-820	1792	585,5	1416	-183,8	-277	401,7	1140
1600	1650	1625	355,2	874,7	2606	-692	1913	926,2	2342	-246,1	-523	680,1	1820
1550	1600	1575	355,7	1230,4	2627	-720	1907	935,0	3277	-256,2	-779	678,8	2498
1500	1550	1525	418,4	1648,8	2594	-752	1842	1086,1	4364	-315,0	-1094	771,1	3270
1450	1500	1475	450,3	2099,1	2578	-763	1814	1161,8	5525	-344,2	-1438	817,6	4087
1400	1450	1425	502,0	2601,1	2580	-815	1764	1296,3	6822	-409,9	-1848	886,4	4974
1350	1400	1375	537,1	3138,2	2511	-922	1588	1349,8	8172	-496,1	-2344	853,8	5827
1300	1350	1325	549,0	3687,2	2363	-1127	1236	1299,4	9471	-619,8	-2964	679,6	6507
1250	1300	1275	518,8	4206,0	2258	-1268	989	1173,8	10645	-659,4	-3623	514,4	7021
1200	1250	1225	463,8	4669,8	2073	-1532	541	964,1	11609	-712,2	-4336	251,9	7273
1150	1200	1175	411,2	5081,0	1899	-1817	82	783,7	12393	-749,6	-5085	34,1	7307
1100	1150	1125	367,9	5448,9	1813	-2035	-221	669,4	13062	-751,2	-5837	-81,9	7225
1050	1100	1075	331,3	5780,2	1726	-2321	-594	574,1	13636	-771,9	-6609	-197,9	7027
1000	1050	1025	306,2	6086,4	1599	-2585	-985	492,0	14128	-795,1	-7404	-303,1	6724
950	1000	975	278,9	6365,3	1472	-2883	-1411	412,2	14540	-807,2	-8211	-395,0	6329
900	950	925	239,7	6605,0	1356	-3109	-1753	326,8	14867	-749,2	-8960	-422,4	5907
850	900	875	216,1	6821,1	1202	-3341	-2138	261,4	15128	-726,1	-9686	-464,7	5442
800	850	825	197,8	7018,9	1056	-3681	-2624	210,7	15339	-734,1	-10420	-523,4	4919
750	800	775	170,7	7189,6	894	-4138	-3244	153,0	15492	-708,2	-11128	-555,2	4364
700	750	725	135,1	7324,7	861	-4545	-3684	116,8	15609	-616,4	-11745	-499,5	3864
650	700	675	101,6	7426,3	831	-4719	-3888	84,8	15694	-481,5	-12226	-396,7	3467
600	650	625	70,3	7496,6	897	-5114	-4217	63,5	15757	-361,5	-12588	-298,0	3169
550	600	575	63,4	7560,0	866	-5400	-4534	55,4	15813	-345,3	-12933	-289,9	2879
500	550	525	44,7	7604,7	743	-5692	-4948	33,6	15846	-257,3	-13190	-223,7	2656
450	500	475	41,4	7646,1	626	-5927	-5300	26,2	15872	-247,8	-13438	-221,6	2434
400	450	425	44,4	7690,5	444	-6201	-5757	20,0	15892	-278,5	-13717	-258,5	2176
350	400	375	40,6	7731,1	94	-6567	-6473	3,9	15896	-270,7	-13987	-266,8	1909
300	350	325	41,1	7772,2	-345	-6908	-7253	-14,4	15882	-288,0	-14275	-302,4	1607
250	300	275	40,4	7812,6	-748	-7382	-8131	-30,6	15851	-301,3	-14577	-331,9	1275
200	250	225	37,9	7850,5	-1082	-8067	-9149	-41,4	15810	-308,3	-14885	-349,7	925
150	200	175	31,6	7882,1	-1326	-8986	-10313	-42,3	15768	-286,3	-15171	-328,6	596
100	150	125	32,4	7914,5	-1613	-9877	-11490	-53,0	15715	-324,7	-15496	-377,7	219
50	100	75	24,7	7939,2	-1758	-10457	-12215	-44,6	15670	-265,1	-15761	-309,7	-91
0	50	25	6,1	7945,3	-2144	-11186	-13330	-13,9	15656	-72,7	-15834	-86,6	-178

Tungnaárjökull

Elevation (m a.s.l.)			ΔS (km^2)	∑ΔS (km^2)	b_w (mm)	b_s (mm)	b_n (mm)	ΔB_w ($10^6 m^3$)	$\sum\Delta B_w$ ($10^6 m^3$)	ΔB_s ($10^6 m^3$)	$\sum\Delta B_s$ ($10^6 m^3$)	ΔB_n ($10^6 m^3$)	$\sum B_n$ ($10^6 m^3$)
1650	1700	1675	2,4	2,4	2383	-1332	1050	5,6	6	-3,2	-3	2,5	3
1600	1650	1625	13,2	15,6	2450	-1179	1270	32,3	38	-15,5	-19	16,7	19
1550	1600	1575	15,3	30,9	2593	-1340	1253	39,6	78	-20,5	-39	19,1	38
1500	1550	1525	15,3	46,2	2693	-1350	1342	41,2	119	-20,6	-60	20,5	59
1450	1500	1475	18,5	64,7	2685	-1416	1269	49,6	168	-26,2	-86	23,4	82
1400	1450	1425	23,3	88,0	2587	-1550	1036	60,3	229	-36,2	-122	24,2	107
1350	1400	1375	21,7	109,7	2425	-2029	396	52,5	281	-44,0	-166	8,6	115
1300	1350	1325	28,1	137,8	2186	-2896	-710	61,3	342	-81,3	-247	-19,9	95
1250	1300	1275	21,8	159,6	2023	-3596	-1573	44,1	387	-78,5	-326	-34,3	61
1200	1250	1225	24,0	183,6	1902	-4319	-2417	45,7	432	-103,8	-430	-58,1	3
1150	1200	1175	21,0	204,6	1832	-4462	-2629	38,4	471	-93,5	-523	-55,1	-52
1100	1150	1125	19,2	223,8	1739	-4197	-2457	33,5	504	-80,8	-604	-47,3	-100
1050	1100	1075	20,0	243,8	1705	-4074	-2368	34,1	538	-81,5	-685	-47,4	-147
1000	1050	1025	18,2	262,0	1640	-4361	-2720	29,8	568	-79,3	-765	-49,5	-197
950	1000	975	18,9	280,9	1496	-4758	-3261	28,3	596	-89,9	-855	-61,6	-258
900	950	925	15,2	296,1	1333	-5019	-3685	20,2	617	-76,2	-931	-55,9	-314
850	900	875	15,1	311,2	1178	-5197	-4018	17,8	634	-78,4	-1009	-60,6	-375
800	850	825	14,1	325,3	965	-5392	-4427	13,6	648	-75,9	-1085	-62,3	-437
750	800	775	10,3	335,6	776	-5629	-4853	8,0	656	-57,8	-1143	-49,8	-487
700	750	725	7,1	342,7	652	-5916	-5264	4,7	661	-42,3	-1185	-37,6	-525
650	700	675	1,6	344,3	636	-6135	-5498	1,1	662	-10,3	-1195	-9,2	-534
600	650	625	0,0	344,3	629	-6341	-5712	0,0	662	-0,4	-1196	-0,3	-534

Sylgjujökull

Elevation (m a.s.l.)			ΔS (km^2)	∑ΔS (km^2)	b_w (mm)	b_s (mm)	b_n (mm)	ΔB_w ($10^6 m^3$)	$\sum\Delta B_w$ ($10^6 m^3$)	ΔB_s ($10^6 m^3$)	$\sum\Delta B_s$ ($10^6 m^3$)	ΔB_n ($10^6 m^3$)	$\sum B_n$ ($10^6 m^3$)
1600	1650	1625	2,0	2,0	2527	-1544	983	5,1	5	-3,1	-3	2,0	2
1550	1600	1575	6,8	8,8	2578	-1461	1117	17,4	23	-9,9	-13	7,5	10
1500	1550	1525	18,9	27,7	2603	-1317	1285	49,1	72	-24,8	-38	24,3	34
1450	1500	1475	12,3	40,0	2600	-1667	933	32,0	104	-20,5	-58	11,5	45
1400	1450	1425	8,2	48,2	2540	-2290	249	20,9	125	-18,8	-77	2,1	47
1350	1400	1375	5,1	53,3	2394	-2661	-267	12,2	137	-13,5	-91	-1,4	46
1300	1350	1325	5,3	58,6	2083	-3259	-1175	11,0	148	-17,2	-108	-6,2	40
1250	1300	1275	10,4	69,0	1895	-3957	-2062	19,6	167	-41,0	-149	-21,3	18
1200	1250	1225	12,6	81,6	1782	-4329	-2546	22,4	190	-54,4	-203	-32,0	-14
1150	1200	1175	14,4	96,0	1654	-4429	-2774	23,8	213	-63,6	-267	-39,9	-54
1100	1150	1125	13,2	109,2	1532	-4296	-2764	20,2	234	-56,6	-324	-36,4	-90
1050	1100	1075	13,4	122,6	1425	-4136	-2710	19,1	253	-55,4	-379	-36,3	-126
1000	1050	1025	9,3	131,9	1342	-4338	-2996	12,5	265	-40,3	-419	-27,8	-154
950	1000	975	3,1	135,0	1276	-4616	-3339	3,9	269	-14,1	-433	-10,2	-164
900	950	925	1,6	136,6	1213	-4937	-3724	1,9	271	-7,9	-441	-6,0	-170
850	900	875	0,2	136,8	1157	-5159	-4001	0,2	271	-0,9	-442	-0,7	-171

Köldukvíslarjökul

Elevation (m a.s.l.)			ΔS (km^2)	∑ΔS (km^2)	b_w (mm)	b_s (mm)	b_n (mm)	ΔB_w ($10^6 m^3$)	$\sum\Delta B_w$ ($10^6 m^3$)	ΔB_s ($10^6 m^3$)	$\sum\Delta B_s$ ($10^6 m^3$)	ΔB_n ($10^6 m^3$)	$\sum B_n$ ($10^6 m^3$)
1950	2000	1975	3,6	3,6	2419	1	2420	8,7	9	0,0	0	8,7	9
1900	1950	1925	12,4	16,0	2410	-275	2135	29,9	39	-3,4	-3	26,5	35
1850	1900	1875	5,9	21,9	2376	-715	1660	13,9	53	-4,2	-8	9,7	45
1800	1850	1825	6,0	27,9	2341	-1036	1304	14,0	67	-6,2	-14	7,8	53
1750	1800	1775	10,5	38,4	2388	-1352	1035	25,2	92	-14,2	-28	10,9	64
1700	1750	1725	17,9	56,3	2340	-1613	726	41,8	133	-28,8	-57	13,0	77
1650	1700	1675	15,6	71,9	2271	-1770	501	35,4	169	-27,6	-85	7,8	84
1600	1650	1625	13,8	85,7	2219	-1921	298	30,7	200	-26,5	-111	4,1	89
1550	1600	1575	19,2	104,9	2198	-1957	240	42,3	242	-37,6	-149	4,6	93
1500	1550	1525	20,9	125,8	2230	-1767	463	46,6	288	-36,9	-186	9,7	103
1450	1500	1475	19,3	145,1	2083	-2082	1	40,2	329	-40,2	-226	0,0	103
1400	1450	1425	14,2	159,3	1911	-2628	-716	27,2	356	-37,4	-263	-10,2	93
1350	1400	1375	15,3	174,6	1787	-3188	-1401	27,3	383	-48,7	-312	-21,4	71
1300	1350	1325	17,5	192,1	1696	-3617	-1921	29,7	413	-63,3	-375	-33,6	38
1250	1300	1275	18,0	210,1	1593	-3611	-2018	28,8	442	-65,4	-441	-36,5	1
1200	1250	1225	18,3	228,4	1471	-3203	-1732	26,9	469	-58,6	-499	-31,7	-31
1150	1200	1175	16,4	244,8	1360	-3006	-1646	22,3	491	-49,3	-549	-27,0	-58
1100	1150	1125	14,9	259,7	1304	-3445	-2140	19,5	510	-51,5	-600	-32,0	-90
1050	1100	1075	13,1	272,8	1260	-4185	-2924	16,6	527	-55,1	-655	-38,5	-128
1000	1050	1025	11,1	283,9	1205	-4757	-3552	13,4	540	-52,9	-708	-39,5	-168
950	1000	975	10,5	294,4	1141	-5087	-3945	12,0	552	-53,3	-761	-41,4	-209
900	950	925	5,6	300,0	1097	-5265	-4168	6,2	559	-29,5	-791	-23,4	-232
850	900	875	0,5	300,5	1047	-5419	-4371	0,6	559	-2,9	-794	-2,4	-235

Dyngjujökull

Elevation (m a.s.l.)			ΔS (km^2)	∑ΔS (km^2)	b_w (mm)	b_s (mm)	b_n (mm)	ΔB_w ($10^6 m^3$)	$\sum\Delta B_w$ ($10^6 m^3$)	ΔB_s ($10^6 m^3$)	$\sum\Delta B_s$ ($10^6 m^3$)	ΔB_n ($10^6 m^3$)	$\sum B_n$ ($10^6 m^3$)
1950	2000	1975	7,4	7,4	2465	-49	2415	18,2	18	-0,4	0	17,9	18
1900	1950	1925	23,2	30,6	2459	-259	2199	56,9	75	-6,0	-6	50,9	69
1850	1900	1875	15,9	46,5	2465	-538	1926	39,3	115	-8,6	-15	30,7	100
1800	1850	1825	9,7	56,2	2492	-558	1934	24,3	139	-5,4	-20	18,8	118
1750	1800	1775	16,0	72,2	2499	-688	1810	39,9	179	-11,0	-31	28,9	147
1700	1750	1725	27,3	99,5	2515	-675	1840	68,6	247	-18,4	-50	50,1	198
1650	1700	1675	71,6	171,1	2540	-603	1936	181,8	429	-43,2	-93	138,6	336
1600	1650	1625	114,0	285,1	2525	-544	1980	287,9	717	-62,1	-155	225,8	562
1550	1600	1575	94,7	379,8	2507	-496	2010	237,5	955	-47,1	-202	190,4	752
1500	1550	1525	89,7	469,5	2413	-588	1824	216,3	1171	-52,8	-255	163,6	916
1450	1500	1475	75,1	544,6	2273	-804	1468	170,7	1342	-60,4	-315	110,2	1026
1400	1450	1425	61,4	606,0	2113	-1091	1021	129,7	1471	-67,0	-382	62,7	1089
1350	1400	1375	49,4	655,4	1919	-1392	527	94,8	1566	-68,8	-451	26,1	1115
1300	1350	1325	37,9	693,3	1691	-1557	133	64,1	1630	-59,1	-510	5,1	1120
1250	1300	1275	41,3	734,6	1429	-1628	-198	59,1	1689	-67,3	-578	-8,2	1112
1200	1250	1225	48,8	783,4	1126	-1727	-600	55,0	1745	-84,4	-662	-29,4	1083
1150	1200	1175	48,2	831,6	869	-1948	-1078	42,0	1786	-94,0	-756	-52,1	1030
1100	1150	1125	44,0	875,6	778	-2252	-1473	34,3	1821	-99,2	-855	-64,9	966
1050	1100	1075	33,1	908,7	718	-2535	-1816	23,8	1845	-84,1	-939	-60,2	905
1000	1050	1025	35,5	944,2	622	-2806	-2184	22,2	1867	-100,1	-1039	-77,9	827
950	1000	975	30,8	975,0	488	-3107	-2619	15,0	1882	-95,8	-1135	-80,8	747
900	950	925	25,6	1000,6	306	-3452	-3145	7,9	1890	-89,1	-1224	-81,2	665
850	900	875	24,9	1025,5	131	-3783	-3651	3,3	1893	-96,1	-1320	-92,7	573
800	850	825	19,7	1045,2	-4	-4056	-4061	0,0	1893	-82,1	-1403	-82,2	491
750	800	775	15,2	1060,4	-83	-4237	-4321	-1,3	1892	-64,2	-1467	-65,5	425
700	750	725	1,7	1062,1	-109	-4295	-4405	-0,2	1892	-7,5	-1474	-7,7	417

Brúarjökull

Elevation (m a.s.l.)			ΔS (km^2)	∑ΔS (km^2)	b_w (mm)	b_s (mm)	b_n (mm)	ΔB_w ($10^6 m^3$)	$\sum\Delta B_w$ ($10^6 m^3$)	ΔB_s ($10^6 m^3$)	$\sum\Delta B_s$ ($10^6 m^3$)	ΔB_n ($10^6 m^3$)	$\sum B_n$ ($10^6 m^3$)
1850	1900	1875	0,8	0,8	2511	-98	2412	2,2	2	0,0	0	2,1	2
1800	1850	1825	4,2	5,0	2595	-28	2567	10,8	13	-0,1	0	10,7	13
1750	1800	1775	3,0	8,0	2594	-132	2462	7,7	21	-0,4	-1	7,3	20
1700	1750	1725	3,7	11,7	2541	-308	2233	9,5	30	-1,2	-2	8,4	28
1650	1700	1675	5,3	17,0	2516	-393	2123	13,3	43	-2,1	-4	11,2	40
1600	1650	1625	44,4	61,4	2558	-590	1968	113,7	157	-26,2	-30	87,5	127
1550	1600	1575	47,6	109,0	2636	-648	1987	125,6	283	-30,9	-61	94,7	222
1500	1550	1525	69,8	178,8	2634	-705	1928	184,0	467	-49,3	-110	134,7	357
1450	1500	1475	73,9	252,7	2574	-759	1815	190,4	657	-56,1	-166	134,3	491
1400	1450	1425	108,1	360,8	2604	-663	1941	281,6	939	-71,7	-238	209,9	701
1350	1400	1375	148,2	509,0	2461	-698	1763	365,1	1304	-103,6	-342	261,5	962
1300	1350	1325	151,3	660,3	2166	-763	1402	327,9	1632	-115,6	-457	212,3	1174
1250	1300	1275	144,8	805,1	2008	-738	1270	290,9	1923	-106,9	-564	184,0	1358
1200	1250	1225	121,8	926,9	1827	-834	992	222,6	2145	-101,7	-666	120,9	1479
1150	1200	1175	105,8	1032,7	1618	-1024	593	171,3	2317	-108,4	-774	62,8	1542
1100	1150	1125	86,8	1119,5	1441	-1266	175	125,1	2442	-109,9	-884	15,2	1557
1050	1100	1075	73,3	1192,8	1270	-1578	-308	93,2	2535	-115,8	-1000	-22,6	1535
1000	1050	1025	65,6	1258,4	1022	-1956	-934	67,1	2602	-128,5	-1129	-61,3	1473
950	1000	975	59,4	1317,8	785	-2353	-1568	46,6	2649	-139,7	-1268	-93,1	1380
900	950	925	48,9	1366,7	600	-2714	-2113	29,4	2678	-132,7	-1401	-103,4	1277
850	900	875	44,9	1411,6	454	-3102	-2647	20,4	2698	-139,2	-1540	-118,8	1158
800	850	825	41,4	1453,0	324	-3456	-3132	13,4	2712	-143,0	-1683	-129,6	1029
750	800	775	36,1	1489,1	195	-3680	-3484	7,1	2719	-132,9	-1816	-125,8	903
700	750	725	23,8	1512,9	107	-3764	-3656	2,6	2721	-89,4	-1906	-86,8	816
650	700	675	12,8	1525,7	49	-3848	-3799	0,6	2722	-49,2	-1955	-48,5	767
600	650	625	0,3	1526,0	33	-3846	-3813	0,0	2722	-1,3	-1956	-1,3	766

Eyjabakkajökull

Elevation (m a.s.l.)			ΔS (km^2)	∑ΔS (km^2)	b_w (mm)	b_s (mm)	b_n (mm)	ΔB_w ($10^6 m^3$)	$\sum\Delta B_w$ ($10^6 m^3$)	ΔB_s ($10^6 m^3$)	$\sum\Delta B_s$ ($10^6 m^3$)	ΔB_n ($10^6 m^3$)	$\sum B_n$ ($10^6 m^3$)
1550	1600	1575	0,0	0,0	3778	35	3813	0,0	0	0,0	0	0,0	0
1500	1550	1525	0,0	0,0	3800	50	3850	0,3	0	0,0	0	0,3	0
1450	1500	1475	1,0	1,0	3680	31	3711	3,6	4	0,0	0	3,6	4
1400	1450	1425	1,8	2,8	3622	4	3626	6,7	11	0,0	0	6,7	11
1350	1400	1375	2,5	5,3	3474	-53	3421	8,8	19	-0,1	0	8,7	19
1300	1350	1325	3,9	9,2	3241	-130	3110	12,7	32	-0,5	-1	12,2	32
1250	1300	1275	13,4	22,6	3009	-263	2745	40,2	72	-3,5	-4	36,7	68
1200	1250	1225	13,3	35,9	2674	-544	2129	35,6	108	-7,2	-11	28,4	97
1150	1200	1175	14,7	50,6	2268	-916	1351	33,3	141	-13,5	-25	19,9	116
1100	1150	1125	12,3	62,9	1937	-1257	680	23,8	165	-15,4	-40	8,3	125
1050	1100	1075	10,6	73,5	1732	-1599	132	18,3	183	-16,9	-57	1,4	126
1000	1050	1025	10,1	83,6	1522	-1946	-424	15,4	199	-19,7	-77	-4,3	122
950	1000	975	7,7	91,3	1298	-2333	-1034	10,0	209	-18,1	-95	-8,0	114
900	950	925	5,2	96,5	1073	-2670	-1597	5,6	214	-13,9	-109	-8,3	106
850	900	875	3,9	100,4	885	-2951	-2066	3,5	218	-11,5	-120	-8,1	98
800	850	825	3,2	103,6	678	-3298	-2619	2,1	220	-10,4	-131	-8,3	89
750	800	775	3,4	107,0	450	-3713	-3262	1,5	222	-12,5	-143	-11,0	78
700	750	725	3,3	110,3	280	-4243	-3963	0,9	222	-14,0	-157	-13,1	65
650	700	675	1,7	112,0	163	-4615	-4452	0,3	223	-7,8	-165	-7,6	58

Hoffellsjökull

Elevation (m a.s.l.)			ΔS (km^2)	∑ΔS (km^2)	b_w (mm)	b_s (mm)	b_n (mm)	ΔB_w ($10^6 m^3$)	$\sum\Delta B_w$ ($10^6 m^3$)	ΔB_s ($10^6 m^3$)	$\sum\Delta B_s$ ($10^6 m^3$)	ΔB_n ($10^6 m^3$)	$\sum B_n$ ($10^6 m^3$)
1450	1500	1475	0,9	0,9	3714	38	3753	3,4	3	0,0	0	3,5	4
1400	1450	1425	6,7	7,6	3342	-58	3284	22,4	26	-0,4	0	22,0	26
1350	1400	1375	10,0	17,6	3247	-105	3141	32,4	58	-1,1	-1	31,3	57
1300	1350	1325	15,4	33,0	3169	-195	2973	48,7	107	-3,0	-4	45,7	103
1250	1300	1275	33,6	66,6	3118	-352	2765	104,6	212	-11,8	-16	92,8	195
1200	1250	1225	26,8	93,4	3232	-815	2417	86,6	298	-21,9	-38	64,8	260
1150	1200	1175	18,2	111,6	3275	-1354	1920	59,6	358	-24,7	-63	35,0	295
1100	1150	1125	17,5	129,1	3193	-1728	1464	55,8	414	-30,2	-93	25,6	321
1050	1100	1075	13,6	142,7	2943	-2141	801	39,9	454	-29,1	-122	10,9	332
1000	1050	1025	10,0	152,7	2702	-2513	189	27,0	481	-25,1	-147	1,9	333
950	1000	975	9,0	161,7	2487	-2892	-405	22,4	503	-26,1	-173	-3,7	330
900	950	925	6,4	168,1	2315	-3204	-888	14,9	518	-20,6	-194	-5,7	324
850	900	875	4,3	172,4	2179	-3433	-1254	9,4	527	-14,9	-209	-5,4	319
800	850	825	3,5	175,9	2059	-3636	-1577	7,4	535	-13,1	-222	-5,7	313
750	800	775	3,8	179,7	1902	-3888	-1985	7,4	542	-15,1	-237	-7,7	305
700	750	725	3,8	183,5	1680	-4173	-2492	6,4	549	-16,0	-253	-9,5	296
650	700	675	3,4	186,9	1417	-4523	-3105	4,8	553	-15,2	-268	-10,4	285
600	650	625	2,5	189,4	1115	-4946	-3830	2,8	556	-12,2	-280	-9,5	276
550	600	575	1,8	191,2	812	-5325	-4512	1,5	558	-9,7	-290	-8,2	268
500	550	525	1,5	192,7	615	-5673	-5058	0,9	558	-8,4	-298	-7,5	260
450	500	475	0,9	193,6	494	-6037	-5543	0,5	559	-5,6	-304	-5,2	255
400	450	425	0,9	194,5	360	-6408	-6047	0,3	559	-6,1	-310	-5,7	249
350	400	375	0,6	195,1	189	-6766	-6576	0,1	559	-4,0	-314	-3,9	245
300	350	325	0,9	196,0	-34	-7162	-7197	0,0	559	-6,5	-321	-6,5	239
250	300	275	2,1	198,1	-344	-7571	-7915	-0,7	559	-16,4	-337	-17,2	222
200	250	225	3,3	201,4	-663	-7718	-8381	-2,2	556	-25,2	-362	-27,4	194
150	200	175	2,6	204,0	-922	-7971	-8893	-2,4	554	-20,7	-383	-23,1	171
100	150	125	2,1	206,1	-1245	-8375	-9621	-2,7	551	-17,8	-401	-20,5	151
50	100	75	2,8	208,9	-1710	-9621	-11332	-4,8	547	-26,9	-428	-31,7	119
0	50	25	0,5	209,4	-1896	-9935	-11832	-1,1	546	-5,6	-433	-6,6	112

Breiðamerkurjökull

Elevation (m a.s.l.)			ΔS (km^2)	∑ΔS (km^2)	b_w (mm)	b_s (mm)	b_n (mm)	ΔB_w ($10^6 m^3$)	$\sum\Delta B_w$ ($10^6 m^3$)	ΔB_s ($10^6 m^3$)	$\sum\Delta B_s$ ($10^6 m^3$)	ΔB_n ($10^6 m^3$)	$\sum B_n$ ($10^6 m^3$)
1900	1950	1925	0,0	0,0	5305	2465	7770	0,2	0	0,0	0	0,3	0
1850	1900	1875	0,4	0,4	5305	2458	7764	1,9	2	0,9	1	2,8	3
1800	1850	1825	0,4	0,8	5200	2364	7565	2,3	5	1,1	2	3,4	7
1750	1800	1775	0,8	1,6	4962	2099	7062	4,1	9	1,7	4	5,8	12
1700	1750	1725	2,5	4,1	4073	845	4918	10,1	19	2,1	6	12,1	25
1650	1700	1675	5,8	9,9	3482	-23	3459	20,1	39	-0,1	6	19,9	44
1600	1650	1625	15,8	25,7	3268	-315	2952	51,6	90	-5,0	1	46,6	91
1550	1600	1575	25,7	51,4	3014	-473	2540	77,5	168	-12,2	-12	65,3	156
1500	1550	1525	32,2	83,6	2751	-589	2161	88,5	256	-19,0	-30	69,5	226
1450	1500	1475	44,3	127,9	2738	-603	2135	121,2	378	-26,7	-57	94,5	320
1400	1450	1425	58,3	186,2	2688	-691	1996	156,9	534	-40,3	-98	116,5	437
1350	1400	1375	88,7	274,9	2650	-833	1816	235,1	770	-73,9	-171	161,1	598
1300	1350	1325	96,9	371,8	2574	-1064	1510	249,6	1019	-103,2	-275	146,4	744
1250	1300	1275	59,4	431,2	2491	-1292	1199	148,1	1167	-76,8	-351	71,3	816
1200	1250	1225	39,7	470,9	2403	-1521	882	95,4	1263	-60,4	-412	35,0	851
1150	1200	1175	32,6	503,5	2299	-1771	527	75,1	1338	-57,8	-470	17,2	868
1100	1150	1125	27,7	531,2	2170	-2062	107	60,2	1398	-57,2	-527	3,0	871
1050	1100	1075	24,1	555,3	2043	-2312	-268	49,2	1447	-55,7	-582	-6,5	865
1000	1050	1025	22,1	577,4	1920	-2534	-613	42,5	1489	-56,1	-639	-13,6	851
950	1000	975	24,5	601,9	1764	-2807	-1043	43,3	1533	-68,9	-707	-25,6	825
900	950	925	27,3	629,2	1599	-2993	-1394	43,8	1576	-81,9	-789	-38,2	787
850	900	875	26,2	655,4	1439	-3250	-1811	37,7	1614	-85,2	-875	-47,4	740
800	850	825	26,0	681,4	1303	-3520	-2216	34,0	1648	-91,8	-966	-57,8	682
750	800	775	25,3	706,7	1166	-3827	-2661	29,5	1678	-96,7	-1063	-67,3	615
700	750	725	23,9	730,6	1076	-4098	-3022	25,7	1703	-98,0	-1161	-72,3	542
650	700	675	30,8	761,4	974	-4291	-3316	30,1	1733	-132,3	-1293	-102,3	440
600	650	625	26,2	787,6	911	-4571	-3660	23,9	1757	-119,8	-1413	-95,9	344
550	600	575	26,8	814,4	867	-5017	-4149	23,4	1781	-135,4	-1549	-112,0	232
500	550	525	15,6	830,0	865	-5256	-4391	13,6	1794	-82,7	-1631	-69,1	163
450	500	475	16,2	846,2	827	-5625	-4798	13,4	1808	-91,4	-1723	-78,0	85
400	450	425	15,8	862,0	673	-5830	-5157	10,7	1818	-92,6	-1815	-81,9	3
350	400	375	12,9	874,9	235	-5975	-5740	3,1	1822	-77,9	-1893	-74,9	-72
300	350	325	12,9	887,8	-440	-6153	-6593	-5,7	1816	-80,4	-1974	-86,1	-158
250	300	275	12,0	899,8	-1083	-6639	-7723	-13,1	1803	-80,0	-2054	-93,1	-251
200	250	225	11,5	911,3	-1528	-7855	-9384	-17,6	1785	-90,3	-2144	-107,8	-359
150	200	175	8,5	919,8	-1797	-9288	-11085	-15,4	1770	-79,7	-2224	-95,1	-454
100	150	125	7,9	927,7	-1990	-10273	-12264	-15,7	1754	-80,9	-2304	-96,5	-550
50	100	75	6,0	933,7	-2152	-10941	-13094	-13,1	1741	-66,4	-2371	-79,5	-630
0	50	25	2,9	936,6	-2240	-11321	-13561	-6,9	1734	-34,6	-2405	-41,5	-671

Síðujökull

Elevation (m a.s.l.)			ΔS (km^2)	∑ΔS (km^2)	b_w (mm)	b_s (mm)	b_n (mm)	ΔB_w ($10^6 m^3$)	$\sum\Delta B_w$ ($10^6 m^3$)	ΔB_s ($10^6 m^3$)	$\sum\Delta B_s$ ($10^6 m^3$)	ΔB_n ($10^6 m^3$)	$\sum B_n$ ($10^6 m^3$)
1700	1750	1725	0,7	0,7	3314	2	3316	2,5	3	0,0	0	2,5	3
1650	1700	1675	5,2	5,9	2915	15	2930	15,0	18	0,0	0	15,1	18
1600	1650	1625	11,1	17,0	2734	-128	2606	30,4	48	-1,4	-1	29,0	47
1550	1600	1575	10,1	27,1	2802	-154	2648	28,3	76	-1,6	-3	26,7	73
1500	1550	1525	20,1	47,2	2806	-45	2761	56,5	133	-0,9	-4	55,6	129
1450	1500	1475	40,1	87,3	2736	-3	2732	109,7	243	-0,2	-4	109,6	239
1400	1450	1425	26,9	114,2	2662	15	2677	71,5	314	0,4	-4	72,0	311
1350	1400	1375	21,3	135,5	2574	33	2608	54,9	369	0,7	-3	55,6	366
1300	1350	1325	17,4	152,9	2478	65	2543	43,2	412	1,1	-2	44,3	410
1250	1300	1275	16,6	169,5	2395	-312	2083	39,7	452	-5,2	-7	34,5	445
1200	1250	1225	21,2	190,7	2342	-573	1768	49,6	501	-12,2	-19	37,5	482
1150	1200	1175	18,1	208,8	2279	-1461	817	41,3	543	-26,5	-46	14,8	497
1100	1150	1125	17,0	225,8	2236	-2187	49	38,1	581	-37,2	-83	0,8	498
1050	1100	1075	18,0	243,8	2178	-2996	-817	39,2	620	-53,9	-137	-14,7	483
1000	1050	1025	21,8	265,6	2080	-3460	-1380	45,3	665	-75,3	-212	-30,0	453
950	1000	975	21,8	287,4	1908	-4256	-2348	41,7	707	-92,9	-305	-51,3	402
900	950	925	22,1	309,5	1706	-4602	-2896	37,8	745	-101,9	-407	-64,1	338
850	900	875	20,9	330,4	1538	-4928	-3390	32,1	777	-102,9	-510	-70,8	267
800	850	825	25,0	355,4	1355	-5092	-3737	33,9	811	-127,3	-637	-93,4	174
750	800	775	25,5	380,9	1150	-5369	-4218	29,3	840	-136,9	-774	-107,5	66
700	750	725	26,0	406,9	850	-5724	-4874	22,1	862	-148,7	-922	-126,6	-60
650	700	675	15,8	422,7	571	-5949	-5377	9,1	871	-94,2	-1017	-85,1	-146
600	650	625	7,4	430,1	397	-6208	-5811	2,9	874	-46,0	-1063	-43,1	-189
550	600	575	0,2	430,3	319	-6355	-6036	0,0	874	-1,3	-1064	-1,3	-190

Skaftárjökull

Elevation (m a.s.l.)			ΔS (km^2)	∑ΔS (km^2)	b_w (mm)	b_s (mm)	b_n (mm)	ΔB_w ($10^6 m^3$)	$\sum\Delta B_w$ ($10^6 m^3$)	ΔB_s ($10^6 m^3$)	$\sum\Delta B_s$ ($10^6 m^3$)	ΔB_n ($10^6 m^3$)	$\sum B_n$ ($10^6 m^3$)
1350	1400	1375	2,4	2,4	2493	-117	2376	6,0	6	-0,3	0	5,8	6
1300	1350	1325	5,5	7,9	2372	-1050	1322	13,0	19	-5,7	-6	7,2	13
1250	1300	1275	4,5	12,4	2260	-2402	-142	10,2	29	-10,8	-17	-0,6	12
1200	1250	1225	6,5	18,9	2193	-3371	-1177	14,2	43	-21,8	-39	-7,6	5
1150	1200	1175	9,3	28,2	2118	-4253	-2134	19,6	63	-39,3	-78	-19,7	-15
1100	1150	1125	12,3	40,5	2054	-4441	-2386	25,2	88	-54,4	-132	-29,2	-44
1050	1100	1075	14,2	54,7	2011	-4182	-2171	28,5	117	-59,3	-192	-30,8	-75
1000	1050	1025	12,1	66,8	1938	-4286	-2348	23,5	140	-51,9	-244	-28,4	-103
950	1000	975	7,6	74,4	1828	-4776	-2948	13,9	154	-36,3	-280	-22,4	-126
900	950	925	5,3	79,7	1684	-5060	-3375	9,0	163	-26,9	-307	-18,0	-144
850	900	875	5,6	85,3	1511	-5236	-3724	8,4	171	-29,1	-336	-20,7	-165
800	850	825	5,7	91,0	1299	-5423	-4124	7,6	179	-31,7	-368	-24,1	-189
750	800	775	5,1	96,1	1127	-5575	-4447	5,8	185	-28,6	-396	-22,8	-211
700	750	725	3,6	99,7	912	-5769	-4856	3,2	188	-20,5	-417	-17,3	-229
650	700	675	2,8	102,5	802	-5855	-5052	2,3	190	-16,5	-433	-14,2	-243
600	650	625	0,8	103,3	621	-6008	-5386	0,5	191	-4,6	-438	-4,1	-247

Vestari Skaftárketill

Elevation (m a.s.l.)			ΔS (km^2)	∑ΔS (km^2)	b_w (mm)	b_s (mm)	b_n (mm)	ΔB_w ($10^6 m^3$)	$\sum\Delta B_w$ ($10^6 m^3$)	ΔB_s ($10^6 m^3$)	$\sum\Delta B_s$ ($10^6 m^3$)	ΔB_n ($10^6 m^3$)	$\sum B_n$ ($10^6 m^3$)
1900	1950	1925	0,7	0,7	2452	-507	1945	1,7	2	-0,3	0	1,3	1
1850	1900	1875	0,6	1,3	2450	-661	1789	1,4	3	-0,4	-1	1,0	2
1800	1850	1825	0,7	2,0	2452	-861	1590	1,8	5	-0,6	-1	1,2	4
1750	1800	1775	2,7	4,7	2474	-1370	1104	6,7	12	-3,7	-5	3,0	7
1700	1750	1725	5,9	10,6	2488	-1546	941	14,6	26	-9,1	-14	5,5	12
1650	1700	1675	6,7	17,3	2476	-1503	972	16,5	43	-10,0	-24	6,5	19
1600	1650	1625	7,4	24,7	2495	-1515	980	18,5	61	-11,2	-35	7,3	26
1550	1600	1575	5,2	29,9	2540	-1444	1096	13,1	74	-7,5	-43	5,7	32
1500	1550	1525	1,5	31,4	2559	-1399	1160	3,8	78	-2,1	-45	1,7	33

Eystri Skaftárketill

Elevation (m a.s.l.)			ΔS (km^2)	∑ΔS (km^2)	b_w (mm)	b_s (mm)	b_n (mm)	ΔB_w ($10^6 m^3$)	$\sum\Delta B_w$ ($10^6 m^3$)	ΔB_s ($10^6 m^3$)	$\sum\Delta B_s$ ($10^6 m^3$)	ΔB_n ($10^6 m^3$)	$\sum B_n$ ($10^6 m^3$)
1750	1800	1775	1,1	1,1	2494	-1448	1045	2,7	3	-1,6	-2	1,2	1
1700	1750	1725	11,1	12,2	2521	-1549	972	28,1	31	-17,3	-19	10,8	12
1650	1700	1675	16,2	28,4	2476	-1508	968	40,1	71	-24,4	-43	15,7	28
1600	1650	1625	9,2	37,6	2475	-1531	943	22,9	94	-14,2	-57	8,7	36
1550	1600	1575	2,2	39,8	2477	-1542	934	5,5	99	-3,4	-61	2,1	38

Gjálp

Elevation (m a.s.l.)			ΔS (km^2)	∑ΔS (km^2)	b_w (mm)	b_s (mm)	b_n (mm)	ΔB_w ($10^6 m^3$)	$\sum\Delta B_w$ ($10^6 m^3$)	ΔB_s ($10^6 m^3$)	$\sum\Delta B_s$ ($10^6 m^3$)	ΔB_n ($10^6 m^3$)	$\sum B_n$ ($10^6 m^3$)
1900	1950	1925	0,5	0,5	2450	-484	1965	1,3	1	-0,3	0	1,1	1
1850	1900	1875	0,6	1,1	2449	-699	1749	1,5	3	-0,4	-1	1,1	2
1800	1850	1825	1,2	2,3	2459	-938	1520	2,9	6	-1,1	-2	1,8	4
1750	1800	1775	4,5	6,8	2498	-1337	1160	11,3	17	-6,1	-8	5,3	9
1700	1750	1725	15,9	22,7	2554	-1444	1109	40,7	58	-23,0	-31	17,7	27
1650	1700	1675	16,5	39,2	2581	-1293	1288	42,7	101	-21,4	-52	21,3	48
1600	1650	1625	0,0	39,2	2600	-1411	1189	0,0	101	0,0	-52	0,0	48

Grímsvötn

Elevation (m a.s.l.)			ΔS (km^2)	∑ΔS (km^2)	b_w (mm)	b_s (mm)	b_n (mm)	ΔB_w ($10^6 m^3$)	$\sum\Delta B_w$ ($10^6 m^3$)	ΔB_s ($10^6 m^3$)	$\sum\Delta B_s$ ($10^6 m^3$)	ΔB_n ($10^6 m^3$)	$\sum B_n$ ($10^6 m^3$)
1700	1750	1725	0,8	0,8	2593	-927	1666	2,1	2	-0,8	-1	1,4	1
1650	1700	1675	40,8	41,6	2555	-1025	1529	104,4	107	-41,9	-43	62,5	64
1600	1650	1625	30,6	72,2	2446	-1033	1413	75,0	181	-31,7	-74	43,3	107
1550	1600	1575	18,6	90,8	2403	-1201	1201	44,8	226	-22,4	-97	22,4	130
1500	1550	1525	16,9	107,7	2413	-1367	1045	40,7	267	-23,1	-120	17,6	147
1450	1500	1475	11,6	119,3	2467	-1255	1211	28,6	296	-14,5	-134	14,0	161
1400	1450	1425	15,1	134,4	2554	-1105	1448	38,5	334	-16,7	-151	21,8	183
1350	1400	1375	0,6	135,0	2400	-449	1951	1,6	336	-0,3	-151	1,3	184

Appendix C: Coordinates at velocity measurement stakes.

Position of velocity measurement stakes determined by GPS sub-metre differential (I), fast static (FS) and kinematic (K).
(Accuracy of horizontal position 0.5 – 1.0 m, and vertical accuracy 1-2 m for DGPS, about 1cm for fast static, and 3 cm for kinematic).
The station Hofn in Höfn í Hornafirði is used as a stationary reference for all measurements, ÍSN93 datum, h_l is elevation above ellipsoid, dL antenna height, N estimated difference between ellipsoid and sea-level, H elevation in metres above sea level (H= h_l+N+dL). X and Y are ÍSN93 Lambert conformal conic projected coordinates. M is a quality marker.

Site	time	Date	#	Calender Day	Year	Latitude		Longitude		h_l (m a. e.)	dL (m)	N (m)	H (m a. s. l.)	X	Y	M
B07q	13,992	11	5	131	2011	64	25,79603	16	17,43439	1424,4	0,0	-67,1	1357,4	630491,51	439245,48	K
B07q	16,833	20	10	293	2011	64	25,79542	16	17,43368	1421,1	0,0	-67,1	1354,0	630492,12	439244,36	K
B09r	16,229	5	5	125	2011	64	45,04451	16	5,47425	832,1	0,0	-66,7	765,4	638440,39	475397,86	K
B09r	10,508	21	10	294	2011	64	45,04287	16	5,47409	824,4	0,0	-66,7	757,8	638440,66	475394,81	K
B10r	13,250	5	5	125	2011	64	43,68511	16	6,70099	882,6	0,0	-66,7	815,9	637583,33	472830,09	K
B10s	13,250	5	5	125	2011	64	43,68511	16	6,70099	882,6	0,0	-66,7	815,9	637583,33	472830,09	K
B10s	10,250	21	10	294	2011	64	43,68485	16	6,70133	878,2	0,0	-66,7	811,5	637583,08	472829,61	K
B11b	17,621	5	5	125	2011	64	40,94029	16	10,49219	1031,7	0,0	-66,8	964,9	634803,33	467599,29	K
B11b	10,863	21	10	294	2011	64	40,94346	16	10,48947	1028,9	0,0	-66,8	962,1	634805,23	467605,28	K
B12q	18,484	5	5	125	2011	64	38,27098	16	14,17658	1146,7	0,0	-66,9	1079,8	632091,91	462514,94	K
B12q	11,421	21	10	294	2011	64	38,27789	16	14,16947	1142,1	0,0	-66,9	1075,2	632097,01	462528,02	K
B13q	10,921	6	5	126	2011	64	34,49778	16	19,77077	1281,6	0,0	-67,0	1214,6	627934,44	455319,08	K
B13q	18,250	20	10	293	2011	64	34,50591	16	19,76095	1279,3	0,0	-67,0	1112,3	627941,63	455334,49	K
B13a25a	20,396	5	5	125	2011	64	34,13188	16	16,73965	1279,2	0,0	-67,0	1212,2	630382,40	454743,06	K
B13a25a	17,546	20	10	293	2011	64	34,14036	16	16,73121	1278,0	0,0	-67,0	1211,1	630388,46	454759,09	K
B13n25a	19,438	5	5	125	2011	64	35,68030	16	18,09924	1246,1	0,0	-67,0	1179,1	629174,51	457570,86	K
B13n25a	9,083	21	10	294	2011	64	35,68734	16	18,09169	1241,2	0,0	-67,0	1174,2	629179,97	457584,18	K
B13n5a	18,892	5	5	125	2011	64	36,77616	16	16,39161	1205,0	0,0	-66,9	1138,0	630448,32	459663,53	K
B13n5a	9,138	21	10	294	2011	64	36,78401	16	16,38417	1203,1	0,0	-66,9	1136,1	630453,62	459678,36	K
B13s25a	11,263	6	5	126	2011	64	33,44235	16	21,64942	1326,5	0,0	-67,1	1259,4	626517,16	453296,79	K
B13s25a	9,988	21	10	294	2011	64	33,45026	16	21,63905	1323,9	0,0	-67,1	1256,9	626524,82	453311,83	K
B13v25a	11,809	6	5	126	2011	64	34,85741	16	22,87137	1299,4	0,0	-67,1	1232,3	625432,53	455883,12	K
B13v25a	18,750	20	10	293	2011	64	34,86537	16	22,85919	1295,5	0,0	-67,1	1228,4	625441,64	455898,30	*
B14s	14,504	6	5	126	2011	64	31,64430	16	24,69198	1379,7	0,0	-67,1	1312,6	624224,37	449858,33	K
B14s	18,000	20	10	293	2011	64	31,65133	16	24,67927	1372,8	0,0	-67,1	1305,7	624234,00	449871,79	*
B15f	15,488	6	5	126	2011	64	28,50147	16	29,99303	1468,2	0,0	-67,2	1400,9	620217,41	443852,87	K
B15f	17,667	20	10	293	2011	64	28,50678	16	29,98219	1458,0	0,0	-67,2	1390,8	620225,70	443863,06	*
B16s	18,263	6	5	126	2011	64	23,56957	16	42,05369	1592,7	0,0	-67,3	1525,4	610889,48	434328,56	K
B16s	12,588	21	10	294	2011	64	23,56895	16	42,05622	1587,9	0,0	-67,3	1520,6	610887,49	434327,35	K
B17q	12,471	6	5	126	2011	64	36,73093	16	28,80248	1277,8	0,0	-67,1	1210,7	620561,68	459168,91	K
B17q	18,500	20	10	293	2011	64	36,73731	16	28,79868	1275,1	0,0	-67,1	1208,0	620564,25	459180,86	*
B18o	8,996	5	5	125	2011	64	31,57107	16	0,13393	1378,3	0,0	-66,9	1311,4	643860,05	450590,26	K
B18o	15,758	20	10	293	2011	64	31,57659	16	0,13706	1374,9	0,0	-66,9	1308,0	643857,07	450600,39	K
B19o	10,513	4	5	124	2011	64	27,93059	15	55,16891	1497,1	0,0	-66,9	1430,2	648157,54	444025,20	K
B19o	18,304	19	10	292	2011	64	27,93012	15	55,16713	1493,6	0,0	-66,9	1426,8	648159,01	444024,39	K
BB0p	19,500	3	5	123	2011	64	22,72030	16	5,05643	1586,5	0,0	-66,9	1519,7	640684,00	433978,90	K
BB0p	14,638	19	10	292	2011	64	22,72013	16	5,05763	1583,3	0,0	-66,9	1516,5	640683,04	433978,52	K
BORaf	18,070	31	5	151	2011	64	24,93740	17	20,15634	1470,0	0,0	-67,7	1402,3	580201,84	435908,97	K
BORaf	14,575	22	10	295	2011	64	24,93251	17	20,15844	1491,9	-0,9	-67,7	1423,3	580200,39	435899,85	K
BORTHNb	18,450	11	1	11	2011	64	25,11105	17	19,14768	1467,7	-4,8	-67,7	1395,2	581003,29	436252,94	K
BORTHNb	12,000	26	3	85	2011	64	25,11083	17	19,14782	1467,9	-2,0	-67,7	1398,2	581003,19	436252,52	K
BORTHNb	9,659	8	5	128	2011	64	25,11075	17	19,14789	1466,7	0,0	-67,7	1399,0	581003,14	436252,37	K
BORTHNb	14,113	22	10	295	2011	64	25,10640	17	19,14743	1497,2	0,0	-67,7	1429,6	581003,73	436244,30	K
Br1f	19,520	5	4	95	2011	64	5,52223	16	19,48437	193,1	0,0	-65,8	127,3	630440,61	401539,98	K
Br7o	15,196	11	5	131	2011	64	22,14315	16	16,91670	1314,6	0,0	-67,0	1247,6	631198,52	432482,53	K
Br7o	17,167	20	10	293	2011	64	22,11973	16	16,91065	1309,0	0,0	-67,0	1242,0	631205,26	432439,26	*
Brup	11,550	5	5	125	2011	64	40,99352	15	55,22186	851,9	0,0	-66,7	785,2	646933,24	468265,21	K
Brup	14,738	20	10	293	2011	64	40,99394	15	55,22181	847,5	0,0	-66,7	780,8	646933,24	468265,99	K
Budp	10,417	5	5	125	2011	64	35,99438	15	59,90883	1201,0	0,0	-66,9	1134,1	643649,90	458808,04	K
Budp	15,192	20	10	293	2011	64	36,00396	15	59,90674	1199,0	0,0	-66,9	1132,1	643650,71	458825,89	K
D05o	12,425	7	5	127	2011	64	42,22287	16	54,63091	1269,2	0,0	-67,4	1201,8	599637,71	468616,48	K
D05o	13,675	21	10	294	2011	64	42,22890	16	54,62140	1266,5	0,0	-67,4	1199,1	599644,90	468627,93	K

D07o	11,667	7	5	127	2011	64	38,29366	16	59,25702	1435,6	0,0	-67,5	1368,1	596194,71	461200,43	K
D07o	13,150	21	10	294	2011	64	38,30568	16	59,24604	1432,3	0,0	-67,5	1364,8	596202,74	461223,03	K
D09n	10,909	7	5	127	2011	64	31,80317	17	0,56823	1647,3	0,0	-67,6	1579,7	595530,08	449114,02	K
D09n	17,612	21	10	294	2011	64	31,80711	17	0,56983	1643,9	0,0	-67,6	1576,4	595528,57	449121,31	K
D12o	10,342	7	5	127	2011	64	28,98941	17	0,13811	1715,1	0,0	-67,6	1647,6	596039,19	443899,54	K
D12o	16,858	21	10	294	2011	64	28,98996	17	0,13710	1710,7	0,0	-67,6	1643,1	596039,96	443900,59	K
E01p	17,479	4	5	124	2011	64	41,51474	15	33,40789	753,9	0,0	-66,7	687,2	664210,46	470127,07	K
E01p	11,783	20	10	293	2011	64	41,51511	15	33,40807	750,2	0,0	-66,7	683,5	664210,27	470127,74	K
E02p	17,992	4	5	124	2011	64	39,13401	15	35,98094	1022,6	0,0	-66,8	955,8	662405,05	465599,36	K
E02p	12,288	20	10	293	2011	64	39,14220	15	35,97657	1018,4	0,0	-66,8	951,7	662407,71	465614,75	K
E03rorq	18,496	4	5	124	2011	64	36,64932	15	36,90984	1254,7	0,0	-66,9	1187,9	661913,40	460949,76	K
E03rorq	10,513	20	10	293	2011	64	36,65399	15	36,91285	1251,3	0,0	-66,9	1184,5	661910,54	460958,28	K
E03virq	18,571	4	5	124	2011	64	36,64659	15	36,90930	1254,0	0,0	-66,9	1187,1	661914,10	460944,70	K
E04p	14,942	4	5	124	2011	64	34,94313	15	37,07640	1354,5	0,0	-66,8	1287,6	661950,31	457777,00	K
E04p	9,775	20	10	293	2011	64	34,94146	15	37,08363	1352,7	0,0	-66,8	1285,9	661944,66	457773,67	K
Fl01b	9,629	4	5	124	2011	64	25,98887	15	55,35216	1396,8	0,0	-66,8	1330,0	648186,32	440414,60	K
Fl01b	17,225	19	10	292	2011	64	25,98094	15	55,33316	1392,5	0,0	-66,8	1325,7	648202,28	440400,63	K
G02h	16,970	31	5	151	2011	64	26,85874	17	17,71553	1628,9	0,0	-67,7	1561,2	582065,75	439529,77	K
G02h	15,771	22	10	295	2011	64	26,85527	17	17,71846	1625,7	-0,6	-67,7	1557,4	582063,57	439523,26	K
G03i	16,200	31	5	151	2011	64	28,44587	17	16,35070	1722,9	0,0	-67,7	1655,2	583079,95	442507,28	K
G03i	16,138	22	10	295	2011	64	28,44427	17	16,35278	1719,0	-1,3	-67,7	1650,0	583078,37	442504,26	K
G04p	13,954	7	5	127	2011	64	29,99793	17	14,98311	1753,2	0,0	-67,7	1685,4	584096,03	445420,04	K
G04p	16,525	22	10	295	2011	64	29,99805	17	14,98413	1750,7	-1,2	-67,7	1681,7	584095,21	445420,25	K
gb2rorb	9,463	5	5	125	2011	64	34,07912	16	0,01740	1268,1	0,0	-66,9	1201,2	643732,15	455249,37	K
gb2rorb	16,058	20	10	293	2011	64	34,08694	16	0,01934	1267,6	0,0	-66,9	1200,7	643729,91	455263,81	K
gb2c	9,463	5	5	125	2011	64	34,07912	16	0,01740	1268,1	-1,4	-66,9	1199,7	643732,15	455249,37	K
gb2c	16,058	20	10	293	2011	64	34,08694	16	0,01934	1267,6	-3,6	-66,9	1197,0	643729,91	455263,81	K
Go1o	15,050	31	5	151	2011	64	34,00467	17	24,94371	1825,4	0,0	-67,8	1757,6	575934,93	452651,83	K
Go1o	18,306	24	10	297	2011	64	34,00309	17	24,94229	1822,9	-0,8	-67,8	1754,2	575936,14	452648,94	K
Hof01i	14,054	4	5	124	2011	64	32,33221	15	35,85017	1207,2	0,0	-66,7	1140,5	663188,92	452985,55	K
Hof01i	21,742	19	10	292	2011	64	32,32547	15	35,85002	1203,7	0,0	-66,7	1137,1	663189,71	452973,04	K
Hosp1f	11,830	6	4	96	2011	64	25,83874	15	28,68425	142,9	0,0	-65,8	77,1	669583,03	441253,13	K
Hosp1g	12,550	6	4	96	2011	64	25,83395	15	28,68004	141,4	0,0	-65,8	75,6	669586,90	441244,42	K
K01r	11,525	10	5	130	2011	64	35,26611	17	52,34994	1089,0	0,0	-67,6	1021,4	554002,69	454525,63	K
K01r	14,696	24	10	297	2011	64	35,26681	17	52,35339	1080,4	0,0	-67,6	1012,8	553999,91	454526,89	K
K02s	10,784	10	5	130	2011	64	34,82846	17	49,69981	1248,3	0,0	-67,6	1180,7	556133,03	453751,10	K
K02s	14,371	24	10	297	2011	64	34,83106	17	49,71298	1244,3	0,0	-67,6	1176,7	556122,42	453755,74	K
K03r	10,209	10	5	130	2011	64	34,24791	17	46,38597	1368,3	0,0	-67,7	1300,7	558799,65	452722,84	K
K03r	13,842	24	10	297	2011	64	34,25063	17	46,40520	1362,8	0,0	-67,7	1295,1	558784,20	452727,59	K
K04rors	12,854	10	5	130	2011	64	33,20968	17	42,23945	1560,2	0,0	-67,7	1492,4	562150,80	450860,31	K
K04virs	12,779	10	5	130	2011	64	33,21140	17	42,24488	1559,2	0,0	-67,7	1491,4	562146,40	450863,41	K
K04virs	13,179	24	10	297	2011	64	33,21479	17	42,26991	1551,9	0,0	-67,7	1484,1	562126,27	450869,30	K
K05s	14,279	10	5	130	2011	64	33,46307	17	35,47549	1749,4	0,0	-67,8	1681,6	567545,61	451446,64	K
K05s	17,317	24	10	297	2011	64	33,46019	17	35,49171	1744,8	-1,1	-67,8	1675,9	567532,77	451441,00	K
K06r	13,050	31	5	151	2011	64	38,35167	17	31,36768	2035,9	0,0	-67,9	1968,0	570615,45	460602,09	K
K06r	19,222	24	10	297	2011	64	38,35154	17	31,36577	2035,5	-2,8	-67,9	1964,9	570616,98	460601,89	K
K07n	8,904	10	5	130	2011	64	29,12275	17	42,08387	1603,4	0,0	-67,7	1535,7	562431,11	443270,95	K
K07n	13,504	24	10	297	2011	64	29,12225	17	42,08460	1599,8	0,0	-67,7	1532,1	562430,55	443270,02	K
S01f	15,233	11	1	11	2011	64	8,73146	17	49,68771	912,4	0,0	-66,9	845,4	557041,48	405271,13	K
S01g	16,871	9	5	129	2011	64	7,00113	17	49,99711	818,1	0,0	-66,8	751,3	556849,83	402052,02	K
S01g	14,704	23	10	296	2011	64	7,00056	17	49,99777	811,8	0,0	-66,8	744,9	556849,32	402050,95	K
S02i	14,417	11	1	11	2011	64	12,14045	17	49,04012	1077,0	0,0	-67,0	1009,9	557448,29	411613,84	K
S02j	15,838	9	5	129	2011	64	12,14325	17	49,03845	1079,8	0,0	-67,0	1012,7	557449,54	411619,07	K
S02j	14,188	23	10	296	2011	64	12,13427	17	49,04311	1073,4	0,0	-67,0	1006,4	557446,09	411602,31	K
S04k	12,742	9	5	129	2011	64	16,20480	17	48,24362	1230,0	0,0	-67,2	1162,8	557950,20	419176,27	K
S04k	13,679	23	10	296	2011	64	16,19452	17	48,25349	1223,6	0,0	-67,2	1156,4	557942,59	419157,03	K
Skf01b	18,246	3	5	123	2011	64	18,00796	16	5,01596	1350,8	0,0	-66,6	1284,1	641120,29	425234,14	K
Skf01b	12,900	19	10	292	2011	64	18,00536	16	5,00003	1345,4	0,0	-66,6	1278,8	641133,35	425229,89	K

T01nm	11,633	11	1	11	2011	64	19,45154	18	8,80336	803,8	0,0	-67,3	736,6	541266,01	424939,08	K
T01nn	10,042	9	5	129	2011	64	19,48504	18	8,22832	829,3	0,0	-67,3	762,0	541728,64	425007,61	K
T01nn	15,967	23	10	296	2011	64	19,48480	18	8,22863	823,0	0,0	-67,3	755,7	541728,39	425007,17	K
T02nm	12,433	11	1	11	2011	64	19,61111	18	3,95840	1016,3	0,0	-67,3	949,0	545166,54	425290,74	K
T02nn	9,259	9	5	129	2011	64	19,61237	18	3,95511	1017,3	0,0	-67,3	950,1	545169,16	425293,12	K
T02nn	16,204	23	10	296	2011	64	19,61273	18	3,96085	1012,8	0,0	-67,3	945,5	545164,53	425293,71	K
T03nn	18,663	8	5	128	2011	64	20,19286	17	58,63078	1147,6	0,0	-67,3	1080,3	549442,48	426437,96	K
T03nn	17,792	23	10	296	2011	64	20,19087	17	58,64078	1141,9	0,0	-67,3	1074,6	549434,48	426434,13	K
T04nn	16,004	8	5	128	2011	64	21,34307	17	51,56165	1292,0	0,0	-67,4	1224,7	555098,61	428672,15	K
T04nn	18,521	23	10	296	2011	64	21,34000	17	51,57231	1285,0	0,0	-67,4	1217,6	555090,14	428666,30	K
T05nl	13,333	11	1	11	2011	64	22,30478	17	42,94705	1412,9	-2,8	-67,5	1342,6	561996,89	430591,66	K
T05nl	20,500	25	3	84	2011	64	22,30413	17	42,95132	1412,5	-0,1	-67,5	1344,9	561993,48	430590,38	K
T05nm	14,913	8	5	128	2011	64	22,30196	17	42,96171	1413,0	0,0	-67,5	1345,5	561985,21	430586,18	K
T05rorf	13,333	11	1	11	2011	64	22,30478	17	42,94705	1412,9	0,0	-67,5	1345,4	561996,89	430591,66	K
T05rorf	20,500	25	3	84	2011	64	22,30413	17	42,95132	1412,5	-0,1	-67,5	1344,9	561993,48	430590,38	K
T05rorf	12,130	30	5	150	2011	64	22,30310	17	42,95310	1412,8	0,0	-67,5	1345,3	561992,09	430588,44	K
T05rorf	19,342	23	10	296	2011	64	22,30074	17	42,96153	1412,7	0,0	-67,5	1345,2	561985,40	430583,91	K
T06nn	14,142	8	5	128	2011	64	24,26697	17	36,62611	1526,6	0,0	-67,6	1459,0	567001,82	434344,09	K
T06nn	15,77	1	6	152	2011	64	24,26656	17	36,62736	1526,5	0,0	-67,6	1458,9	567000,82	434343,29	K
T06nn	13,025	23	10	296	2011	64	24,26343	17	36,63607	1523,5	0,0	-67,6	1455,9	566993,96	434337,34	K
T07nk	16,933	11	1	11	2011	64	25,30297	17	31,18202	1629,9	-2,8	-67,7	1559,4	571331,01	436367,75	K
T07nk	22	25	3	84	2011	64	25,30200	17	31,18561	1629,9	-0,6	-67,7	1561,6	571328,17	436365,88	K
T07nl	11,546	8	5	128	2011	64	25,31568	17	31,11354	1631,9	0,0	-67,7	1564,2	571385,44	436392,66	K
T07rorh	16,933	11	1	11	2011	64	25,30297	17	31,18202	1629,9	-1,0	-67,7	1561,2	571331,01	436367,75	K
T07rori	16,933	11	1	11	2011	64	25,30297	17	31,18202	1629,9	0,0	-67,7	1562,2	571331,01	436367,75	K
T07rori	22	25	3	84	2011	64	25,30200	17	31,18561	1629,9	-0,1	-67,7	1562,1	571328,17	436365,88	K
T07rori	14,28	30	5	150	2011	64	25,30113	17	31,18830	1630,3	-1,0	-67,7	1561,6	571326,05	436364,22	K
T07rorj	14,28	30	5	150	2011	64	25,30113	17	31,18830	1630,3	0,0	-67,7	1562,6	571326,05	436364,22	K
T07rorj	12,075	23	10	296	2011	64	25,29926	17	31,19532	1629,5	0,0	-67,7	1561,8	571320,49	436360,61	K
T07rorj	12,075	23	10	296	2011	64	25,29926	17	31,19532	1629,5	1,0	-67,7	1562,8	571320,49	436360,61	K
T08nn	10,8	8	5	128	2011	64	26,30265	17	27,79928	1704,1	0,0	-67,8	1636,4	574002,06	438289,43	K
T08nn	11,733	23	10	296	2011	64	26,30205	17	27,80069	1698,9	0,0	-67,8	1631,1	574000,96	438288,29	K

Appendix D: Measured surface velocity on Vatnajökull in 2011.

Site	Calendar day date	#	Calendar day date	#	# of days	translation (m)	(°)	velocity (cm/day)	(m/annum)
B07q	110511	131	111020	293	162	1,27	153	0,78	2,85
B09r	110505	125	111021	294	169	3,04	178	1,80	6,57
B10r	101007	280	110505	125	210	0,27	57	0,13	0,48
B10s	110505	125	111021	294	169	0,55	209	0,33	1,19
B10s	111021	294	120510	131	202	0,40	47	0,20	0,73
B11b	110505	125	111021	294	169	6,26	20	3,70	13,51
B11b	111021	294	120510	131	202	0,44	80	0,22	0,80
B12q	110505	125	111021	294	169	13,99	24	8,28	30,22
B13q	110506	126	111020	293	167	16,98	28	10,16	37,10
B13a25a	110505	125	111020	293	168	17,09	23	10,17	37,13
B13n5a	110505	125	111021	294	169	15,70	22	9,29	33,91
B13s25a	110506	126	111021	294	168	16,83	29	10,02	36,56
B13v25a	110506	126	111020	293	167	17,66	33	10,57	38,60
B14s	111020	293	110506	126	-167	16,52	218	-9,89	-36,10
B14s	110506	126	121010	284	523	39,19	38	7,49	27,35
B15f	110506	126	111020	293	167	13,12	41	7,86	28,68
B16s	110506	126	111021	294	168	2,34	241	1,39	5,07
B17q	110506	126	111020	293	167	12,20	14	7,30	26,66
B18o	110505	125	111020	293	168	10,53	346	6,26	22,87
B19o	110504	124	111019	292	168	1,67	121	0,99	3,63
BB0p	110503	123	111019	292	169	1,02	252	0,60	2,19
BORaf	110531	151	111022	295	144	9,21	191	6,40	23,35
BORTHNb	101010	283	110111	11	93	3,24	189	3,48	12,72
BORTHNb	110111	11	110326	85	74	0,42	195	0,57	2,08
BORTHNb	110326	85	110508	128	43	0,16	201	0,37	1,35
BORTHNb	110508	128	111022	295	167	8,06	177	4,83	17,63
BORTHNb	111022	295	120506	127	197	7,15	181	3,63	13,25
Br1f	101013	286	110405	95	174	3,44	172	1,98	7,22
Br7o	110511	131	111020	293	162	43,65	174	26,94	98,34
Brup	110505	125	111020	293	168	0,78	3	0,46	1,69
Budp	110505	125	111020	293	168	17,82	5	10,61	38,72
D05o	110507	127	111021	294	167	13,48	34	8,07	29,47
D07o	110507	127	111021	294	167	23,92	21	14,32	52,27
D09n	110507	127	111021	294	167	7,41	350	4,44	16,19
D12o	110507	127	111021	294	167	1,30	38	0,78	2,84
E01p	110504	124	111020	293	169	0,70	348	0,41	1,51
E02p	110504	124	111020	293	169	15,56	13	9,21	33,61
E03rorq	110504	124	111020	293	169	8,98	344	5,31	19,39
E04p	110504	124	111020	293	169	6,55	242	3,87	14,14
Fl01b	110504	124	111019	292	168	21,17	134	12,60	45,99
G02h	110531	151	111022	295	144	6,84	200	4,75	17,34
G03i	110531	151	111022	295	144	3,40	209	2,36	8,62
G04p	110507	127	111022	295	168	0,85	285	0,50	1,84
gb2rorb	101006	279	110505	125	211	10,50	355	4,98	18,17
gb2rorb	110505	125	111020	293	168	14,57	354	8,67	31,64
gb2rorb	111020	293	120508	129	201	11,26	354	5,60	20,44

Go1o	110531	151	111024	297	146	3,14	159	2,15	7,85
Hof01i	110504	124	111019	292	168	12,48	179	7,43	27,12
Hosp1f	100824	236	110406	96	225	11,19	164	4,97	18,15
K01r	110510	130	111024	297	167	3,04	295	1,82	6,65
K02s	110510	130	111024	297	167	11,56	295	6,92	25,27
K03r	110510	130	111024	297	167	16,16	288	9,68	35,32
K04virs	110510	130	111024	297	167	20,96	287	12,55	45,81
K05s	110510	130	111024	297	167	14,01	248	8,39	30,63
K06r	110531	151	111024	297	146	1,54	99	1,05	3,85
K07n	110510	130	111024	297	167	1,10	212	0,66	2,39
S01g	110509	129	111023	296	167	1,18	207	0,71	2,59
S02i	100511	131	110111	11	245	22,11	193	9,03	32,94
S02j	110509	129	111023	296	167	17,05	193	10,21	37,27
S04k	110509	129	111023	296	167	20,64	203	12,36	45,11
Skf01b	110503	123	111019	292	169	13,72	111	8,12	29,63
T01nm	100504	124	110111	11	252	0,55	190	0,22	0,79
T01nn	110509	129	111023	296	167	0,51	209	0,31	1,11
T01nn	111023	296	120504	125	194	0,98	216	0,51	1,84
T02nm	100504	124	110111	11	252	8,52	272	3,38	12,33
T02nn	110509	129	111023	296	167	4,67	278	2,80	10,21
T03nn	110508	128	111023	296	168	8,86	245	5,27	19,24
T04nn	110508	128	111023	296	168	10,29	236	6,13	22,36
T05rorf	101009	282	110111	11	94	4,48	235	4,77	17,40
T05rorf	110111	11	110325	84	73	3,64	251	4,99	18,20
T05rorf	110325	84	110530	150	66	2,39	217	3,61	13,19
T05rorf	110530	150	111023	296	146	8,07	237	5,53	20,17
T05rorf	111023	296	120504	125	194	9,57	237	4,93	18,01
T06nn	110508	128	110601	152	24	1,26	233	5,25	19,15
T06nn	110601	152	111023	296	144	9,09	230	6,31	23,03
T07rorh	101009	282	110111	11	94	4,30	235	4,58	16,71
T07rori	110111	11	110325	84	73	3,40	238	4,65	16,98
T07rori	110325	84	110530	150	66	2,69	233	4,08	14,90
T07rorj	110530	150	111023	296	146	6,62	238	4,53	16,54
T07rorj	111023	296	120505	126	195	9,37	244	4,80	17,54
T08nn	110508	128	111023	296	168	1,59	226	0,94	3,45

Appendix E: Melt water runoff to selected rivers in summer 2011, derived from summer balance.

ΔS: area in a given elevation range where summer balance is negative, **∑ΔS**: cumulative area above a given elevation, **ΔQ_s**: melt water runoff from a given elevation range, **$\sum \Delta Q_s$** : cumulative melt water runoff from an area above given elevation.

Tungnaá water drainage basin

Elevation (m a. s. l.)		ΔS km^2	∑ΔS km^2	ΔQ_s $(10^6 m^3)$	$\sum \Delta Q_s$ $(10^6 m^3)$
1350	1400	0,6	0,6	1,6	1,6
1300	1350	6,2	6,8	20,9	22,5
1250	1300	10,7	17,5	45,2	67,7
1200	1250	11,4	28,9	52,3	120,0
1150	1200	10,8	39,7	47,6	167,6
1100	1150	12,8	52,5	52,5	220,1
1050	1100	11,9	64,4	48,8	268,8
1000	1050	9,7	74,1	42,3	311,1
950	1000	10,8	84,9	51,0	362,2
900	950	9,0	93,9	45,0	407,2
850	900	8,3	102,2	43,3	450,5
800	850	8,6	110,8	46,1	496,6
750	800	6,3	117,1	35,3	531,9
700	750	4,2	121,3	24,3	556,1
650	700	0,5	121,8	3,3	559,4

Sylgja water drainage basin

Elevation (m a. s. l.)		ΔS km^2	∑ΔS km^2	ΔQ_s $(10^6 m^3)$	$\sum \Delta Q_s$ $(10^6 m^3)$
1300	1350	1,3	1,3	4,8	4,8
1250	1300	3,6	4,9	15,0	19,9
1200	1250	6,4	11,3	29,3	49,2
1150	1200	8,3	19,6	38,3	87,5
1100	1150	6,6	26,2	29,0	116,5
1050	1100	7,6	33,8	31,2	147,6
1000	1050	3,8	37,6	16,6	164,2
950	1000	1,5	39,1	6,9	171,1
900	950	0,6	39,7	2,8	173,9
850	900	0,0	39,7	0,1	174,0

Western Skaftá cauldron water drainage basin

Elevation (m a. s. l.)		ΔS km^2	∑ΔS km^2	ΔQ_s $(10^6 m^3)$	$\sum \Delta Q_s$ $(10^6 m^3)$
1700	1750	3,2	3,2	4,9	4,9
1650	1700	7,0	10,2	10,5	15,4
1600	1650	8,4	18,6	12,8	28,2
1550	1600	5,0	23,6	7,3	35,5
1500	1550	1,5	25,1	2,0	37,5

Eastern Skaftár cauldoron water drainage basin

Elevation (m a. s. l.)		ΔS km^2	∑ΔS km^2	ΔQ_s ($10^6 m^3$)	$\sum\Delta Q_s$ ($10^6 m^3$)
1750	1800	2,5	2,5	3,6	3,6
1700	1750	10,6	13,1	16,4	20,0
1650	1700	14,8	27,9	22,3	42,2
1600	1650	9,3	37,2	14,2	56,5
1550	1600	2,2	39,4	3,4	59,9

Grímsvötn water drainage basin

Elevation (m a. s. l.)		ΔS km^2	∑ΔS km^2	ΔQ_s ($10^6 m^3$)	$\sum\Delta Q_s$ ($10^6 m^3$)
1900	1950	0,6	0,6	0,3	0,3
1850	1900	1,3	1,9	0,9	1,2
1800	1850	1,6	3,5	1,5	2,7
1750	1800	3,9	7,4	5,3	8,0
1700	1750	15,9	23,3	22,9	30,9
1650	1700	54,1	77,4	62,5	93,4
1600	1650	28,9	106,3	32,0	125,4
1550	1600	18,1	124,4	22,5	147,9
1500	1550	16,4	140,8	22,9	170,8
1450	1500	11,3	152,1	14,6	185,3
1400	1450	14,9	167,0	16,7	202,0
1350	1400	0,6	167,6	0,3	202,3

Kaldakvísl water drainage basin

Elevation (m a. s. l.)		ΔS km^2	∑ΔS km^2	ΔQ_s ($10^6 m^3$)	$\sum\Delta Q_s$ ($10^6 m^3$)
1950	2000	1,3	1,3	0,0	0,0
1900	1950	12,3	13,6	3,4	3,5
1850	1900	6,4	20,0	4,4	7,9
1800	1850	6,4	26,4	6,6	14,5
1750	1800	11,7	38,1	15,8	30,2
1700	1750	21,1	59,2	33,8	64,0
1650	1700	16,7	75,9	29,2	93,2
1600	1650	14,2	90,1	27,1	120,3
1550	1600	19,4	109,5	38,3	158,6
1500	1550	27,2	136,7	44,6	203,2
1450	1500	28,5	165,2	56,1	259,2
1400	1450	23,1	188,3	58,6	317,8
1350	1400	21,6	209,9	66,0	383,8
1300	1350	21,3	231,2	74,8	458,7
1250	1300	22,6	253,8	80,6	539,3
1200	1250	22,6	276,4	74,8	614,1
1150	1200	20,2	296,6	64,7	678,8
1100	1150	18,3	314,9	65,7	744,5
1050	1100	17,2	332,1	72,0	816,5
1000	1050	14,9	347,0	69,4	885,8
950	1000	10,7	357,7	54,1	940,0
900	950	5,6	363,3	29,5	969,5
850	900	0,5	363,8	2,9	972,4

Jökulsá á Fjöllum water drainage basin

Elevation (m a. s. l.)		ΔS km^2	$\sum\Delta S$ km^2	ΔQ_s $(10^6 m^3)$	$\sum\Delta Q_s$ $(10^6 m^3)$
2000	2050	0,0	0,0	0,0	0,0
1950	2000	8,0	8,0	0,4	0,4
1900	1950	25,6	33,6	6,5	6,9
1850	1900	18,2	51,8	8,9	15,8
1800	1850	12,7	64,5	6,1	21,9
1750	1800	22,0	86,5	13,3	35,2
1700	1750	34,2	120,7	21,1	56,3
1650	1700	79,5	200,2	47,3	103,6
1600	1650	116,5	316,7	63,0	166,5
1550	1600	100,9	417,6	50,2	216,7
1500	1550	97,8	515,4	58,4	275,2
1450	1500	85,7	601,1	70,0	345,2
1400	1450	74,3	675,4	81,9	427,1
1350	1400	60,2	735,6	83,3	510,4
1300	1350	49,1	784,7	75,9	586,3
1250	1300	52,5	837,2	85,8	672,1
1200	1250	57,4	894,6	99,9	772,1
1150	1200	54,5	949,1	107,1	879,2
1100	1150	45,9	995,0	103,9	983,1
1050	1100	34,1	1029,1	86,6	1069,7
1000	1050	36,4	1065,5	102,1	1171,7
950	1000	31,5	1097,0	97,7	1269,4
900	950	26,2	1123,2	90,5	1359,9
850	900	25,4	1148,6	96,2	1456,0
800	850	20,2	1168,8	82,1	1538,1
750	800	15,2	1184,0	64,2	1602,4
700	750	1,7	1185,7	7,5	1609,9

Kreppa and Kverká water drainage basin

Elevation (m a. s. l.)		ΔS km^2	∑ΔS km^2	ΔQ_s ($10^6 m^3$)	$\sum\Delta Q_s$ ($10^6 m^3$)
1900	1950	0,0	0,0	0,0	0,0
1850	1900	1,0	1,0	0,1	0,1
1800	1850	2,5	3,5	0,2	0,3
1750	1800	2,8	6,3	0,3	0,6
1700	1750	3,6	9,9	1,1	1,7
1650	1700	5,0	14,9	1,9	3,7
1600	1650	37,9	52,8	21,2	24,9
1550	1600	22,6	75,4	13,6	38,5
1500	1550	14,3	89,7	9,6	48,2
1450	1500	15,4	105,1	11,5	59,7
1400	1450	19,3	124,4	15,8	75,5
1350	1400	25,2	149,6	23,0	98,6
1300	1350	20,5	170,1	19,8	118,3
1250	1300	16,4	186,5	15,5	133,8
1200	1250	18,1	204,6	16,1	149,9
1150	1200	18,2	222,8	18,1	167,9
1100	1150	17,5	240,3	20,9	188,9
1050	1100	11,6	251,9	17,0	205,9
1000	1050	14,1	266,0	26,4	232,2
950	1000	16,1	282,1	36,8	269,0
900	950	14,4	296,5	38,2	307,3
850	900	14,5	311,0	44,8	352,1
800	850	11,5	322,5	39,6	391,8
750	800	9,3	331,8	34,5	426,3
700	750	4,2	336,0	15,9	442,2
650	700	0,4	336,4	1,7	443,9

Jökulsá á Brú water drainage basin

Elevation (m a. s. l.)		ΔS km^2	∑ΔS km^2	ΔQ_s ($10^6 m^3$)	$\sum\Delta Q_s$ ($10^6 m^3$)
1600	1650	8,3	8,3	5,6	5,6
1550	1600	30,4	38,7	20,8	26,4
1500	1550	60,6	99,3	43,3	69,7
1450	1500	63,6	162,9	49,1	118,8
1400	1450	93,2	256,1	61,0	179,8
1350	1400	124,5	380,6	81,6	261,3
1300	1350	133,2	513,8	96,3	357,6
1250	1300	128,3	642,1	91,4	449,0
1200	1250	102,8	744,9	85,1	534,1
1150	1200	87,3	832,2	90,0	624,1
1100	1150	69,3	901,5	88,9	713,0
1050	1100	61,8	963,3	99,0	812,0
1000	1050	51,8	1015,1	102,6	914,6
950	1000	43,4	1058,5	103,1	1017,7
900	950	34,6	1093,1	94,7	1112,4
850	900	30,4	1123,5	94,4	1206,8
800	850	29,9	1153,4	103,4	1310,2
750	800	26,8	1180,2	98,4	1408,6
700	750	19,6	1199,8	73,5	1482,1
650	700	12,3	1212,1	47,5	1529,5
600	650	0,3	1212,4	1,3	1530,8

Jökulsá á Fljótsdal water drainage basin

Elevation (m a. s. l.)		ΔS km^2	ΣΔS km^2	ΔQ_s ($10^6 m^3$)	$\Sigma\Delta Q_s$ ($10^6 m^3$)
1400	1450	0,6	0,6	0,0	0,0
1350	1400	2,8	3,4	0,2	0,2
1300	1350	5,2	8,6	0,8	1,0
1250	1300	15,8	24,4	4,2	5,2
1200	1250	15,9	40,3	8,7	13,9
1150	1200	17,6	57,9	16,0	29,8
1100	1150	15,1	73,0	19,6	49,4
1050	1100	12,7	85,7	21,4	70,8
1000	1050	11,9	97,6	24,5	95,2
950	1000	9,0	106,6	21,7	117,0
900	950	5,8	112,4	15,7	132,6
850	900	4,3	116,7	12,9	145,5
800	850	3,3	120,0	10,9	156,4
750	800	3,4	123,4	12,6	169,0
700	750	3,3	126,7	14,0	183,0
650	700	1,7	128,4	7,8	190,8

Hornafjarðarfljót water drainage basin

Elevation (m a. s. l.)		ΔS km^2	∑ΔS km^2	ΔQ_s ($10^6 m^3$)	$\sum\Delta Q_s$ ($10^6 m^3$)
1400	1450	5,2	5,2	0,6	0,6
1350	1400	11,8	17,0	1,6	2,2
1300	1350	18,3	35,3	5,1	7,2
1250	1300	36,6	71,9	14,5	21,7
1200	1250	30,2	102,1	25,1	46,8
1150	1200	20,8	122,9	28,2	75,1
1100	1150	19,8	142,7	34,2	109,3
1050	1100	15,3	158,0	32,7	142,0
1000	1050	11,7	169,7	29,2	171,2
950	1000	11,1	180,8	31,6	202,8
900	950	8,2	189,0	26,0	228,8
850	900	5,5	194,5	18,9	247,7
800	850	4,4	198,9	16,1	263,8
750	800	4,1	203,0	16,0	279,8
700	750	4,0	207,0	16,6	296,4
650	700	3,5	210,5	15,6	312,0
600	650	2,6	213,1	12,8	324,8
550	600	2,0	215,1	10,7	335,5
500	550	1,8	216,9	10,1	345,6
450	500	1,4	218,3	8,1	353,7
400	450	1,3	219,6	7,9	361,6
350	400	0,8	220,4	5,2	366,8
300	350	1,1	221,5	7,9	374,7
250	300	2,3	223,8	17,7	392,5
200	250	3,5	227,3	26,9	419,4
150	200	2,7	230,0	21,4	440,8
100	150	2,1	232,1	18,0	458,8
50	100	2,8	234,9	26,9	485,7
0	50	0,6	235,5	5,6	491,3

Jökulsá á Breiðamerkursandi water drainage basin

Elevation (m a. s. l.)		ΔS km^2	∑ΔS km^2	ΔQ_s ($10^6 m^3$)	$\sum\Delta Q_s$ ($10^6 m^3$)
1700	1750	0,8	0,8	0,4	0,4
1650	1700	4,0	4,8	1,9	2,3
1600	1650	12,9	17,7	6,5	8,8
1550	1600	19,1	36,8	10,5	19,3
1500	1550	23,0	59,8	14,6	33,9
1450	1500	35,2	95,0	20,4	54,2
1400	1450	49,6	144,6	32,8	87,1
1350	1400	83,3	227,9	68,7	155,8
1300	1350	85,4	313,3	89,7	245,5
1250	1300	53,1	366,4	68,8	314,2
1200	1250	35,1	401,5	53,8	368,0
1150	1200	28,9	430,4	51,8	419,8
1100	1150	24,6	455,0	51,2	471,1
1050	1100	20,7	475,7	48,7	519,7
1000	1050	17,8	493,5	46,7	566,4
950	1000	19,0	512,5	54,1	620,5
900	950	20,2	532,7	60,5	681,0
850	900	20,5	553,2	66,5	747,6
800	850	20,2	573,4	70,2	817,8
750	800	19,5	592,9	74,4	892,2
700	750	21,1	614,0	86,1	978,2
650	700	26,7	640,7	113,6	1091,8
600	650	18,5	659,2	84,1	1175,9
550	600	18,5	677,7	93,1	1269,0
500	550	7,0	684,7	36,7	1305,8
450	500	7,7	692,4	44,0	1349,7
400	450	5,8	698,2	34,3	1384,0
350	400	5,5	703,7	32,6	1416,6
300	350	6,5	710,2	39,8	1456,3
250	300	6,0	716,2	39,3	1495,7
200	250	6,3	722,5	49,8	1545,5
150	200	5,1	727,6	47,9	1593,5
100	150	5,1	732,7	52,4	1645,9
50	100	4,1	736,8	44,8	1690,7
0	50	2,7	739,5	30,3	1721,0

Breiðárlón/Fjallsárlón water drainage basin

Elevation (m a. s. l.)		ΔS km^2	∑ΔS km^2	ΔQ_s ($10^6 m^3$)	$\sum\Delta Q_s$ ($10^6 m^3$)
1550	1600	0,1	0,1	0,0	0,0
1500	1550	3,6	3,7	0,9	0,9
1450	1500	4,4	8,1	2,0	2,9
1400	1450	5,2	13,3	3,4	6,3
1350	1400	6,4	19,7	5,6	11,9
1300	1350	12,6	32,3	14,5	26,4
1250	1300	6,7	39,0	8,7	35,0
1200	1250	5,6	44,6	8,2	43,3
1150	1200	5,1	49,7	8,6	51,9
1100	1150	4,5	54,2	8,9	60,8
1050	1100	5,0	59,2	10,9	71,6
1000	1050	6,0	65,2	13,9	85,5
950	1000	7,0	72,2	18,8	104,3
900	950	8,4	80,6	25,1	129,4
850	900	6,7	87,3	21,9	151,3
800	850	8,4	95,7	29,3	180,6
750	800	8,8	104,5	33,6	214,3
700	750	6,1	110,6	25,1	239,4
650	700	7,4	118,0	32,4	271,8
600	650	8,3	126,3	38,6	310,4
550	600	8,8	135,1	44,1	354,4
500	550	9,5	144,6	49,6	404,1
450	500	9,6	154,2	53,0	457,1
400	450	11,1	165,3	64,3	521,4
350	400	8,5	173,8	51,1	572,5
300	350	7,7	181,5	47,5	620,0
250	300	7,4	188,9	49,7	669,7
200	250	6,8	195,7	52,7	722,4
150	200	4,6	200,3	42,4	764,8
100	150	4,3	204,6	44,1	808,8
50	100	3,7	208,3	39,9	848,8
0	50	1,8	210,1	20,3	869,1

Skeiðarársandur water drainage basin (Gígja)

Elevation (m a. s. l.)		ΔS km^2	∑ΔS km^2	ΔQ_s ($10^6 m^3$)	$\sum\Delta Q_s$ ($10^6 m^3$)
1700	1750	1,0	1,0	0,4	0,4
1650	1700	17,2	18,2	12,7	13,2
1600	1650	70,7	88,9	51,4	64,5
1550	1600	80,2	169,1	58,9	123,4
1500	1550	100,1	269,2	75,7	199,2
1450	1500	94,4	363,6	79,1	278,3
1400	1450	91,4	455,0	84,0	362,3
1350	1400	80,6	535,6	88,3	450,5
1300	1350	68,9	604,5	94,5	545,0
1250	1300	59,5	664,0	97,4	642,4
1200	1250	49,9	713,9	94,9	737,3
1150	1200	40,7	754,6	89,0	826,3
1100	1150	31,1	785,7	72,3	898,6
1050	1100	24,3	810,0	64,8	963,4
1000	1050	22,0	832,0	64,6	1028,0
950	1000	23,6	855,6	71,4	1099,3
900	950	24,8	880,4	74,4	1173,7
850	900	27,8	908,2	86,0	1259,7
800	850	22,5	930,7	78,3	1338,0
750	800	19,6	950,3	80,5	1418,5
700	750	19,1	969,4	90,3	1508,9
650	700	11,9	981,3	62,9	1571,8
600	650	13,1	994,4	74,6	1646,4
550	600	12,4	1006,8	73,4	1719,8
500	550	8,3	1015,1	51,9	1771,7
450	500	5,5	1020,6	36,5	1808,1
400	450	6,7	1027,3	46,0	1854,1
350	400	11,1	1038,4	79,7	1933,9
300	350	14,2	1052,6	109,8	2043,7
250	300	15,3	1067,9	125,2	2168,8
200	250	12,4	1080,3	109,1	2277,9
150	200	11,3	1091,6	106,1	2384,0
100	150	13,5	1105,1	135,9	2519,9
50	100	5,0	1110,1	52,6	2572,6

Súla water drainage basin

Elevation (m a. s. l.)		ΔS km^2	∑ΔS km^2	ΔQ_s ($10^6 m^3$)	$\sum\Delta Q_s$ ($10^6 m^3$)
1600	1650	0,0	0,0	0,0	0,0
1550	1600	0,6	0,6	0,0	0,0
1500	1550	1,1	1,7	0,0	0,0
1450	1500	3,7	5,4	0,0	0,0
1400	1450	4,0	9,4	0,0	0,0
1350	1400	3,2	12,6	0,0	0,0
1300	1350	2,5	15,1	0,0	0,0
1250	1300	1,6	16,7	0,0	0,0
1200	1250	2,3	19,0	0,0	0,0
1150	1200	3,6	22,6	0,0	0,0
1100	1150	6,7	29,3	0,1	0,1
1050	1100	4,9	34,2	0,0	0,2
1000	1050	1,1	35,3	0,0	0,2
900	950	0,3	35,6	0,0	0,3
850	900	1,6	37,2	0,2	0,5
800	850	8,8	46,0	5,5	6,0
750	800	6,3	52,3	13,5	19,5
700	750	5,4	57,7	20,1	39,6
650	700	4,4	62,1	21,5	61,1
600	650	8,8	70,9	48,5	109,6
550	600	11,7	82,6	69,9	179,5
500	550	8,9	91,5	56,3	235,8
450	500	7,2	98,7	47,0	282,8
400	450	6,3	105,0	42,8	325,6
350	400	4,8	109,8	34,5	360,0
300	350	1,8	111,6	14,1	374,1
250	300	0,9	112,5	7,8	382,0
200	250	0,8	113,3	6,8	388,8
150	200	0,8	114,1	7,5	396,4
100	150	0,8	114,9	8,5	404,9
50	100	0,6	115,5	7,0	411,8

Djúpá water drainage basin

Elevation (m a. s. l.)		ΔS km^2	∑ΔS km^2	ΔQ_s ($10^6 m^3$)	$\sum\Delta Q_s$ ($10^6 m^3$)
1350	1400	0,0	0,0	0,0	0,0
1300	1350	0,1	0,1	0,0	0,0
1100	1150	0,2	0,3	0,0	0,0
1050	1100	2,7	3,0	4,8	4,8
1000	1050	6,5	9,5	14,2	19,1
950	1000	5,9	15,4	19,2	38,3
900	950	5,8	21,2	20,3	58,5
850	900	5,7	26,9	22,6	81,1
800	850	8,4	35,3	34,6	115,7
750	800	6,6	41,9	30,5	146,2
700	750	4,0	45,9	21,6	167,8
650	700	3,0	48,9	16,2	184,0
600	650	0,4	49,3	2,4	186,3

Brunná water drainage basin

Elevation (m a. s. l.)		ΔS km^2	∑ΔS km^2	ΔQ_s ($10^6 m^3$)	$\sum\Delta Q_s$ ($10^6 m^3$)
1050	1100	0,0	0,0	0,3	0,3
1000	1050	1,1	1,1	4,7	4,9
950	1000	3,3	4,4	14,9	19,8
900	950	4,2	8,6	20,3	40,0
850	900	4,3	12,9	22,2	62,2
800	850	4,9	17,8	25,6	87,8
750	800	5,4	23,2	29,3	117,1
700	750	6,4	29,6	35,8	152,9
650	700	3,9	33,5	23,2	176,1
600	650	2,3	35,8	14,5	190,6
550	600	0,0	35,8	0,2	190,8

Hverfisfljót water drainage basin

Elevation (m a. s. l.)		ΔS km^2	$\sum\Delta S$ km^2	ΔQ_s $(10^6 m^3)$	$\sum\Delta Q_s$ $(10^6 m^3)$
1650	1700	0,3	0,3	0,0	0,0
1600	1650	3,0	3,3	0,5	0,6
1550	1600	3,4	6,7	0,8	1,4
1500	1550	3,4	10,1	0,7	2,1
1450	1500	8,1	18,2	0,2	2,3
1400	1450	3,7	21,9	0,1	2,4
1350	1400	3,8	25,7	0,2	2,6
1300	1350	7,4	33,1	6,5	9,1
1250	1300	8,8	41,9	12,2	21,3
1200	1250	8,9	50,8	15,7	37,0
1150	1200	10,0	60,8	21,0	58,0
1100	1150	10,4	71,2	28,2	86,2
1050	1100	10,2	81,4	37,5	123,6
1000	1050	9,3	90,7	39,6	163,2
950	1000	9,4	100,1	43,8	207,0
900	950	8,9	109,0	44,9	251,9
850	900	7,4	116,4	38,4	290,3
800	850	9,3	125,7	49,4	339,7
750	800	11,5	137,2	63,5	403,1
700	750	13,7	150,9	80,2	483,3
650	700	7,8	158,7	48,0	531,4
600	650	4,6	163,3	28,7	560,0
550	600	0,2	163,5	1,1	561,2

Skaftá water drainage basin

Elevation (m a. s. l.)		ΔS km^2	$\sum\Delta S$ km^2	ΔQ_s $(10^6 m^3)$	$\sum\Delta Q_s$ $(10^6 m^3)$
1650	1700	2,9	2,9	3,7	3,7
1600	1650	16,1	19,0	17,9	21,6
1550	1600	23,8	42,8	31,8	53,4
1500	1550	29,5	72,3	39,9	93,3
1450	1500	24,1	96,4	34,0	127,3
1400	1450	22,4	118,8	37,5	164,8
1350	1400	20,7	139,5	42,3	207,0
1300	1350	22,9	162,4	63,9	270,9
1250	1300	16,4	178,8	53,1	324,0
1200	1250	21,5	200,3	84,8	408,8
1150	1200	23,9	224,2	104,2	513,0
1100	1150	24,5	248,7	106,9	619,9
1050	1100	26,8	275,5	111,7	731,6
1000	1050	26,3	301,8	112,8	844,4
950	1000	20,3	322,1	96,6	941,1
900	950	15,8	337,9	79,7	1020,7
850	900	16,2	354,1	84,6	1105,3
800	850	14,7	368,8	79,4	1184,7
750	800	11,6	380,4	65,0	1249,7
700	750	8,5	388,9	49,6	1299,3
650	700	5,1	394,0	30,3	1329,6
600	650	0,9	394,9	5,5	1335,1

Appendix F: MODIS satellite images of Vatnajökull and vicinity 2010_11.

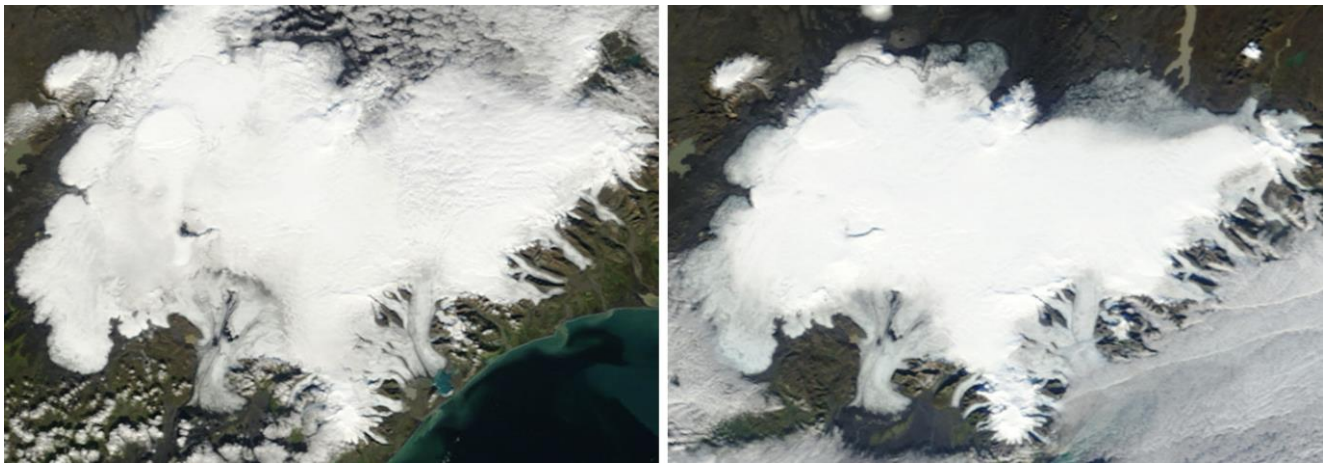

Left: September 19th 2010, snow is already starting to accumulate in the upper regions. Right: October 10th 2010, winter has settled in, this week the mass balance survey team observed up to 120 cm fresh snow at the highest elevations.

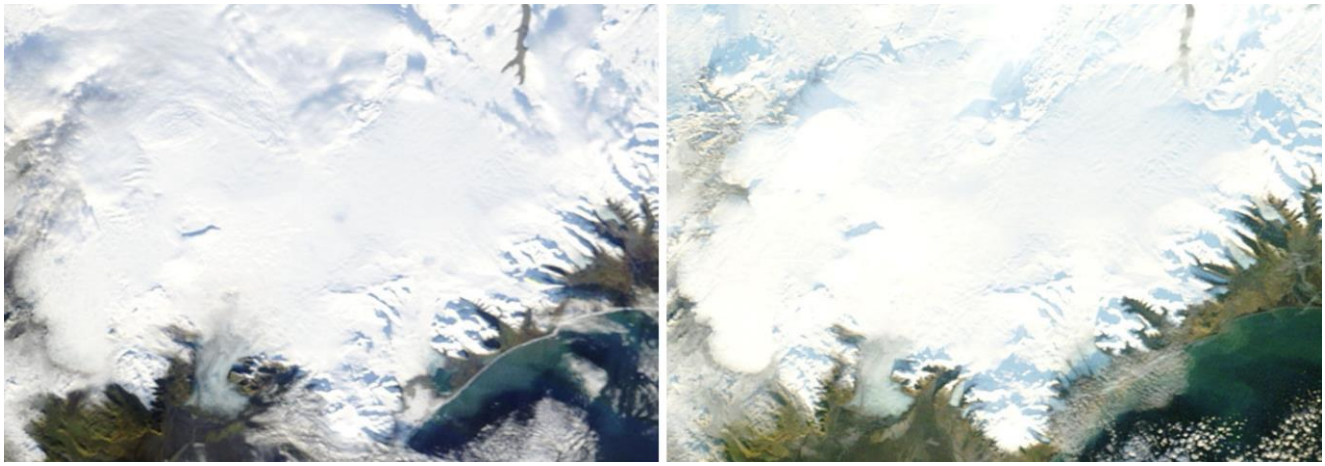

There are no cloud free days between October 10th and November 22nd. Left: November 2nd, in the SW there is no snow below ~800m. Right: November 22nd, the snow line has lowered to about 700 m, Hálslón is still not frozen over.

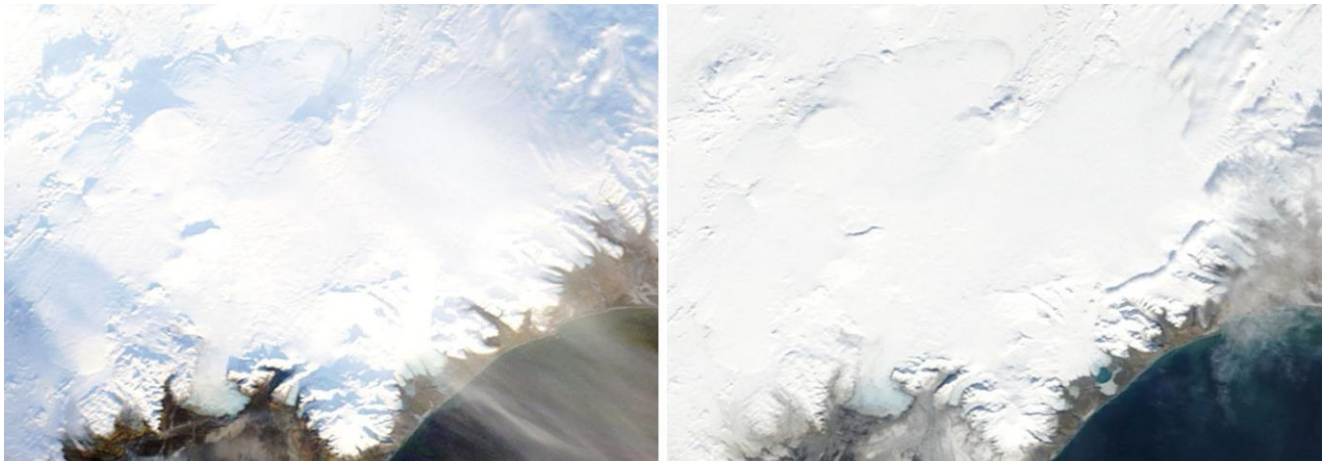

Left: January 18th 2011, the snow line is at ~200 m; however the snow on Dyngjujökull snout is very thin, the tephra on the surface there is visible. Right: March 12th, little visible change, the lowland still snow-free.

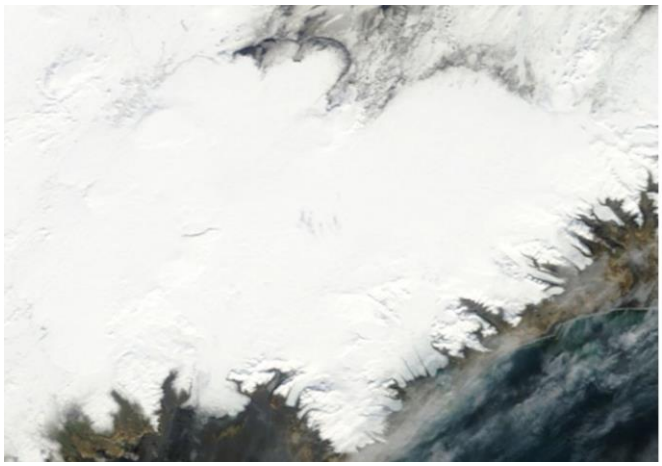
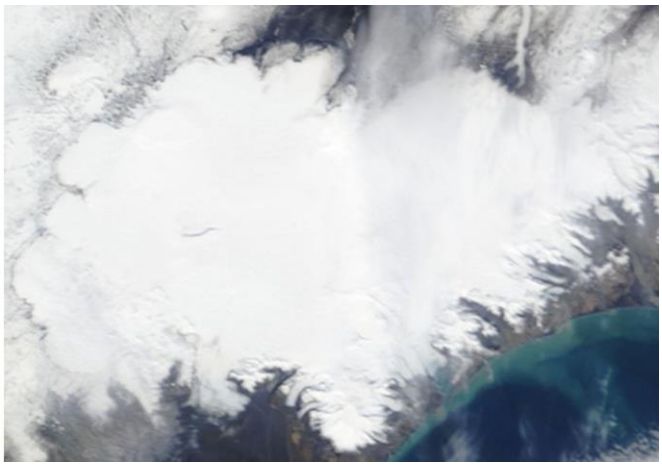

Left: April 17th, the snow line is rising, much of the snow in the north highland has melted. Right: May 2nd, now some of the snow-cover west of Vatnajökull has also melted.

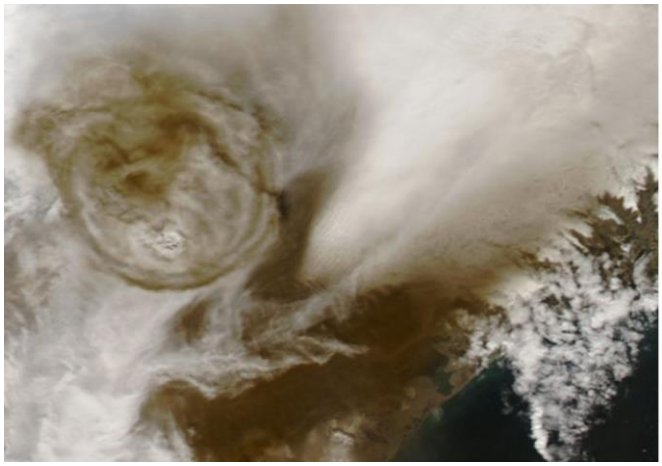
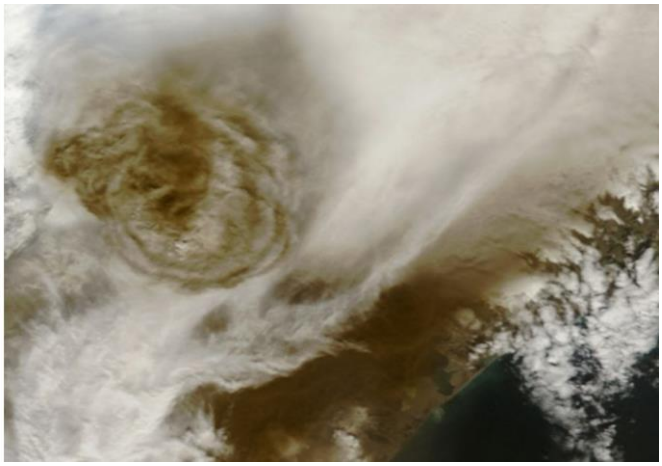

May 22st, an eruption in Grímsvötn started in the afternoon on the 21st, the images show the eruption plume at close to peak power of the eruption, the eruption ended at May 30th.

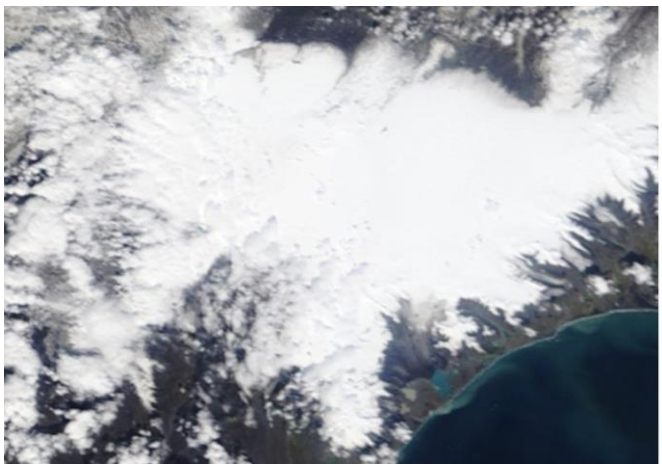
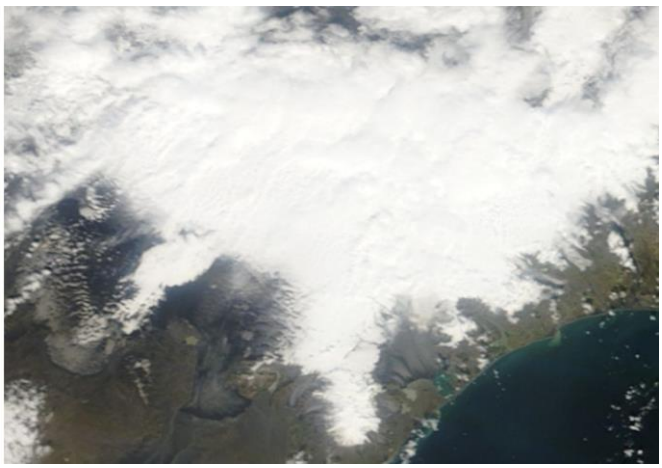

Left: June 3rd, through the cloud-cover tephra is visible south and west of Grímsvötn. Extreme melting has already started in the lower SW (observed in the annual expedition of the Iceland Glaciological Society this week). There is some fresh snow on top of and mixed with the tephra downfall. Since wind was from the north during most of the eruption period, the tephra cover was thickest south of the eruption site (~1 m thick 6 km south of the eruption site). E and NE of Grímsvötn the tephra was very thin, but substantial (~1 cm thick 10 km away) amounts were deposited W and NW of Grímsvötn in short spells of E and SE wind.

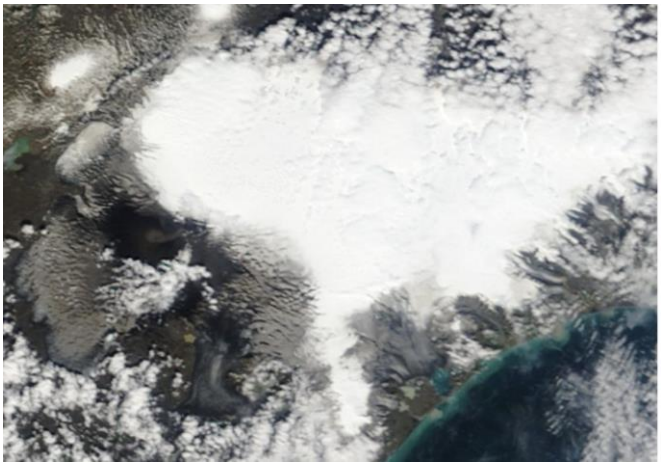


Left: June 21st, 2011, bare ice is visible in the lowest areas in the SW, the tephra washes of the ice surface. In the darkest areas the tephra is thick enough to insulate, no melting. Although clouds block view to parts of the glacier, there is obviously fresh snow on much of the surface covering the tephra; snowfall in the height of the melting season greatly reduces ablation. July 11th, snowline has significantly moved upwards, and most of the fresh snow has melted exposing the tephra and thus greatly enhancing ablation.


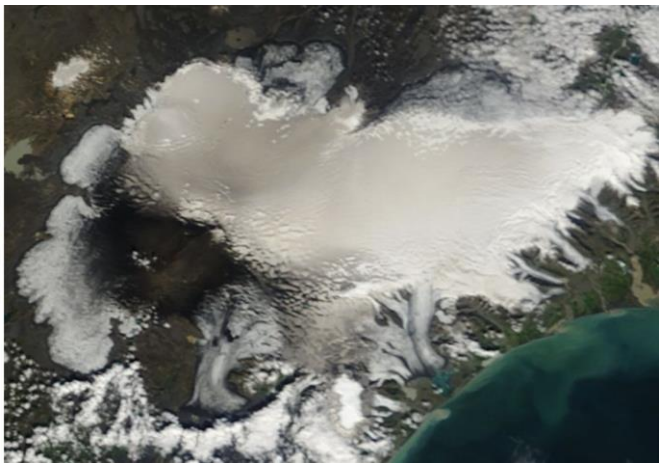

Left: July 23rd, some fresh snow still in the highest regions, snowline in the north moving fast upwards. Right: August 8th, now tephra is visible everywhere on the surface except where it has washed away in the ablations zone. The darkest area is where tephra thickness in more than a few cm (upto a few m south of Grímsvötn, in this region there is no ablation.

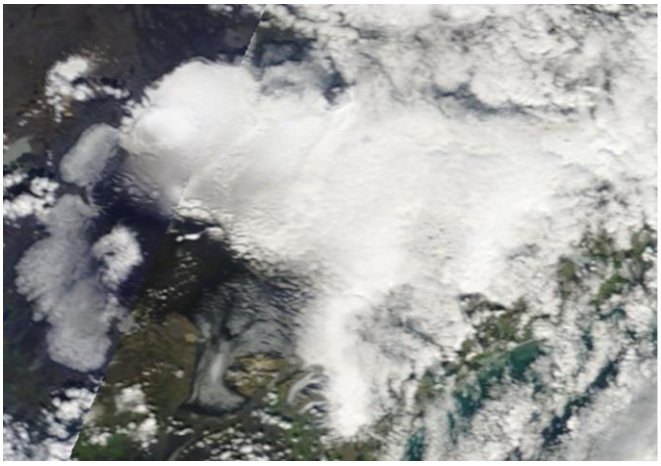
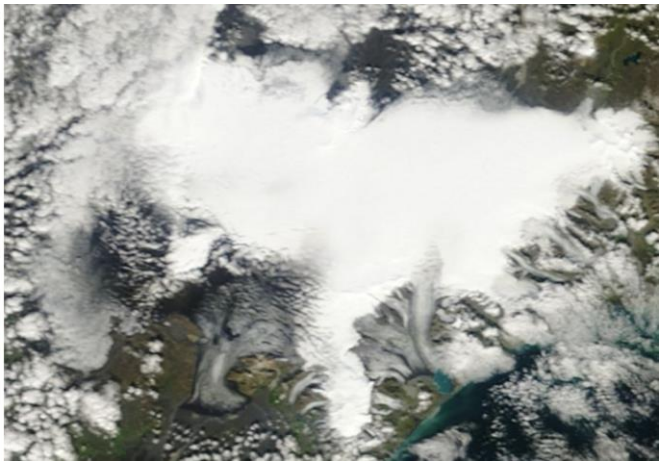

Left: August 20th and right August 25th. Snow is starting to accumulate above ~1000 m in the north and east, ablation comes to a halt, winter starts early.

Left: September 13th. In high and dry northern winds large amounts of tephra are blown to the south and southwest, some of this tephra was deposited in Reykjavík. Right: September 14th, less cloud cover reveals winter conditions on the

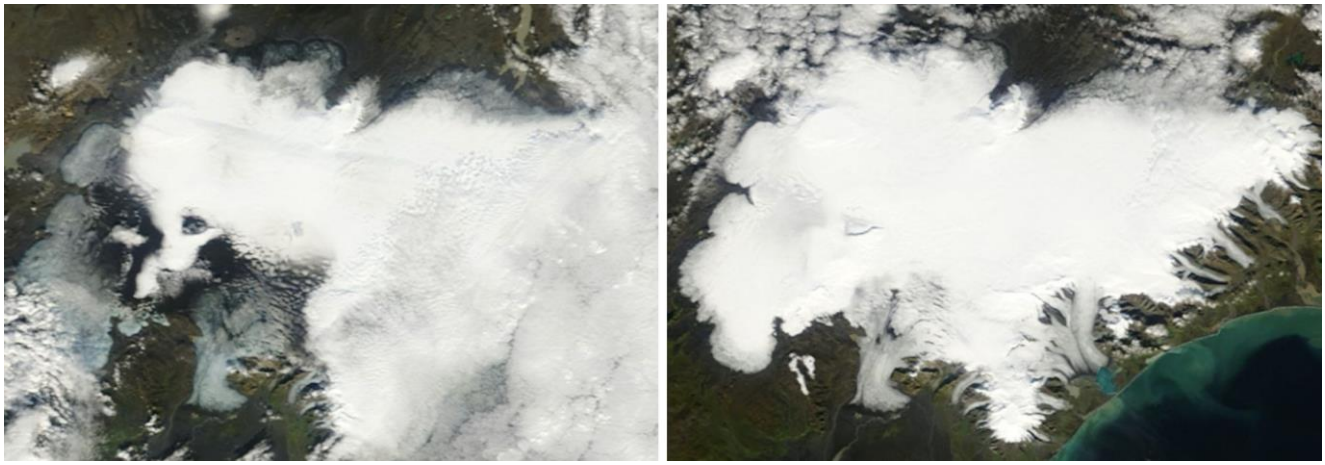

Left: September 17th, the fresh snow has melted in the ablation zone of the northern outlets, the western glacier is still snow free up to ~ 1400 m. Right: September 22nd, winter conditions on the glacier.

The images are either from the MODIS Aqua or MODIS Terra satellites, visible light, 250m resolution.
http://rapidfire.sci.gsfc.nasa.gov/
The Moderate Resolution Imaging Spectroradiometer (MODIS) flies onboard NASA's Aqua and Terra satellites as part of the NASA-centered international Earth Observing System. Both satellites orbit the Earth from pole to pole, seeing most of the globe every day. Onboard Terra, MODIS sees the Earth during the morning, while Aqua MODIS orbits the Earth in the afternoon.

On the next pages MODIS images for all days of May, June, July, August and September are shown.

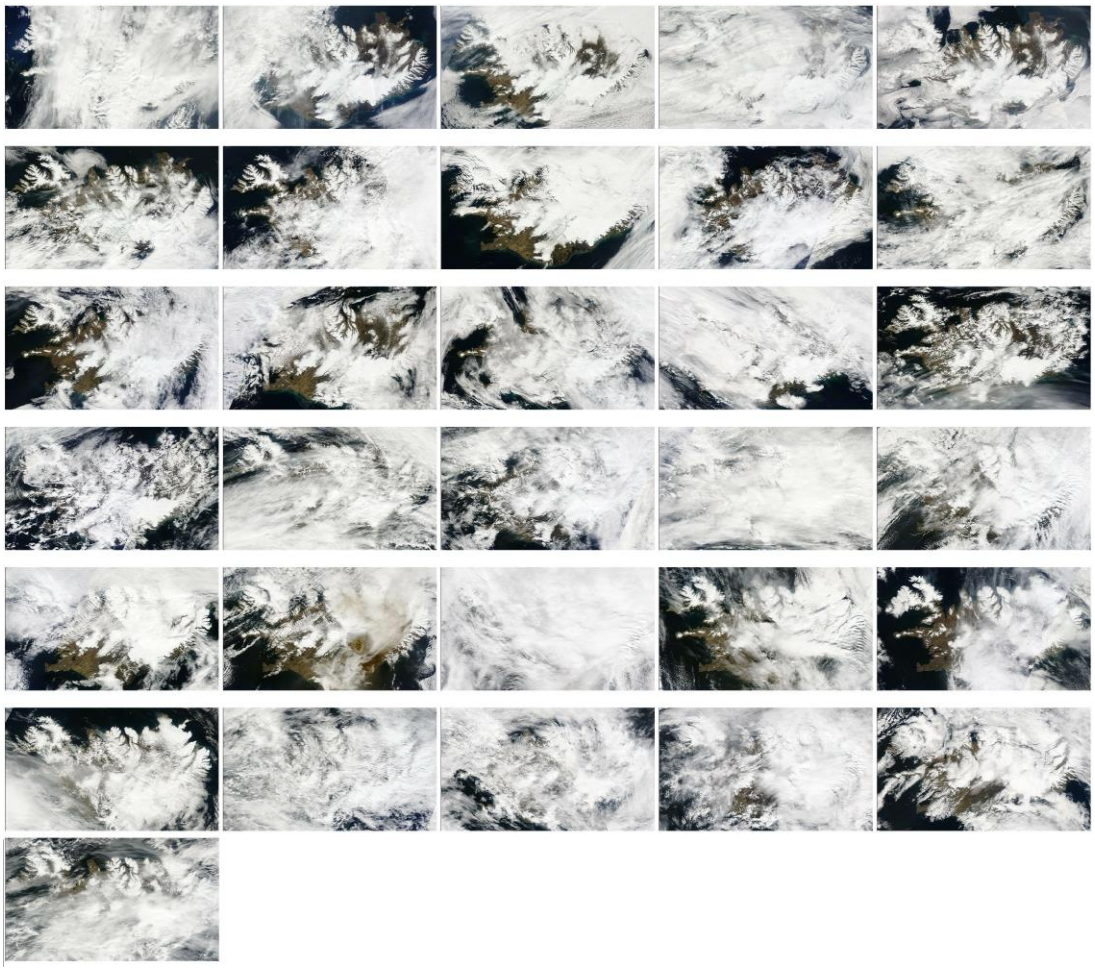

MODIS: May 2011 (read from left to right and downwards).

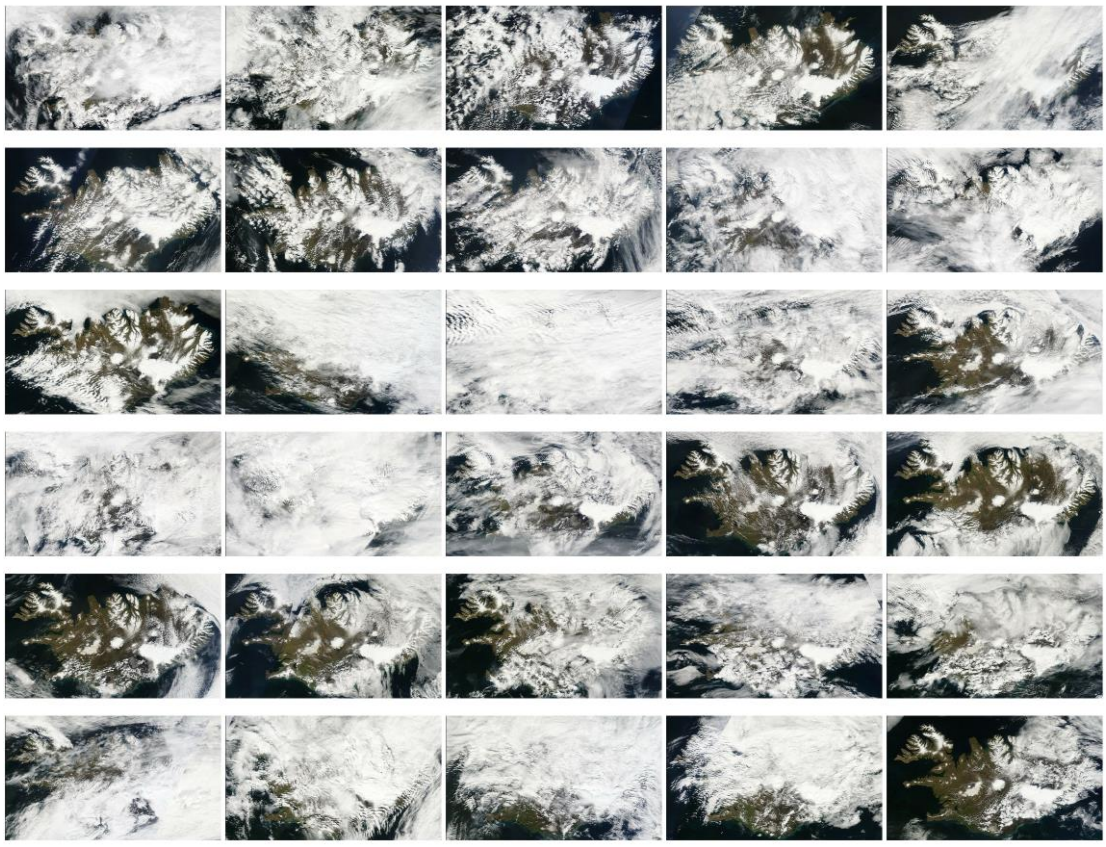

MODIS: June 2011 (read from left to right and downwards).

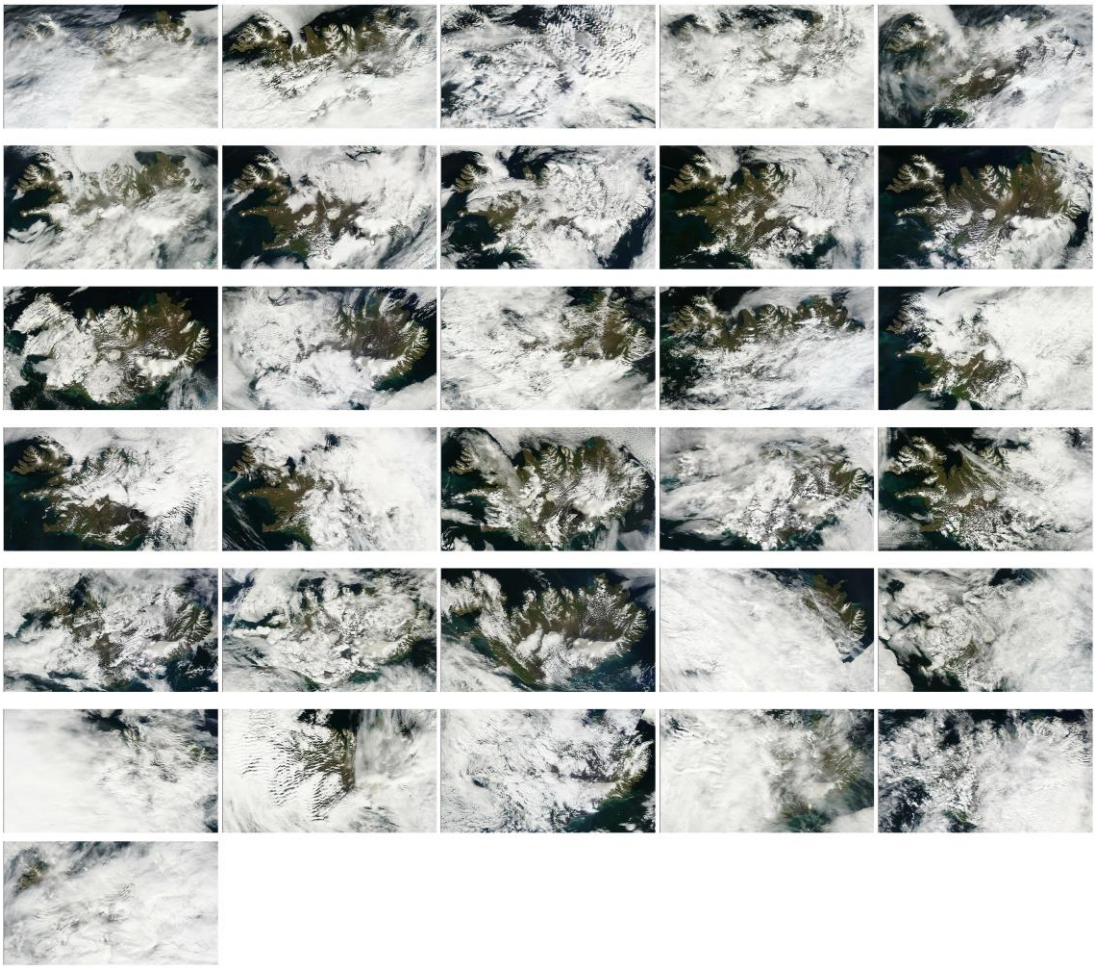

MODIS: July 2011 (read from left to right and downwards).

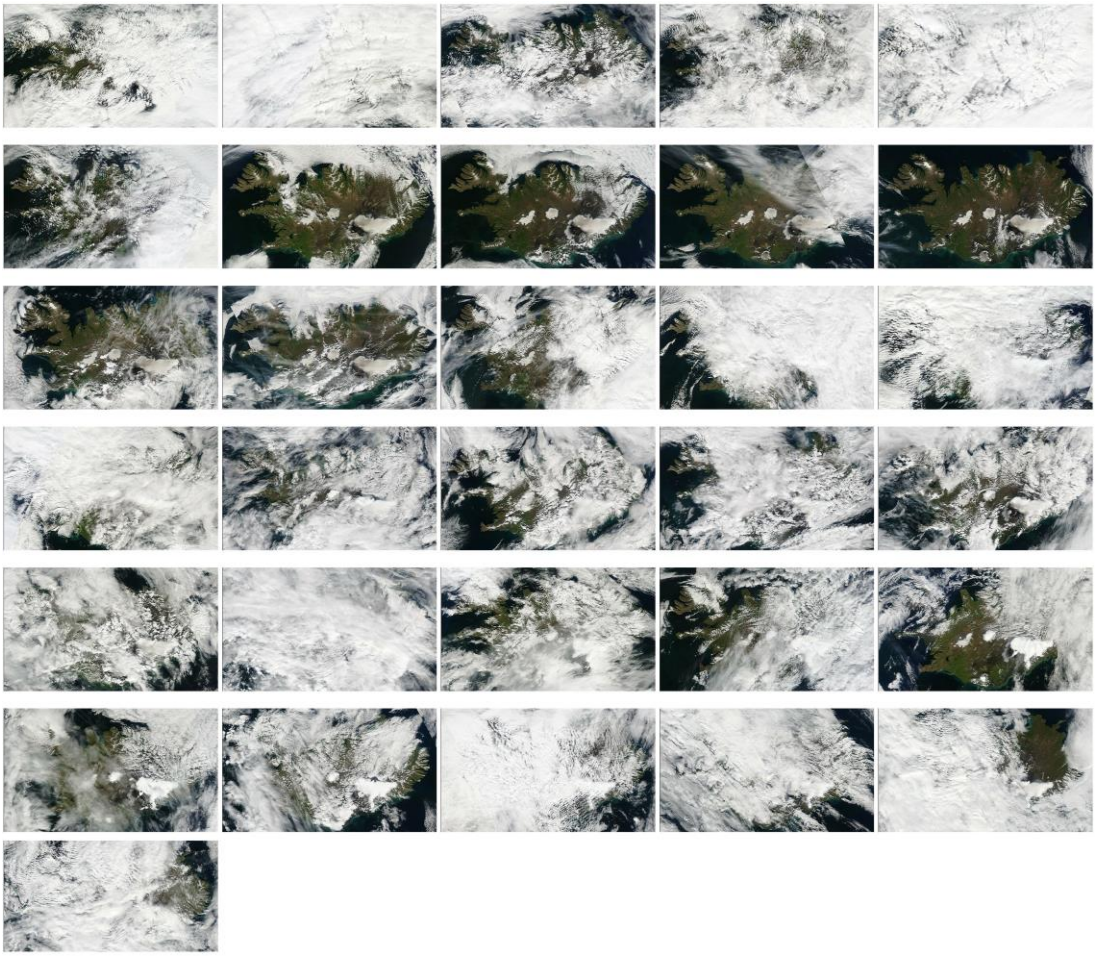

MODIS: August 2011 (read from left to right and downwards).

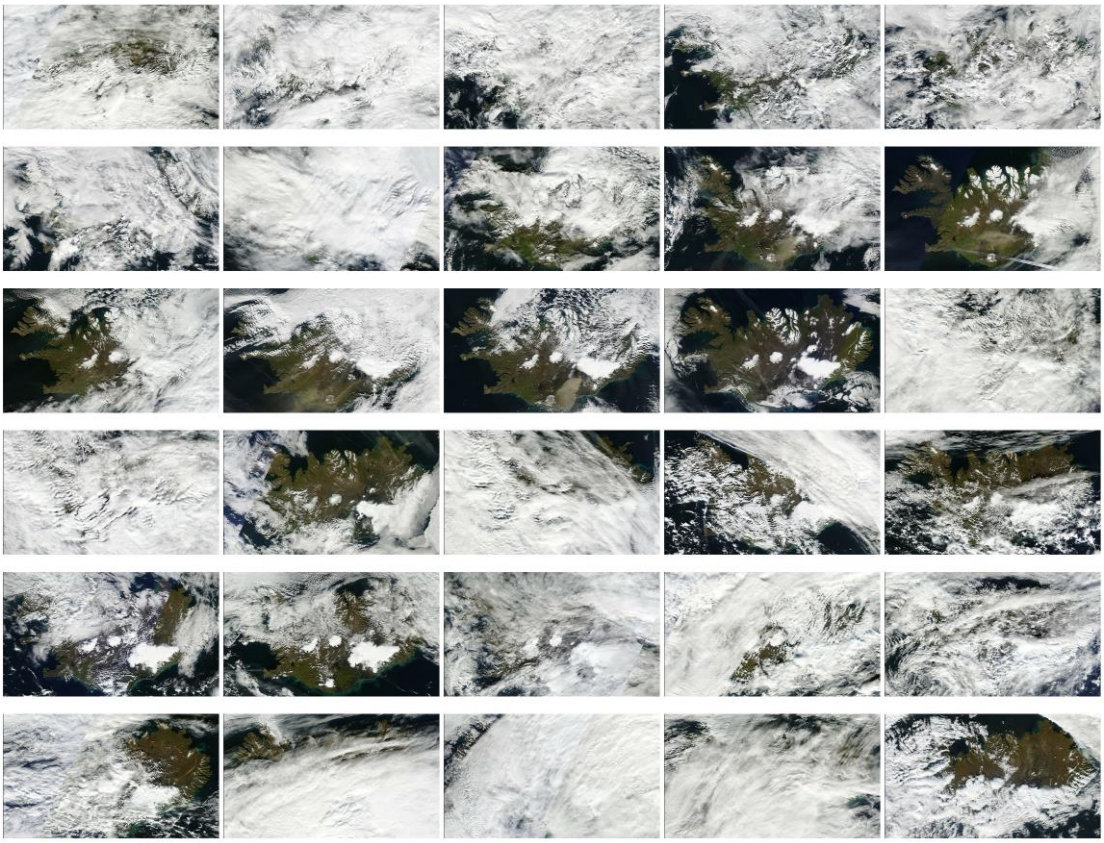

MODIS: September 2011 (read from left to right and downwards).